

**Elucidation of the sesquiterpene lactone
biosynthetic pathway in feverfew
(*Tanacetum parthenium*)**

Qing Liu

Thesis committee

Promotor

Prof. dr. ir. H.J. Bouwmeester
Professor of Plant Physiology
Wageningen University

Co-promotor

Dr. S.V.D. Krol
Associate professor, Laboratory of Plant Physiology
Wageningen University

Other members

Prof. dr. A. Ferrer, Centre for Research in Agricultural Genomics, Bellaterra,
Spain
Dr. M.C.R. Franssen, Wageningen University
Prof. dr. M.E. Schranz, Wageningen University
Dhr. dr. ir. R.C. Schuurink, University of Amsterdam

This research was conducted under the auspices of the Graduate School of
Experimental Plant Sciences.

**Elucidation of the sesquiterpene lactone
biosynthetic pathway in feverfew
(*Tanacetum parthenium*)**

Qing Liu

Thesis

submitted in fulfilment of the requirements for the degree of doctor
at Wageningen University
by the authority of the Rector Magnificus
Prof. dr. M.J. Kropff,
in the presence of the
Thesis Committee appointed by the Academic Board
to be defended in public
on Monday 2nd December 2013
at 1:30 p.m. in the Aula.

Qing Liu

Elucidation of the sesquiterpene lactone biosynthetic pathway in feverfew
(*Tanacetum parthenium*)

134 pages

PhD thesis, Wageningen University, Wageningen, the Netherlands (2013)
With summaries in English and Dutch

ISBN 978-94-6173-756-4

Contents

Chapter 1	General introduction	7
Chapter 2	Biosynthesis and localization of parthenolide in glandular trichomes of feverfew (<i>Tanacetum parthenium</i> L. Schulz Bip.)	19
Chapter 3	Reconstitution of the costunolide biosynthetic pathway in yeast and <i>Nicotiana benthamiana</i>	39
Chapter 4	<i>In planta</i> reconstitution of the parthenolide biosynthetic pathway	59
Chapter 5	Kauniolide synthase, a cytochrome P450 terpenoid cyclase that catalyses the first step in guaianolide sesquiterpene lactone biosynthesis	87
Chapter 6	General discussion	105
	Summary	121
	Samenvatting	123
	Acknowledgements	125
	<i>Curriculum vitae</i>	128
	Publication list	129
	Education statement	131
	Funding	133

Chapter 1

General introduction

Qing Liu

Plant secondary metabolites and terpenoids

Plants produce a diverse group of secondary metabolites that are required for adaptation to their environment. The majority of plant secondary metabolites include alkaloids, cyanogenic glycosides, saponins, tannins, flavonoids, anthocyanins and terpenoids. These compounds are involved in many aspects of plants during development, such as defense against herbivores and pathogens, attraction of pollinators, regulation of symbiosis, control of seed germination, and chemical inhibition of competing plant species (Makkar *et al.*, 2007).

Terpenoids are the most numerous and structurally diverse class of secondary metabolites. As built of basic five-carbon units, they can be categorized as mono- (C₁₀), sesqui- (C₁₅), di- (C₂₀), tri- (C₃₀), tetra- (C₄₀) and poly- (>C₄₀) terpenoids. Terpenoids play diverse function roles in plants as hormones (strigolactones, gibberellins and abscisic acid), electron carriers (plastoquinone and ubiquinone), mediators of polysaccharide assembly (polyprenyl phosphates), structural components of membranes (phytosterols), and photosynthetic pigments (carotenoids) (Theis & Lerdau, 2003). Besides the importance for the plant itself, terpenoids are also important to humans as many of them can be used as commercial flavourings, fragrances, antimalarial drugs and anticancer drugs (Jirschitzka *et al.*, 2012). They are usually the major constituents of essential oils (commonly C₅, C₁₀, C₁₅ and C₂₀ terpenoids) of most plants offering a wide variety of pleasant scents, such as flowery, fruity, woody or balsamic notes, which makes them a very important class of compounds for flavour and fragrance industries, e.g. menthol from wild mint (*Mentha arvensis*); D-carvone from caraway (*Carum carvi*); D-limonene from citrus species; citral from lemongrass (*Cymbopogon citratus*); 1,8-cineole from eucalyptus (*Eucalyptus globulus*) (Caputi & Aprea, 2011). Some terpenoids are widely applied either directly as drugs, or as lead compound for the synthesis of drugs that mimic terpenoids found in nature (Feher & Schmidt, 2003). A sesquiterpene lactone artemisinin, an antimalarial drug, was isolated from a herb *Artemisia annua* which has been used for many centuries in Chinese tradition medicine as a treatment for fever and malaria (Klayman, 1985). Another terpenoid paclitaxel (taxol), first isolated from the pacific yew tree (*Taxus brevifolia*), has been considered as the most successful anticancer drugs (Heinig *et al.*, 2013).

Sesquiterpenoids

Sesquiterpenoids are terpenoids with a skeleton of 15 carbons. They occur as hydrocarbons or in oxygenated forms, such as ketones, alcohols, aldehydes, acids, and lactones. Often these oxygen containing sesquiterpenoids are further modified, for example by double bond reduction or to form glycosides and acetyl esters. When a lactone is contained in the sesquiterpene skeleton, the compound's name is given the suffix 'olide'. Sesquiterpene lactones (STLs) are a major class of plant secondary metabolites, which are found in most species of the *Asteraceae*. Many of these colourless, bitter tasting, lipophilic molecules are the active constituents of a variety of medicinal plants used in traditional medicine (Rodriguez *et al.*, 1976; Zhang *et al.*, 2005). Over 4000 different STLs have been identified so far (de Kraker *et al.*, 2002). Although sesquiterpene lactones generally are present throughout the plant, they are most commonly

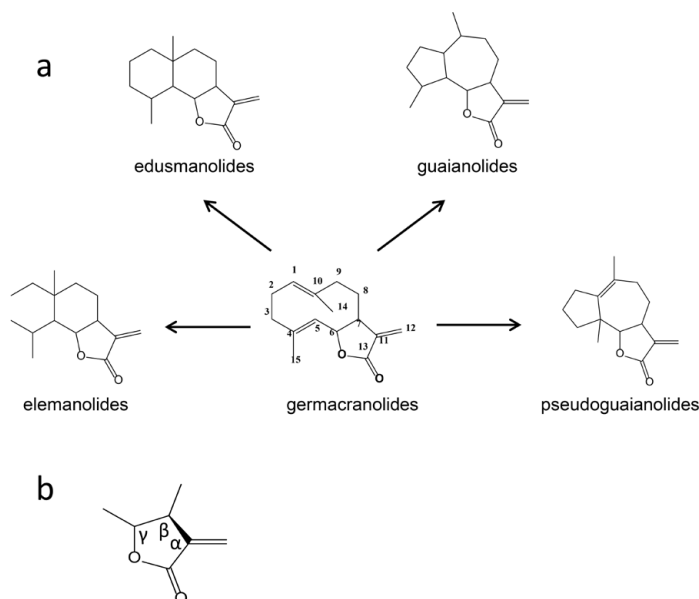


Figure 1. Different types of germacrane-derived sesquiterpene lactones (a), and structure of α -methylene- γ -lactone (b), a major functional group for biological activity of all the sesquiterpene lactones.

located in glandular trichomes on flowers, leaves and stems (Kelsey & Shafizadeh, 1980; Seigler, 1998). There are five subclasses of STLs categorised according to their carbon skeleton: germacranolide, eudesmanolide, elemanolides, guaianolide, and pseudoguaianolide (Rodriguez *et al.*, 1976; Picman, 1986; Fischer, 1990). Germacranolides are the most common type. Generally, they contain a *trans,trans*-cyclodecadiene system, but also a number of *cis,cis*-germacranolides have been reported. All the sesquiterpene lactones are considered to be derived from a germacrane precursor, likely germacrene A (Figure 1) (de Kraker *et al.*, 1998). The germacrane precursor undergoes cyclisation, ring fusion, and sometimes methyl migration to yield the other skeletal types of STLs.

Sesquiterpene lactones in feverfew

Feverfew (*Tanacetum parthenium*) is one of the most prominent medicinal species in the *Asteraceae* family (Bedoya *et al.*, 2008). Feverfew is a daisy-like annual or perennial herb (Figure 2). The term *parthenium* has been considered to originate from the Greek word *parthenios*

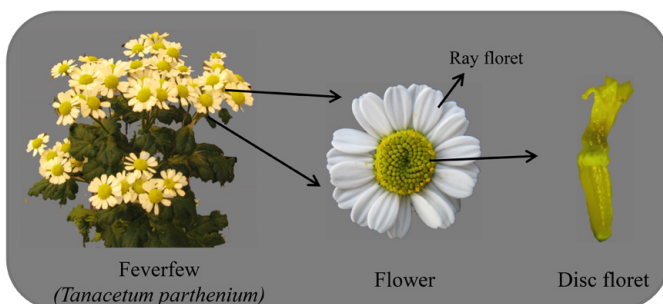


Figure 2. Plant, flower, ray floret and disc floret of feverfew and its botanical classification.

meaning ‘virgin’, probably because the herb has been used as an anti-dote for women’s ailments (Jackson & McDonald, 1986). An alternative explanation comes from a Greek story about an accident where feverfew was used to save the life of someone who had fallen from the Parthenon during its construction in the 5th century BC (Johnson, 1984). The herb has been used since ancient times as a general *febrifuge*, which means ‘fever reducer’, hence its common name.

Feverfew is native in southern Europe, but it has become naturalized throughout Europe, Asia, North Africa, Australia and North

America. During summer, the plant flowers and most of the aerial parts are harvested when they are required for use in herbal medicine. Feverfew has been used for at least two millennia for the treatment of fever, as well as headache, menstrual irregularities, stomach-ache and as an aid for those suffering from arthritis and inflammation (Pareek *et al.*, 2011). Its extracts have been approved in Europe as a herbal drug for the treatment of migraine without prescription. The clinical safety of these extracts has been verified.

More than 30 STLs have been identified in feverfew, including parthenolide, costunolide, 3 β -hydroxyparthenolide, 3 β -hydroxycostunolide, artemecanin, artemorin, balchanin, canin, 10-epicanin, epoxyartemorin, 1 β -hydroxyarbusculin, 8 α -hydroxyestagiatin, 8 β -hydroxyreynosin, manolialide, reynosin, santamarine, epoxysantamarine, secotanaparthanolide A, secotanaparthanolide B, tanaparthin- α -peroxide, and 3,4 β -epoxy-8-deoxycumambrin B (Pareek *et al.*, 2011; Fishedick *et al.*, 2012). These STLs belong to three structural types: eudesmanolides, germacranolides, and guaianolides. The structures of some representative STLs are shown in Figure 3. Parthenolide is the principal bioactive STL component in feverfew (0.1~0.9 %, dry weight) (Bork *et al.*, 1997).

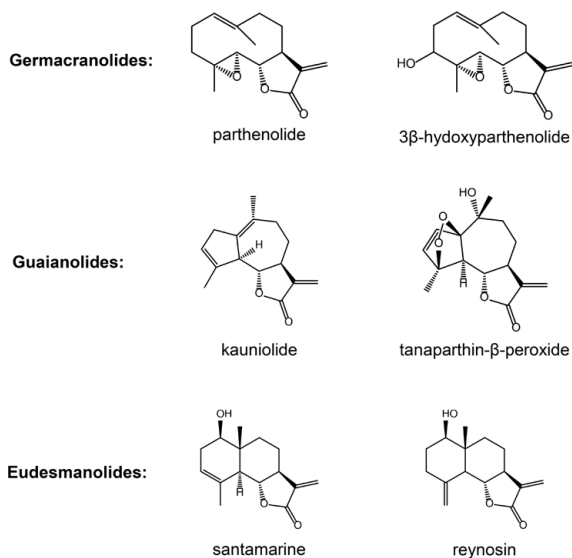


Figure 3. Structures of representative sesquiterpene lactones reported in feverfew.

Why do sesquiterpene lactones have such exceptional bioactivities?

Parthenolide exhibits exceptional anti-cancer, anti-inflammatory, and anti-microbial activity (Mathema *et al.*, 2012). It has been reported to induce reactive oxygen species (ROS) exclusively in tumor cells (Zhang *et al.*, 2004; Zunino *et al.*, 2007; Juliana *et al.*, 2010), enhance platelet production and attenuate platelet activation through the inhibitory activity of NF- κ B signalling pathway (Sahler *et al.*, 2011), and interfere with microtubule formation by reducing

impaired control of spindle positioning (Fonrose *et al.*, 2007). It has also been reported to induce apoptosis of human acute myelogenous leukemia stem and progenitor cells (Guzman *et al.*, 2005), act as inhibitor of inflammasomes (Juliana *et al.*, 2010), and prevent human lens epithelial cells from oxidative stress-induced apoptosis through inhibition of the activation of inflammation-related genes (Li-Weber *et al.*, 2005). However, despite promising activity, this potent natural product has one major limitation which precludes its further development as a therapeutic agent and that is its poor water-solubility (Sweeney *et al.*, 2005). Hence, there is a great need for derivatives with similar bioactivity but improved water solubility. An analogue of parthenolide, dimethylamino-parthenolide (DMAPT), was shown to retain the biological activity of parthenolide, while exhibiting oral-bioavailability (Guzman *et al.*, 2007). Eight additional, water-soluble, parthenolide analogues were found to exhibit good anti-leukemic activity (Neelakantan *et al.*, 2009).

The biological activity of most STLs is due to alkylation of biological macromolecules by Michael-type additions. The cytotoxic activity of STLs has been attributed to the reaction of the α,β -unsaturated lactone moiety with thiols, such as cysteine residues in proteins, which leads to the disruption of various cysteine-dependent structural enzymes and proteins. In addition, the redox balance in biological tissues is altered by the reaction of the lactone moiety with free intracellular reduced glutathione (Rodriguez *et al.*, 1976).

The α -methylene- γ -lactone group and α,β -unsaturated carbonyl (Figure 1b), as well as conjugated aldehyde groups, are considered to be the reactive groups (Lee *et al.*, 1971; Mersfort, 2011). The cytotoxic activity of STLs decreases strongly through reduction of the double bond of the α,β -unsaturated ketone (Lee, 2010). When the α -methylene- γ -lactone moiety is the only alkylating centre, a conjugated ester side chain increases cytotoxicity regardless of its lipophilic properties (Ghantous *et al.*, 2010). These alkylating STLs can react with nucleophiles, which consequently react reversibly with sulfhydryl groups in the cell, including those on free cysteine residues (Ghantous *et al.*, 2010). Guaianolide and pseudoguaianolide skeletal types are found to be among the most active STLs through *in vitro* cytotoxicity assays (Fernandes *et al.*, 2008).

Biosynthesis of sesquiterpene lactones

MEP and Mevalonate pathway

The STLs in feverfew are thought to be located in trichomes on the abaxial side of the leaves as well as in the flowers and seeds (Blakeman & Atkinson, 1979). Parthenolide is found in highest concentration in the flowers and fruits. The amounts present in leaves are normally well in excess of 2 mg g⁻¹. Other sesquiterpene lactones are only present in mg kg⁻¹ quantities (Hewlett *et al.*, 1996). Sesquiterpene lactones are derived from the universal C5 precursor isopentenyl diphosphate (IPP) which can be synthesized via two different pathways: the mevalonate (MVA) pathway and the 2-C-methyl-D-erythritol 4-phosphate (MEP) pathway (Figure 4). Both pathways exist in plants but have different subcellular localisation. The MEP pathway enzymes are located in plastids, while the MVA enzymes are found in the cytosol

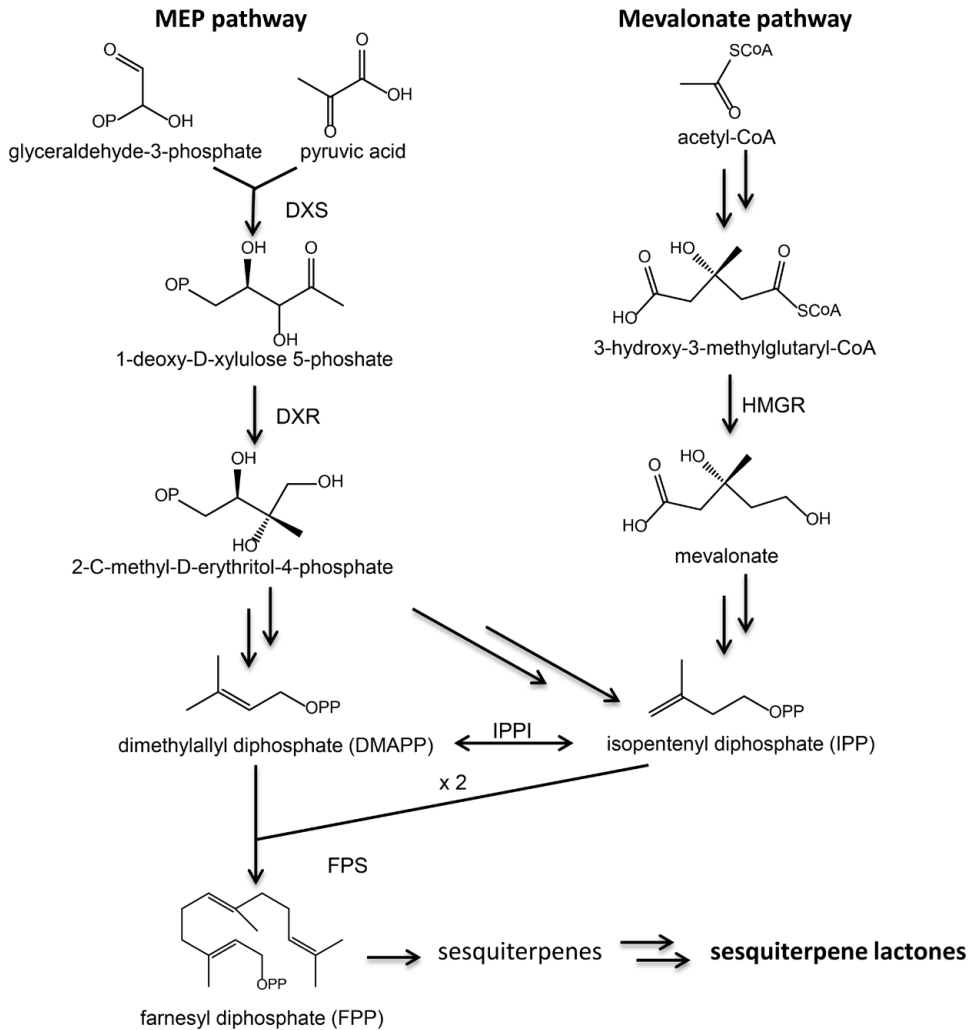


Figure 4. Overview of sesquiterpene lactone biosynthesis. DXS, 1-deoxy-D-xylulose 5-phosphate synthase; DXR, 1-deoxy-D-xylulose 5-phosphate reductoisomerase; HMGR, 3-hydroxy-3-methylglutaryl-CoA reductase; IDI, IPP-isomerase; FPS, farnesyl diphosphate synthase.

(Vranová *et al.*, 2013).

In the MEP pathway, glyceraldehyde-3-phosphate and pyruvic acid are transformed to IPP and DMAPP in a ratio of 5:1 through seven enzymes. In the MVA pathway, acetyl-CoA is transformed to IPP through 6 steps, followed by an IPP isomerase (IPPI) that maintains a balance between IPP and DMAPP. Two IPPs and one DMAPP are then converted to farnesyl diphosphate (FPP), the precursor for all sesquiterpenes, through farnesyl diphosphate synthase (FPS). FPP can be converted to sesquiterpenes by sesquiterpene synthases. The sesquiterpenes are often further modified by hydroxylation and/or other oxidation reactions, usually

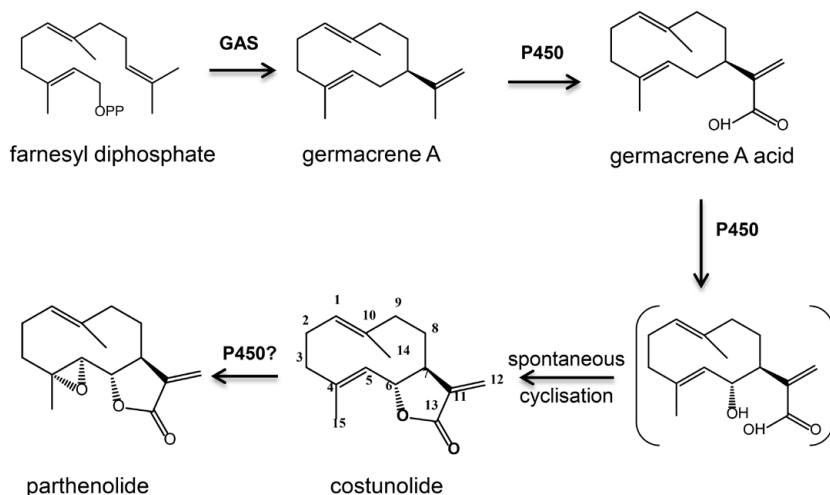


Figure 5. Presumed biosynthetic pathway for parthenolide. GAS, germacrene A synthase. P450, cytochrome P450 monooxygenase.

mediated by cytochrome P450 enzymes. Cytochrome P450 monooxygenases are heme protein-dependent mixed-function oxidases that utilize NADPH and/or NADH to reductively cleave atmospheric dioxygen to produce a functionalized organic substrate and a molecule of water (Schuler & Werck-Reichhart, 2003). In many cases, the result of a cytochrome P450 catalysed reaction is insertion of oxygen (hydroxylation), but in a number of cases, P450s mediate dehydrogenation, isomerization, dimerization, carbon-carbon bond cleavage, reduction, as well as N-, O- and S-dealkylations, sulphoxidations, epoxidations, deaminations, and desulphurations (Weitzel & Simonsen, 2013). The term 'P450' originated from their shared ability to display a typical absorption peak at 450 nm when carbon monoxide is bound to the reduced form of the enzyme (Omura & Sato, 1964).

Several P450s have been reported to be involved in sesquiterpene biosynthesis. CYP71AV1, amorpha-4,11-diene oxidase of *Artemisia annua*, was found to catalyse the conversion of amorpha-4,11-diene into artemisinic acid in three consecutive hydroxylation steps (Ro *et al.*, 2006). By co-expressing amorpha-4,11-diene synthase (ADS) and CYP71AV1 in *Nicotiana benthamiana*, artemisinic acid was produced, which was partially conjugated to form a diglucoside (van Herpen *et al.*, 2010). A cytochrome P450 enzyme, CYP71D20, was reported to catalyse the regio- and stereospecific insertion of two hydroxyl moieties into the bicyclic sesquiterpene 5-epiaristolochene (Takahashi *et al.*, 2005). Another P450 CYP71D55, prenaspirodiene oxygenase from *Hyoscyamus muticus* (Solanaceae), was found to be capable of hydroxylating valencene, 5-*epi*-eremophilene, and 5-*epi*-aristolochene in addition to its native substrate prenaspirodiene (Takahashi *et al.*, 2007).

Biosynthesis of sesquiterpene lactones in feverfew

The biosynthesis pathway of parthenolide, the most prominent compound in feverfew, was postulated to proceed as shown in Figure 5 when the work of this PhD thesis was initiated.

First, germacrene A synthase (GAS) catalyses the cyclization of FPP to germacrene A (de Kraker *et al.*, 1998). GAS has been cloned from chicory (Bouwmeester *et al.*, 2002), lettuce (Bennett *et al.*, 2002) and *A. annua* (Bertea *et al.*, 2006). In a number of additional steps, germacrene A is then oxidized to germacranoic carboxylic acid (de Kraker *et al.*, 2001). This sequence of reactions is very similar to the biosynthesis of artemisinic acid, hydroxylation of amorphadiene to artemisinic alcohol, artemisinic aldehyde, and then artemisinic acid by CYP71AV1 (Ro *et al.*, 2006; Teoh *et al.*, 2006; Zhang *et al.*, 2008). Thus, it is likely that the oxidation of germacrene A to germacranoic acid in *Tanacetum parthenium* is performed by a similar P450 monooxygenase. The subsequent hydroxylation of germacranoic acid, required to form costunolide (Figure 5), is likely also catalysed by a P450 monooxygenase. Parthenolide is produced through epoxidation of costunolide at the C4-C5 double bond of costunolide, possibly by another P450 monooxygenase.

Thesis outline

This thesis is part of a project within the “Food, Agriculture and Fisheries, and Biotechnology” theme of the Seventh Framework Programme of the European Commission project entitled ‘Plant Terpenoids for Human Health: a chemical and genomic approach to identify and produce bioactive compounds’ (acronym: TERPMED).

As part of the TERPMED project, this thesis aimed to elucidate the biosynthetic pathway of parthenolide and other sesquiterpene lactones in feverfew (*Tanacetum parthenium*), and to improve parthenolide production - and produce novel STLs through combinatorial biochemistry - through genetic engineering of plants. Enzymes involved in the different steps of the biosynthesis of these bioactive STLs are characterized at molecular and biochemical level and the corresponding genes used for metabolic engineering.

The present chapter, **Chapter 1**, gives an introduction to the sesquiterpene lactones in general and parthenolide and feverfew in particular, the medicinal properties of the STLs and what is known and postulated about their biosynthesis.

Chapter 2 describes work on the localisation of parthenolide biosynthesis to provide the basis for the subsequent characterisation of the pathway. The work shows that parthenolide is produced and localized mainly in trichomes on feverfew flowers. Isolated trichomes are subsequently used to isolate the sesquiterpene synthase encoding the first dedicated step in parthenolide biosynthesis, germacrene A synthase (*TpGAS*).

During my work on *TpGAS*, *germacrene A oxidase (GAO)*, the gene that likely encodes the next step in the pathway, was reported from lettuce (Nguyen *et al.*, 2010) and chicory (*Cichorium intybus* L.) (Cankar *et al.*, 2011). As the feverfew trichome transcriptomics data were not yet available, in **Chapter 3** I used a chicory root 454 cDNA library to identify the gene that is responsible for the next step of the pathway, costunolide synthase, *CiCOS*. I used this gene, in combination with *TpGAS* and *CiGAO* for reconstitution of the costunolide biosynthesis pathway through transient expression in *N. benthamiana*. This resulted in formation of the expected product, costunolide, but also new costunolide conjugates, which have never been

reported before in plants.

Chapter 4 describes the isolation and characterization of *TpGAO*, *TpCOS* and *TpPTS* using feverfew trichome cDNA sequences. Together with *TpGAS* that I characterised in Chapter 2, these are all the pathways genes required for biosynthesis of parthenolide from farnesyl diphosphate. I used these genes to reconstitute the entire parthenolide biosynthesis pathway in *N. benthamiana*. Parthenolide was formed, mostly as conjugates, and these are tested for bioactivity against cancer cells.

The feverfew trichome EST data yielded a wealth of other interesting gene candidates and **Chapter 5** describes the isolation and characterization of a *kauniolide synthase* (*TpKS*). *TpKS* is also a cytochrome P450 and catalyses ring closure in the germacranolide costunolide to form a guaianolide STL, kauniolide.

Chapter 6 integrates and discusses all the results from this thesis in a broader perspective. Some future perspectives are also discussed.

References

- Ashour M, Wink M, Gershenzon J 2010. Biochemistry of terpenoids: Monoterpenes, sesquiterpenes and diterpenes. *Annual Plant Reviews Volume 40: Biochemistry of Plant Secondary Metabolism*: Wiley-Blackwell, 258-303.
- Bedoya LM, Abad MJ, Bermejo P. 2008. The role of parthenolide in intracellular signalling processes: Review of current knowledge. *Current Signal Transduction Therapy* 3(2): 82-87.
- Bennett MH, Mansfield JW, Lewis MJ, Beale MH. 2002. Cloning and expression of sesquiterpene synthase genes from lettuce (*Lactuca sativa* L.). *Phytochemistry* 60(3): 255-261.
- Berteau CM, Voster A, Verstappen FWA, Maffei M, Beekwilder J, Bouwmeester HJ. 2006. Isoprenoid biosynthesis in *Artemisia annua*: Cloning and heterologous expression of a germacrene A synthase from a glandular trichome cDNA library. *Archives of biochemistry and biophysics* 448(1-2): 3-12.
- Blakeman JP, Atkinson P. 1979. Anti-microbial properties and possible role in host-pathogen interactions of parthenolide, a sesquiterpene lactone isolated from glands of *Chrysanthemum parthenium*. *Physiological Plant Pathology* 15(2): 183-190.
- Bork PM, Schmitz ML, Kuhnt M, Escher C, Heinrich M. 1997. Sesquiterpene lactone containing Mexican Indian medicinal plants and pure sesquiterpene lactones as potent inhibitors of transcription factor NF- κ B. *FEBS Letters* 402(1): 85-90.
- Bouwmeester HJ, Kodde J, Verstappen FWA, Altug IG, de Kraker JW, Wallaart TE. 2002. Isolation and characterization of two germacrene A synthase cDNA clones from chicory. *Plant Physiology* 129(1): 134-144.
- Cankar K, Houwelingen Av, Bosch D, Sonke T, Bouwmeester H, Beekwilder J. 2011. A chicory cytochrome P450 mono-oxygenase CYP71AV8 for the oxidation of (+)-valencene. *FEBS Letters* 585(1): 178-182.
- Caputi L, Aprea E. 2011. Use of terpenoids as natural flavouring compounds in food industry. *Recent Patents on Food, Nutrition & Agriculture* 3(1): 9.
- de Kraker JW, Franssen MCR, Dalm MCF, de Groot A, Bouwmeester HJ. 2001. Biosynthesis of germacrene A carboxylic acid in chicory roots. Demonstration of a cytochrome P450 (+)-germacrene A hydroxylase and NADP(+)-dependent sesquiterpenoid dehydrogenase(s) involved in sesquiterpene lactone biosynthesis. *Plant Physiology* 125(4): 1930-1940.
- de Kraker JW, Franssen MCR, de Groot A, König WA, Bouwmeester HJ. 1998. (+)-Germacrene A biosynthesis - The committed step in the biosynthesis of bitter sesquiterpene lactones in chicory. *Plant Physiology* 117(4): 1381-1392.
- de Kraker JW, Franssen MCR, Joerink M, de Groot A, Bouwmeester HJ. 2002. Biosynthesis of costunolide, dihydrocostunolide, and leucodin. Demonstration of cytochrome P450-catalyzed formation of the lactone ring present in sesquiterpene lactones of chicory. *Plant Physiology* 129(1): 257-268.
- Fehér M, Schmidt JM. 2003. Property distributions: differences between drugs, natural products, and molecules from combinatorial chemistry. *Journal of Chemical Information and Computer Sciences* 43(1): 218-227.
- Fernandes MB, Scotti MT, Ferreira MJ, Emerenciano VP. 2008. Use of self-organizing maps and molecular descriptors to predict the cytotoxic activity of sesquiterpene lactones. *European Journal of Medicinal Chemistry*

- 43(10): 2197-2205.
- Fischedick JT, Standiford M, Johnson DA, De Vos RCH, Todorović S, Banjanac T, Verpoorte R, Johnson JA. 2012.** Activation of antioxidant response element in mouse primary cortical cultures with sesquiterpene lactones isolated from *Tanacetum parthenium*. *Planta Medica*(EFirst).
- Fischer NH. 1990.** *Biochemistry of the mevalonic acid pathway to terpenoids*. New York: Plenum Press.
- Fonrose X, Ausseil F, Soleilhac E, Masson V, David B, Pouny I, Cintrat J-C, Rousseau B, Barette C, Massiot G. 2007.** Parthenolide inhibits tubulin carboxypeptidase activity. *Cancer research* 67(7): 3371-3378.
- Ghantous A, Gali-Muhtasib H, Vuorela H, Saliba NA, Darwiche N. 2010.** What made sesquiterpene lactones reach cancer clinical trials? *Drug Discovery Today* 15(15-16): 668.
- Guzman ML, Rossi RM, Karnischky L, Li X, Peterson DR, Howard DS, Jordan CT. 2005.** The sesquiterpene lactone parthenolide induces apoptosis of human acute myelogenous leukemia stem and progenitor cells. *Blood* 105(11): 4163-4169.
- Guzman ML, Rossi RM, Neelakantan S, Li XJ, Corbett CA, Hassane DC, Becker MW, Bennett JM, Sullivan E, Lachowicz JL, Vaughan A, Sweeney CJ, Matthews W, Carroll M, Liesveld JL, Crooks PA, Jordan CT. 2007.** An orally bioavailable parthenolide analog selectively eradicates acute myelogenous leukemia stem and progenitor cells. *Blood* 110(13): 4427-4435.
- Heinig U, Scholz S, Jennewein S. 2013.** Getting to the bottom of taxol biosynthesis by fungi. *Fungal Diversity*: 1-10.
- Hewlett MJ, Begley MJ, Groenewegen WA, Heptinstall S, Knight DW, May J, Salan U, Toplis D. 1996.** Sesquiterpene lactones from feverfew, *Tanacetum parthenium*: Isolation, structural revision, activity against human blood platelet function and implications for migraine therapy. *Journal of the Chemical Society-Perkin Transactions 1*(16): 1979-1986.
- Jackson B, McDonald RL. 1986.** Magic and medicine of plants. In: *The Reader's Digest* Montral. 182.
- Jirschtzka J, Mattern DJ, Gershenzon J, D'Auria JC. 2012.** Learning from nature: new approaches to the metabolic engineering of plant defense pathways. *Current Opinion in Biotechnology* 24(2): 320-328.
- Johnson S. 1984.** *Feverfew: A traditional herbal remedy for migraine and arthritis*. London: Sheldon Press.
- Juliana C, Fernandes-Alnemri T, Wu J, Datta P, Solorzano L, Yu J-W, Meng R, Quong AA, Latz E, Scott CP. 2010.** Anti-inflammatory compounds parthenolide and Bay 11-7082 are direct inhibitors of the inflammasome. *Journal of Biological Chemistry* 285(13): 9792-9802.
- Kelsey RG, Shafizadeh F. 1980.** Glandular trichomes and sesquiterpene lactones of *Artemisia nova* (Asteraceae). *Biochemical Systematics and Ecology* 8(4): 371-377.
- Klayman DL. 1985.** Qinghaosu (artemisinin): an antimalarial drug from China. *Science* 228(4703): 1049-1055.
- Lee K-H. 2010.** Discovery and development of natural product-derived chemotherapeutic agents based on a medicinal chemistry approach. *Journal of Natural Products* 73(3): 500-516.
- Lee K-H, Huang E-S, Piantadosi C, Pagano JS, Geissman T. 1971.** Cytotoxicity of sesquiterpene lactones. *Cancer research* 31(11): 1649-1654.
- Li-Weber M, Palfi K, Giaisi M, Krammer P. 2005.** Dual role of the anti-inflammatory sesquiterpene lactone: regulation of life and death by parthenolide. *Cell Death & Differentiation* 12(4): 408-409.
- Makkar HP, Siddhuraju P, Becker K. 2007.** *Plant secondary metabolites*: Humana Press.
- Martin VJJ, Pitera DJ, Withers ST, Newman JD, Keasling JD. 2003.** Engineering a mevalonate pathway in *Escherichia coli* for production of terpenoids. *Nature Biotechnology* 21(7): 796-802.
- Mathema V, Koh Y-S, Thakuri B, Sillanpää M. 2012.** Parthenolide, a sesquiterpene lactone, expresses multiple anti-cancer and anti-inflammatory activities. *Inflammation* 35(2): 560-565.
- Merfort I. 2011.** Perspectives on sesquiterpene lactones in inflammation and cancer. *Current Drug Targets* 12(11): 1560-1573.
- Neelakantan S, Nasim S, Guzman ML, Jordan CT, Crooks PA. 2009.** Aminoparthenolides as novel anti-leukemic agents: Discovery of the NF- κ B inhibitor, DMAPT (LC-1). *Bioorganic & Medicinal Chemistry Letters* 19(15): 4346-4349.
- Nguyen DT, Gopfert JC, Ikezawa N, Macnevin G, Kathiresan M, Conrad J, Spring O, Ro DK. 2010.** Biochemical conservation and evolution of germacrene A oxidase in asteraceae. *Journal of Biological Chemistry* 285(22): 16588-16598.
- Omura T, Sato R. 1964.** The carbon monoxide-binding pigment of liver microsomes. I. Evidence for its hemoprotein nature. *Journal of Biological Chemistry* 239(7): 2370-2378.
- Pareek A, Suthar M, Rathore SG, Bansal V. 2011.** Feverfew (*Tanacetum parthenium* L.): A systematic review. *Pharmacognosy Review* 5(9): 103-110.
- Picman AK. 1986.** Biological activities of sesquiterpene lactones. *Biochemical Systematics and Ecology* 14(3): 255-281.
- Ro DK, Paradise EM, Ouellet M, Fisher KJ, Newman KL, Ndungu JM, Ho KA, Eachus RA, Ham TS, Kirby J,**

- Chang MCY, Withers ST, Shiba Y, Sarpong R, Keasling JD. 2006.** Production of the antimalarial drug precursor artemisinic acid in engineered yeast. *Nature* **440**(7086): 940-943.
- Rodriguez E, Towers GHN, Mitchell JC. 1976.** Biological activities of sesquiterpene lactones. *Phytochemistry* **15**(11): 1573-1580.
- Sahler J, Bernard JJ, Spinelli SL, Blumberg N, Phipps RP. 2011.** The Feverfew plant-derived compound, parthenolide enhances platelet production and attenuates platelet activation through NF- κ B inhibition. *Thrombosis Research* **127**(5): 426-434.
- Schuler MA, Werck-Reichhart D. 2003.** Functional genomics of P450s. *Annual Review of Plant Biology* **54**: 629-667.
- Seigler DS. 1998.** *Plant secondary metabolism*: Kluwer Academic Pub.
- Sweeney CJ, Mehrotra S, Sadaria MR, Kumar S, Shortle NH, Roman Y, Sheridan C, Campbell RA, Murry DJ, Badve S, Nakshatri H. 2005.** The sesquiterpene lactone parthenolide in combination with docetaxel reduces metastasis and improves survival in a xenograft model of breast cancer. *Molecular Cancer Therapeutics* **4**(6): 1004-1012.
- Takahashi S, Yeo Y-S, Zhao Y, O'Maille PE, Greenhagen BT, Noel JP, Coates RM, Chappell J. 2007.** Functional characterization of premnaspirodiene oxygenase, a cytochrome P450 catalyzing regio- and stereo-specific hydroxylations of diverse sesquiterpene substrates. *Journal of Biological Chemistry* **282**(43): 31744-31754.
- Takahashi S, Zhao Y, O'Maille PE, Greenhagen BT, Noel JP, Coates RM, Chappell J. 2005.** Kinetic and molecular analysis of 5-epiaristolochene 1, 3-dihydroxylase, a cytochrome P450 enzyme catalyzing successive hydroxylations of sesquiterpenes. *Journal of Biological Chemistry* **280**(5): 3686-3696.
- Teoh KH, Polichuk DR, Reed DW, Nowak G, Covello PS. 2006.** *Artemisia annua* L. (Asteraceae) trichome-specific cDNAs reveal CYP71AV1, a cytochrome P450 with a key role in the biosynthesis of the antimalarial sesquiterpene lactone artemisinin. *FEBS Letters* **580**(5): 1411-1416.
- Theis N, Lerdau M. 2003.** The evolution of function in plant secondary metabolites. *International Journal of Plant Sciences* **164**(S3): S93-S102.
- van Herpen TWJM, Cankar K, Nogueira M, Bosch D, Bouwmeester HJ, Beekwilder J. 2010.** *Nicotiana benthamiana* as a production platform for Artemisinin precursors. *PLoS ONE* **5**(12): e14222.
- Vranová E, Coman D, Gruijsem W. 2013.** Network analysis of the MVA and MEP pathways for isoprenoid synthesis. *Annual Review of Plant Biology* **64**: 665-700.
- Weitzel C, Simonsen HT. 2013.** Cytochrome P450-enzymes involved in the biosynthesis of mono- and sesquiterpenes. *Phytochemistry Reviews*: 1-18.
- Zhang S, Ong C-N, Shen H-M. 2004.** Involvement of proapoptotic Bcl-2 family members in parthenolide-induced mitochondrial dysfunction and apoptosis. *Cancer Letters* **211**(2): 175-188.
- Zhang S, Won YK, Ong CN, Shen HM. 2005.** Anti-cancer potential of sesquiterpene lactones: bioactivity and molecular mechanisms. *Current Medicinal Chemical - Anti-cancer Agents* **5**(3): 239-249.
- Zhang Y, Teoh KH, Reed DW, Maes L, Goossens A, Olson DJH, Ross ARS, Covello PS. 2008.** The molecular cloning of artemisinic aldehyde Δ 11(13) reductase and its role in glandular trichome-dependent biosynthesis of artemisinin in *Artemisia annua*. *Journal of Biological Chemistry* **283**(31): 21501-21508.
- Zunino SJ, Ducore JM, Storms DH. 2007.** Parthenolide induces significant apoptosis and production of reactive oxygen species in high-risk pre-B leukemia cells. *Cancer Letters* **254**(1): 119-127.

Chapter 2

Biosynthesis and localization of parthenolide in glandular trichomes of feverfew (*Tanacetum parthenium* L. Schulz Bip.)

Mohammad Majdi¹, Qing Liu¹, Ghasem Karimzadeh, Mohammad Ali Malboobi, Jules Beekwilder, Katarina Canka, Ric de Vos, Sladjana Todorović, Ana Simonović and Harro Bouwmeesterauthors

¹ These two authors contributed equally to this work.

Published as Majdi, M, et al., (2011) *Phytochemistry* 72, 1739-1750.

Abstract

Feverfew (*Tanacetum parthenium*) is a perennial medicinal herb and is a rich source of sesquiterpene lactones. Parthenolide is the main sesquiterpene lactone in feverfew and has attracted attention because of its medicinal potential for treatment of migraine and cancer. In the present work the parthenolide content in different tissues and developmental stages of feverfew was analyzed to study the timing and localization of parthenolide biosynthesis. The strongest accumulating tissue was subsequently used to isolate sesquiterpene synthases with the goal to isolate the gene encoding the first dedicated step in parthenolide biosynthesis. This led to the isolation and characterization of a germacrene A synthase (*TpGAS*) and an (E)- β -caryophyllene synthase (*TpCarS*). Transcript level patterns of both sesquiterpene synthases were analyzed in different tissues and glandular trichomes. Although *TpGAS* was expressed in all aerial tissues, it was expressed higher in tissues with higher concentrations of parthenolide and particularly in the biosynthetically active stages of flower development. The high expression of *TpGAS* in glandular trichomes which also contain the highest concentration of parthenolide, suggests that glandular trichomes are the organ where parthenolide biosynthesis and accumulation occur.

Introduction

Terpenoids are the largest class of plant secondary metabolites with over 20,000 compounds known (Davis & Croteau, 2000). Sesquiterpene lactones are a major class of terpenoids that arise from the assembly of a 15-carbon skeleton into bisabolane, cuparane, cadinane, humulane and germacrane backbones and the addition of functional groups to these backbones (Chappell et al., 2010; Chappell, 2010). They are particularly abundant in the Asteracea family and are biologically significant because of key roles in plant environment interaction, for example as chemical defense compounds against pathogens and insects (Cheng et al., 2007; Hristozov et al., 2007; Chappell et al., 2010; Chappell, 2010). Sesquiterpenes have various biological activities and uses for humans, including antimicrobial, anticancer and anti-inflammatory properties (Min Li-Weber, 2002); (Elisa Saranitzky, 2009; Trusheva et al., 2010). Feverfew ($2n=2x=18$) is a perennial herb belonging to the Asteracea that has been used traditionally as a fever-reducer (Palevitch et al., 1997). The most important constituent (up to 85% of total sesquiterpenes) among the 30 sesquiterpene lactones identified in feverfew is parthenolide (Williams et al., 1995; Brown et al., 1997; Cretnik et al., 2005). Parthenolide (Fig.1) is a germacranolide lactone which recently raised quite a lot of attention because clinical trials showed medicinal value and pharmacological activities especially as a migraine prophylaxis agent and also for treatment of cancer (Knight, 1995; Palevitch et al., 1997; Vogler et al., 1998; Min Li-Weber, 2002; Pfaffenrath et al., 2002; Lesiak K, 2010).

Considering these promising applications, the need for parthenolide may be increasing in the near future. In order to increase the availability of parthenolide several approaches can be envisaged, such as heterologous engineering into other plant species or microbial platforms. In order to be able to do so knowledge about the biosynthetic pathway of parthenolide is mandatory.

Sesquiterpene lactones are mostly derived from the mevalonic acid (MVA) pathway (van Klink et al., 2003). They are classified on the basis of their carbon skeletons as germacranolides, guaianolides, pseudoguanolides and eudesmanolides (de Kraker et al., 1998). Parthenolide has a germacranolide backbone structure and costunolide has been proposed to be the common precursor of all germacranolide-derived sesquiterpene lactones (de Kraker et al., 2002) (Fig. 1). The first committed step in the biosynthesis of costunolide is the cyclization of farnesyl diphosphate (FDP) to germacrene A by a germacrene A synthase (de Kraker et al., 1998; Bouwmeester et al., 2002). Recently two research groups showed that the cytochrome P450, germacrene A oxidase, is responsible for the conversion of germacrene A to germacrenoic acid (germacra-1(10),4,11(13)-trien-12oic acid) (Fig. 1) (Cankar et al.; Nguyen et al., 2010).

To verify this pathway in feverfew and to identify the genes missing in the parthenolide pathway, it is crucial to study the spatial and temporal regulation of the pathway. The biosynthesis and accumulation of secondary metabolites in plants is closely associated with the transcription level of the relevant genes in organs, tissues, as well as in different developmental stages. Biosynthesis and accumulation of metabolites may occur at the same place

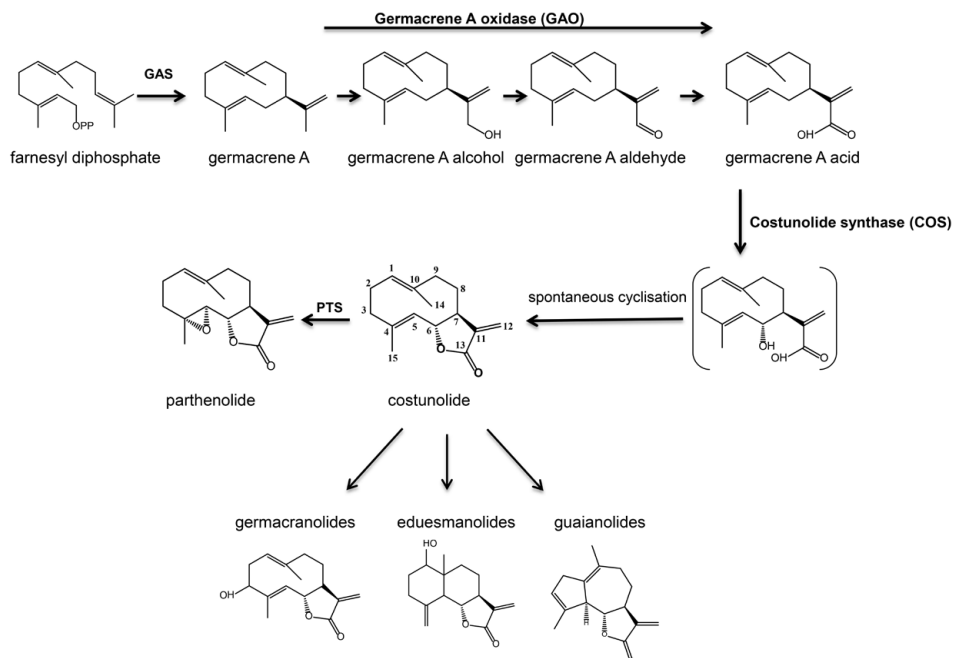


Fig. 1. Presumed biosynthetic pathway of parthenolide. GAS, germacrene A synthase; PTS, parthenolide synthase.

(cells, tissues) or be spatially separated. For example, biosynthesis as well as accumulation of artemisinin have been observed in the glandular trichomes of *Artemisia annua* (Bertea et al., 2006; Teoh et al., 2006). In the Asteracea, several different specialized accumulation/biosynthesis structures for secondary metabolites have been reported e.g cavities in *Solidago canadensis* (Curtis & Lersten, 1990; Cury & Appezzato-da-Gloria, 2009), ducts in *Ambrosia trifida* (Curtis, 1988), laticifers in *Lactuca sativa* (Esau, 1965; Sessa et al., 2000) and glandular trichomes in *Artemisia annua* (Kelsey, 1980).

Glandular trichomes are specialized structures consisting of usually 6 to 10 cells, that produce secondary metabolites which are stored in a sub-cuticular cavity on top of the trichome, such that the phytotoxic secondary metabolites are stored away from primary metabolism (Wagner, 1991). Glandular trichomes have been used in several species of the Asteracea to elucidate the biosynthesis of terpenes, using the fact that they are the most active or even exclusive organ for biosynthesis e.g in *A. annua* (Bertea et al., 2006; Covello et al., 2007; Olsson et al., 2009; Lies Maes, 2010) and *Helianthus annuus* (Gopfert et al., 2009).

The objectives of the present investigation were to determine the developmental and spatial regulation of parthenolide biosynthesis in feverfew. This detailed analysis should provide the crucial knowledge necessary for further characterization of the parthenolide biosynthetic pathway, for example to identify the right tissue and developmental stage to create an EST library that can be used for gene discovery. In addition, we set out to identify and characterize the sesquiterpene synthase that catalyses the first dedicated step in parthenolide biosynthesis.

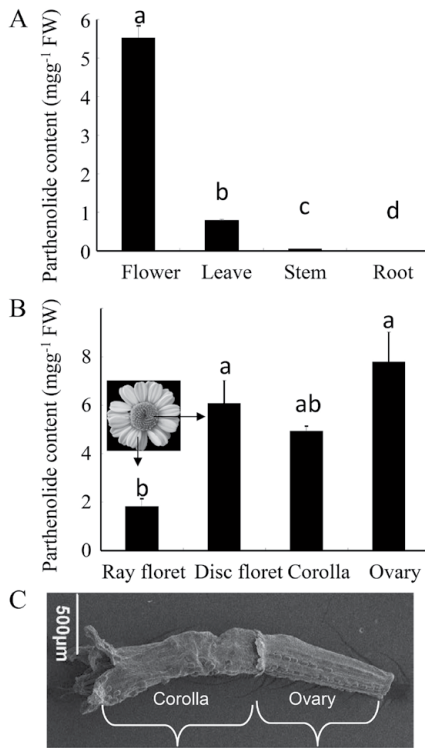


Fig. 2. Parthenolide concentration in A) different tissues of *Tanacetum parthenium* B) within different flower parts of *T. parthenium*. Bars represent means ($n = 3$) \pm S.E. Bars with different letters are significantly ($P < 0.01$) different according to Duncan's test. C) Trichome distribution over disc florets parts, ovary (right) and corolla (left). Bar= 500 μ m.

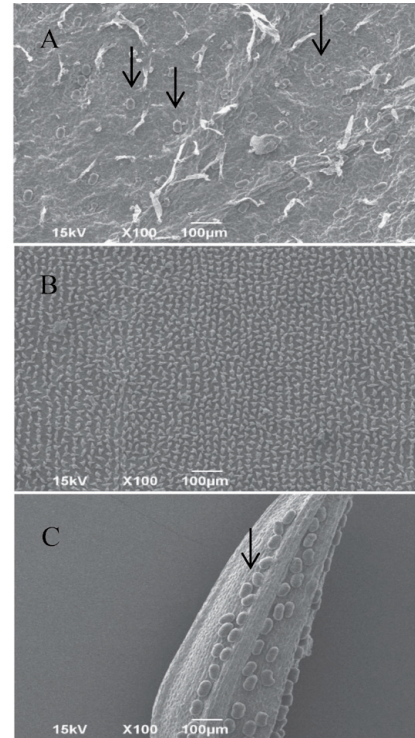


Fig. 3. Scanning electron microscope pictures of trichomes on A) leaves B) ray florets and C) disc florets of *Tanacetum parthenium*. Arrows indicate glandular trichomes. Bar= 100 μ m.

Results

Parthenolide concentrations in feverfew

To see which organs of feverfew contain parthenolide, several different tissues including flower, leaf, stem and root were analyzed by LC-QTOF-MS. There were significant differences between different tissues in term of parthenolide concentration ($P < 0.01$) (Fig. 2A). The highest amount of parthenolide was observed in flowers, followed by leaves and stems. No parthenolide was detected in feverfew roots.

Considering the high parthenolide concentration in flowers compared to the other tissues we further investigated which part(s) of the flower contains the highest amount of parthenolide. The parthenolide concentration differed between the two main parts of the flower, with the highest amount of parthenolide being observed in the disc florets when compared with the ray florets ($P < 0.01$) (Fig. 2B). Scanning electron microscopy (SEM) showed that

the ray florets do not contain trichomes (Fig. 3B) in contrast to the disc florets (Fig. 3C). Disc florets consist of two parts, the upper (corolla) and lower part (ovary), of which the latter contained more parthenolide (Fig. 2B). SEM showed that the trichome density on disc florets is higher on the ovary than the corolla (Fig. 2C). When comparing the trichome density in several other plant organs it showed to be highest on the disc florets (Fig. 3C), followed by leaves (Fig. 3A) while stems contain an even lower density of trichomes (data not shown). To elucidate whether parthenolide is present in the glandular trichomes, chloroform dipping was used, which extracts the glandular trichomes but not - or to a much lesser extent - the remainder of the plant tissue (Duke et al., 1994). Indeed, scanning electron microscopy showed that a chloroform dip of 30 sec extracts most of the trichomes on a disc floret without inducing visible damage to the epidermal cells (Fig. 4). Chloroform-dipped disc florets contained significantly ($P < 0.01$) less parthenolide than non-dipped disc florets. More than 80% of the parthenolide was extracted from disc florets by the 30-sec chloroform dip.

Isolation of sesquiterpene synthases

The degenerate primer approach followed by 3'- and 5'-rapid amplification of cDNA ends (RACE), resulted in the isolation of two full-length feverfew sesquiterpene synthase cDNAs, *TpGAS* and *TpCarS*. The *TpGAS* ORF showed a length of 1,677 bp encoding 559 amino acids. A Blast search in GenBank revealed that *TpGAS* has high homology with other GASs of the Asteraceae, such as germacrene A synthase short form from *C. intybus* (highest identity, 87%), germacrene A synthase LTC1 from *Lactuca sativa*, germacrene A synthase 1 from *H. annuus*, germacrene A synthase from *Crepidiastrum sonchifolium*, germacrene A synthase from *A. annua* and germacrene A synthase long form from *C. intybus* (lowest identity, 73%). The molecular weight of the *TpGAS* protein was calculated to be 64.5 kDa with an isoelectric point (pI) of 5.03. The deduced *TpGAS* protein alignment with other germacreneA synthases is shown in Fig. 5A. Phylogenetic analysis using ClustalW (<http://www.ebi.ac.uk/Tools/clustalw2/index.html>) showed that *TpGAS* and *A. annua* GAS are in the same cluster and have the shortest evolutionary distance from each other. In spite of the higher similarity between *TpGAS* and short form GAS from chicory they have been categorized in different clusters (Fig. 5B). The *TpCarS* ORF has a length of 1,647 bp encoding for 549 amino acids. Blast search in GenBank showed high identity (93%) with (E)- β -caryophyllene synthase from *A. annua* and 61% with GAS from *Solidago canadensis*. The molecular weight of the predicted *TpCarS* protein was calculated to be 63.5 kDa with isoelectric point (pI) of 5.48. A protein sequence alignment and a phylogenetic tree of *TpCarS* with a number of other sesquiterpene synthases

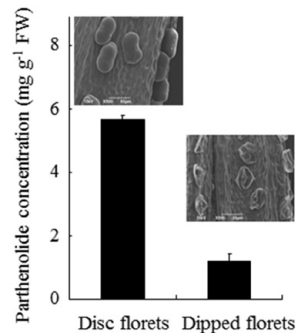


Fig. 4. Parthenolide concentration in disc florets and chloroform dipped disc florets and corresponding Scanning Electron Microscope pictures. Bars represent means ($n = 3$) \pm S.E.

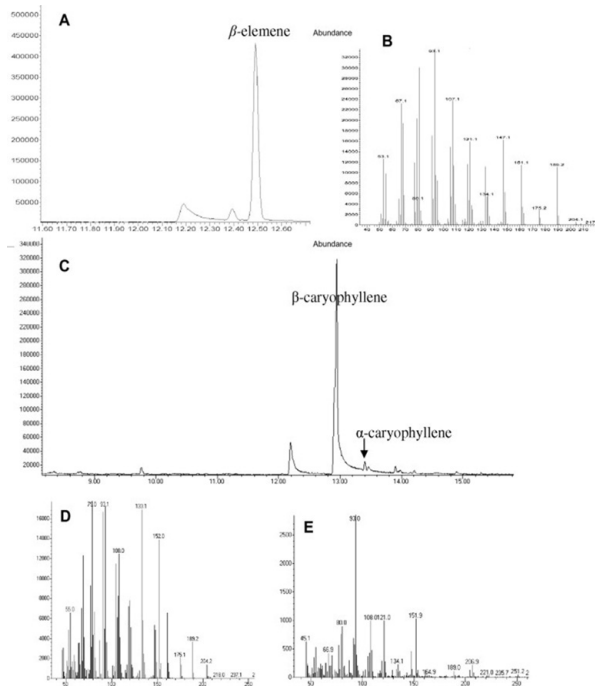


Fig. 6. GC-MS analysis of the products of recombinantly expressed feverfew sesquiterpene synthases using FPP as substrate. (A) Product of *TpGAS* *in vitro* assay is β -elemene (a cope-rearrangement product of germacrene A). (B) Mass spectrum of β -elemene. (C) Products of *TpCarS* *in vitro* assay are β -caryophyllene and α -caryophyllene (α -humulene); (D) Mass spectrum of β -caryophyllene. (E) Mass spectrum of α -caryophyllene (α -humulene).

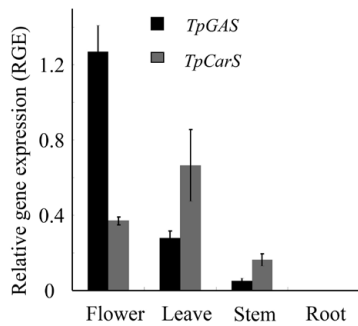


Fig. 7. Relative gene expression (RGE) of *TpGAS* and *TpCarS* in different tissues of *Tanacetum parthenum*. Real-time qPCR was based on the Ct values (see materials and methods). The Ct value for each sample was normalized using the house-keeping gene *TpActin*.

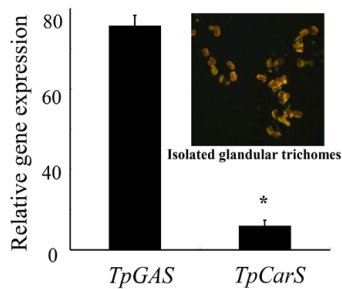


Fig. 8. Relative gene expression (RGE) of *TpGAS* and *TpCarS* in purified glandular trichomes (see insert). Bars represent means ($n = 3$) \pm S.E. * indicates significant ($P < 0.01$) difference according to Student's t-test. Real-time qPCR was based on the Ct values (see materials and methods). The Ct value for each sample was normalized using the housekeeping gene *TpActin*.

are shown in Fig. S2 and S3.

Functional characterization of *TpGAS* and *TpCarS*

TpGAS and *TpCarS* were functionally characterized by cloning of the ORF in pACYCDuetTM-1 vector and heterologous expression in *E. coli*. An enzyme assay with the recombinant *TpGAS* in the presence of FDP, followed by GC-MS analysis showed a single peak which was

identified as β -elemene by comparing its spectrum and retention index with library data (Fig. 6 A,B). β -Elemene is the Cope rearrangement product of germacrene A that is formed upon injection into the hot injection port of the GC-MS (de Kraker et al., 1998). A comparable enzyme assay with *TpCarS* generated mostly β -caryophyllene and a trace of α -humulene (also called α -caryophyllene) (Fig. 6 C, D and E).

Expression of *TpGAS* and *TpCarS*

In order to assess the expression of *TpGAS* and *TpCarS* in different organs of feverfew, qRT-PCR experiments were carried out using cDNA templates from whole flowers, leaves, stems and roots as well as glandular trichomes. Comparison of relative gene expression (RGE) patterns for *TpGAS* and *TpCarS* revealed that the expression of *TpCarS* was higher in leaves than in flowers and stems whereas the expression of *TpGAS* in flowers was more than 4-fold higher than in leaves and 25-fold higher than in stems (Fig. 7). Both genes were not expressed in roots. The highest expression of *TpGAS* was observed in trichomes (RGE of more than 100), which is at least 10-fold higher than the RGE of *TpCarS* in trichomes (Fig. 8).

Analysis of variance showed significant differences in parthenolide concentration of ovaries of different developmental stages of flowers ($P < 0.001$) (Fig. 9A). Mean comparison with Duncan's test showed that the parthenolide concentration significantly increased with flower developmental stage, reaching a peak at stage 5 (2-fold higher than in stage 2) and subsequently declining gradually during stage 6 and 7 (Fig. 9A). The parthenolide concentration in stage 7 was still higher than in stage 2 (Fig. 9A). Analysis of variance showed that also for *TpGAS* expression significant differences existed in the RGE in ovaries of different developmental stages ($P < 0.001$) (Fig. 9B). RGE increased significantly with flower developmental stage, reaching a peak at stage 3 and 4 (about 2-fold increase compared with stage 2) then strongly decreasing in stage 5 (>4-fold lower than in stages 3 and 4). The lowest RGEs were observed for stage 6 and 7 ovaries. *TpCarS* displayed a stable, low expression pattern (RGE < 1) in all different developmental stages (Fig. 9B).

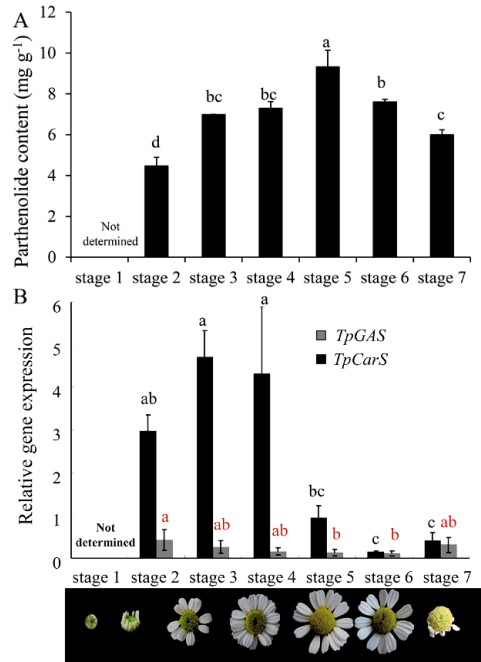


Fig. 9. (A) Parthenolide concentration and (B) relative gene expression of *TpGAS* and *TpCarS* in ovaries from different developmental stages of *Tanacetum parthenium* flowers. Bars represent means ($n = 3$) \pm S.E. Bars with different letters are significantly ($P < 0.05$) different according to Duncan's test.

Discussion

Parthenolide is mainly accumulating in glandular trichomes

Our work shows that the parthenolide present in feverfew is particularly concentrated in the flowers, which is in accordance with the results of others (Awang, 1991; Majdi et al., 2010). Within the flowers, the disc florets contain a higher concentration of parthenolide than the ray florets which coincide with a higher glandular trichome density on the disc florets. Within the disc florets the ovary contains a higher concentration of parthenolide than the corolla and also here this coincides with a higher glandular trichome density on the former (Fig. 2B-C). All this suggests that the glandular trichomes are likely the place where parthenolide accumulation occurs. The mild chloroform dipping extraction method, which extracted about 80% of parthenolide from the disc florets without visible damage to the epidermis, further proved the presence of parthenolide in the glandular trichomes (Fig. 4). The presence of sesquiterpene lactones has usually been associated with other structures such as cavities, ducts and laticifers (Esau, 1965; Kelsey, 1980; Curtis, 1988; Curtis & Lersten, 1990; Cury & Appezzato-da-Gloria, 2009). On the other hand, the presence of sesquiterpenes, including oxidized derivatives, in glandular trichomes has been reported in other plants as well such as *A. annua* (Bertea et al., 2006), *Solanum habrochaites* (Gianfagna TJ, 1992), *Mentha x piperita* (McCaskill & Croteau, 1995) and *Solanum lycopersicum* (Schillmiller et al., 2010).

TpGAS expression reveals glandular trichomes as the site of parthenolide biosynthesis

As discussed above, the parthenolide concentration is associated with the distribution of glandular trichomes in several different organs. The highest density of glandular trichomes occurred in flowers (ovaries) followed by leaves and stems and the same pattern was observed for the parthenolide concentration (Fig. 2 and 3) as well as the expression of *TpGAS* (Fig. 7). *TpGAS* is encoding the enzyme that highly likely catalyses the first step in parthenolide biosynthesis, germacrene A synthase (Fig. 1). The expression of *TpCarS* - another feverfew sesquiterpene synthase - showed a very different profile and was for example highest in leaves (Fig. 7). Also parthenolide concentration and *TpGAS* expression in trichomes - isolated from different developmental stages of ovaries - correlated, in contrast to *TpCarS* of which expression did not correlate with parthenolide concentration (Fig. 9). The association of parthenolide with glandular trichomes is further substantiated by the fact that parthenolide was not detected in roots which do not have glandular trichomes (Fig. 2 and 7). Also closely related plant species belonging to the Asteraceae such as *A. annua* make and store sesquiterpene lactones in the glandular trichomes (Bertea et al., 2006; Covello et al., 2007). Consistent with our results, the relationship between the density of glandular trichomes and the essential oil content has also been reported in other plant species (Maffei et al., 1989; McCaskill & Croteau, 1999; Bertea et al., 2006). In feverfew, *TpGAS* is only expressed in the aerial parts in which also parthenolide exists, while the expression of *GAS* in roots of other Asteraceae - that produce sesquiterpene lactones in their roots - has been reported e.g. *C. intybus* and *H. annuus* (Bouwmeester et al., 2002; Gopfert et al., 2009). In the latter case, not only has different

regulation of transcription of biosynthetic genes allowed for biosynthesis of sesquiterpene lactones in the roots but also storage of the sesquiterpene lactones was adapted to accommodate for the absence of trichomes on the roots (Gopfert et al., 2009).

The much higher expression of *TpGAS* in trichomes when compared with other tissues (Fig. 7) shows that *TpGAS* is a glandular trichome specific gene. In consistence with our work there have been many reports on different plant species which have demonstrated a strong correlation between terpene amount (or emission) and the level of the corresponding mRNA, indicating that terpenoid biosynthesis is mainly regulated at the transcript level (Nagegowda, 2010). Also gene expression analysis in different cell types of glandular trichomes of *A. annua* including apical, sub-apical and mesophyl cells showed that the expression of three enzymes specific to the artemisinin biosynthetic pathway are active only in the apical cells (Olsson et al., 2009). These apical cells are likely the ones in which artemisinin biosynthesis occurs, close to the subcuticular cavity where artemisinin and/or its precursors are stored. In contrast, FDP synthase which is not specific only for artemisinin biosynthesis was expressed in all the glandular trichomes cell types (Olsson et al., 2009). All this suggests that also for uncovering the regulation and site of parthenolide biosynthesis, analysis of *TpGAS* expression and its localisation is a reliable approach.

Developmental changes in *TpGAS* expression and parthenolide concentration

Analysis of parthenolide concentration and *TpGAS* expression in different developmental stages of flowers showed that parthenolide accumulation and *TpGAS* expression closely correlate. Although *TpCarS* gene expression was observed in the trichomes in several flower developmental stages, both the level of transcript and the pattern of transcript change do not show any relationship with parthenolide biosynthesis, excluding that *TpCarS* is involved in parthenolide biosynthesis. Parthenolide accumulation is developmentally regulated and displays three distinct phases (Fig. 9). The first phase (stage 1 to stage 4) can be considered as “parthenolide accumulation phase” in which there is a direct relationship between the increase in *TpGAS* expression and the increase in parthenolide concentration (Fig. 9). The second phase (stage 5) can be considered as “parthenolide saturation phase” in which the parthenolide concentration reaches its maximum while the expression of *TpGAS* is down-regulated compared with the previous phase. This may indicate a feed back regulatory mechanism or a developmental program controlling parthenolide accumulation by down-regulating the expression of the gene(s) in the biosynthetic pathway of parthenolide, in this case *TpGAS*. Also feedback inhibition of artemisinin biosynthesis by repression of *ADS* and *CYP71AV1* expression by artemisinic acid and artemisinin has recently been suggested (Arsenault et al., 2010). Considering the relationship between flower development and glandular trichome development (Werker, 2000; Gopfert et al., 2005), this phase may represent physiological maturity of the glandular trichomes which coincides with the end of cell expansion in floret development. The third phase (stage 6-7) can be considered as “parthenolide reduction phase”, in which a decrease in parthenolide concentration was observed, along with the strongly reduced expression of *TpGAS* (Fig. 9). The *TpGAS* expression pattern resembles that of the *H. annuus*

germacrene A synthase. In this species, up-regulation of the germacrene A synthase during the secretory stage and down-regulation during the post-active secretory phase has been reported confirming developmental stage-specific expression in glandular trichomes (Gopfert et al., 2009). The high expression of *TpGAS* during the parthenolide accumulation phase and continued expression of *TpGAS* during the parthenolide decrease phase show the necessity of active and continuous transcription of *TpGAS* (and likely other genes downstream of *TpGAS*) for parthenolide accumulation. This is consistent with the high positive correlation between the expression of *ADS* and *CYP71AV1* and the accumulation of the artemisinin precursor dihydroartemisinic acid in *A. annua* (Arsenault et al., 2010). Also in peppermint a high rate of monoterpene biosynthesis and high enzyme activities were observed during early leaf development (Gershenzon, 1994). The strong developmental changes in parthenolide concentration that we find (Fig. 9) are supported by the literature. For example, Omidbaigi et al. (2007) reported developmental changes in feverfew essential oil content and composition in flowers at various harvesting times. Developmental regulation appears to be an important factor in parthenolide biosynthesis and this is consistent with other reports on terpene biosynthesis (McConkey et al., 2000; Lommen et al., 2006; Kim et al., 2008; Arsenault et al., 2010). The decrease in parthenolide concentration during the reduction phase is more difficult to explain. Volatilization and leaching have been postulated as possible mechanisms that cause a loss of sesquiterpene lactones (Gershenzon, 1994). However, parthenolide is not volatile and leaching is not likely to occur in a greenhouse or climate room. Possibly, parthenolide decrease in the reduction phase is caused by a biodegradation mechanism or further conversion to another compound(s). Further conversion of parthenolide to epoxyparthenolide and hydroxyparthenolide in *Anvillea radiata* a member of the Asteracea has been reported (Hassany et al., 2004). Biodegradation or further conversion could also explain the diurnal changes in parthenolide content (decrease during the night) in feverfew leaves (Fonseca et al., 2005; Fonseca et al., 2006). The decrease in parthenolide concentration in phase 3 could also indicate trichome collapse, as has been reported for *A. annua* (Lommen et al., 2006; Arsenault et al., 2010). Lommen et al. (2006) have proposed that trichome collapse in *A. annua* is responsible for the decrease in artemisinin content during the later stages of leaf development.

Conclusion

Cloning of *TpGAS* and the study of its transcript patterns in different tissues and developmental stages of flowers in feverfew shows that the expression of *TpGAS* is closely associated with parthenolide biosynthesis. The high expression of *TpGAS* in glandular trichomes and the localization of parthenolide in the trichomes show that the trichomes are the specific site of parthenolide biosynthesis and accumulation. Hence, isolation of feverfew glandular trichomes will be a powerful tool to generate an EST library, which can be used for high throughput transcript sequencing and identification of additional genes involved in the biosynthetic pathway of parthenolide. This approach has been successful in other plant species and has led to the identification of genes involved in the biosynthesis of several secondary metabolites (Bertea et al., 2006; Covello et al., 2007; Nagel et al., 2008). Transcript profiling

in combination with metabolite profiling (untargeted large scale metabolomics) of glandular trichomes isolated from flowers in different developmental stages could also provide insight into the regulation of accumulation and loss of parthenolide in *Tanacetum parthenium*.

Materials and methods

Plant growth condition

Tanacetum parthenium L. plants were grown under controlled conditions in a climate room with a 16h day length supplied with a photosynthetic photon flux density of $320 \mu\text{mol m}^{-2} \text{s}^{-1}$ with day/night temperature of 24/18 °C. Samples for phytochemical and gene expression analysis were immediately frozen in liquid nitrogen and then stored at -80 °C until further use.

Seven developmental stages of feverfew flower development were defined based on a scale developed for *Chrysanthemum cinerariaefolium* (Head, 1966). Stage 1 (well developed closed buds), stage 2 (ray florets vertical), stage 3 (ray florets horizontal and first row of disc florets open), stage 4 (approximately three rows of disc florets open), stage 5 (all disc florets open, fully mature), stage 6 (early senescence; color of disc florets diminishing but ray florets still intact), stage 7 (late senescence; disc florets dried out) (Head, 1966). Ovaries were isolated from all these stages except stage 1.

Parthenolide measurement

Plant materials (flower, leaf, stem, root and ovary) were ground to a fine powder using a mortar and pestle in liquid nitrogen. Non-volatile compounds were analyzed using a protocol for untargeted metabolomics of plant tissues (De Vos et al., 2007).

Three biological replicates were used for each sample. In brief, 100 mg of sample for each replicate (leaves from one month old plants in the vegetative stage, whole stage 3 flowers, ovaries from different flower developmental stages, stems and roots) were ground in liquid nitrogen and extracted with 0.3 mL methanol:formic acid (1000:1, v/v). The extracts were briefly vortexed and then sonicated for 15 min. Subsequently, the extracts were centrifuged and filtered through a 0.2 μm inorganic membrane filter (RC4, Sartorius, Germany). LC-PDA-MS analysis was performed using a Waters Alliance 2795 HPLC connected to a Waters 2996 PDA detector and a QTOF Ultima V4.00.00 mass spectrometer (Waters, MS technologies, UK) operating in positive ionization mode. The column used was an analytical column (2.0 \times 150 mm; Phenomenex, USA) with a C18 pre-column (2.0 \times 4 mm; Phenomenex, USA). Degassed eluent A (ultra pure water:formic acid; 1000:1, v/v) and eluent B (acetonitril:formic acid; 1000:1, v/v) were pumped at 0.19 mL min⁻¹ into the HPLC system. The gradient started at 5% B and increased linearly to 35% B in 45 min. Then the column was washed and equilibrated for 15 min before the next injection.

An authentic standard of parthenolide (Sigma-Aldrich, USA) was used to make a calibration curve by injecting different concentrations of parthenolide for quantification.

Chloroform dipping

To 100 mg of ovaries from feverfew in a 2 mL Eppendorf vial, 1 mL of chloroform was added followed by vortexing for 30 seconds and short centrifugation. The chloroform phase was removed and the chloroform evaporated in a fume hood for 3 minutes. Then the parthenolide content of dipped and non-dipped ovaries was measured by LC-MS as described above.

Isolation of glandular trichomes and RNA extraction

Ovaries (about 300 flowers) were separated from the rest of the flower for trichome isolation. About 3 gram of ovaries were placed in a 50 mL pre-cooled Greiner tube and 10 mL liquid nitrogen was added. The tube was covered using a 20 µm mesh followed by vortexing for 1 min and addition of another 10 mL liquid nitrogen. The vortexing was repeated 6 to 10 times. The isolated trichomes were separated from the other cells and debris by passing through a 120 µm mesh and collection on a 20 µm mesh. RNA was isolated from the glandular trichomes using the Spectrum™ Plant Total RNA isolation kit (Sigma, USA).

RNA extraction and cDNA synthesis for sesquiterpene synthases

Flowers of *Tanacetum parthenium* were used for RNA extraction. Tripure isolation reagent (Roche, Mannheim, Germany) was used for extraction of total RNA according to the manufacturer's instructions with minor modifications. Isolated RNA was subsequently treated with DNase I (Invitrogen, USA) and then purified through a silica column using the RNeasy RNA clean up kit (Qiagen #74104, USA). The quantity and quality of RNA was determined using a NanoDrop (NanoDrop Technologies, USA) and agarose gel electrophoresis. The reverse transcription reaction was carried out with the Taqman Reverse Transcription Reagent kit (Applied Biosystems, USA) using 1µg of total RNA and 50µM oligo dT according to the manufacturer's instructions.

To clone sesquiterpene synthases, a homology-based PCR cloning strategy was used. Sequence alignments of published Asteracea sesquiterpene synthase cDNAs in public databases were used to design degenerate oligonucleotide primers. Primer pairs were designed corresponding to the conserved regions, avoiding degeneracy at the 3' end: forward primer 5'-TATWCNGTNCAYCGTCTYGG 3' and reverse primer 5'- AYYKCATATCRTTCCACCAC 3'. The temperature program for PCR was initial denaturation at 94 °C for 5 min, followed by 30 cycles of 94 °C for 30 s, 50 °C for 30 s, 72 °C for 1 min and the final elongation at 72 °C for 5 min.

A second set of degenerate primers (set 2 degenerate primers) consisted of: forward primer 5'-GAY GAR AAY GGI AAR TTY AAR GA-3' and reverse primer 5'- CCR TAI GCR TCR AAI GTR TCR TC-3' (Wallaart et al., 2001) . The temperature program for PCR was initial denaturation at 94 °C for 3 min, followed by 35 cycles of 94 °C for 30 s, 48 °C for 1 min, 72 °C for 1 min and the final elongation at 72 °C for 5 min. The resulting purified fragments were cloned into pGEM-T Easy Vector (Promega, USA) and sequenced.

cDNA extension using 5' and 3'-RACE

5'-RACE and 3'-RACE were performed using the SMART-RACE cDNA amplification kit (Clontech, USA) according to the manufacturer's protocol. The first strand cDNA for 5' and

3' RACE were synthesized from 1 µg of total RNA extracted from ovaries according to the protocol (Clontech, USA). According to the partial sequence of the TpGAS fragment (550 bp) amplified using degenerate primers set 1, high annealing temperature (70 °C) primers were designed for both 5' and 3' RACE. Nested primers were designed according to the protocol suggestions. The Gsp1-GAS (Gene specific primer 5') and NGsp1-GAS (Nested gene specific primer 5') for 5'-RACE were 5' GCATCCCTTGATGGAATGGTCTCCTT -3' and 5' CCCAACATACCCCTCACATCACTCG -3', respectively. The Gsp2-GAS (Gene specific primer 3') and NGsp2-GAS (Nested gene specific primer 3') for 3'-RACE were 5'-GTGATGTGAGGGGTATGTTGGGCTTA-3' and 5' TGCACAGTTGAGAATAAGAGG -3', respectively.

Two additional sesquiterpene synthase like sequences were generated using the second set of degenerate primers. For one of them the 5' and 3' RACE did not produce the expected cDNA fragments, while the other did. The Gsp1-CarS (Gene specific primer 5') and NGsp1-CarS (Nested gene specific primer 5') for 5'-RACE were 5'CTTCGCCTTGCACCCCAAGTATGT 3' and 5' CAAGCAGGCCTTCTACATCGTTGGTG 3', respectively. The Gsp2-CarS (Gene specific primer 3') and NGsp2-CarS (Nested gene specific primer 3') for 3'-RACE were 5'- GGCCTGCTTGAGCTGTATGAGGCAAC -3' and 5' TTCGCTGGCCACTGTTCTTGACGATA -3', respectively. 5'-RACE and 3'-RACE products were cloned into the pGEM-T easy vector (Promega) and sequenced. Assembly of the sequences from the 3' RACE and 5' RACE products using SeqMan software yielded the full-length cDNA sequences of TpGAS and TpCarS.

Heterologous expression of *TpGAS* and *TpCarS* in *Escherichia coli*

According to the 5' and 3' ends new primers were designed introducing BamHI and NotI restriction sites to clone the fragment into pACYC-DUET-1 (Novagen). A full length of TpGAS was amplified using 5' Race cDNA as a template, using primers forward 5'-ACTACGGATCGGCAGCGGTTCAAGCTACTAC -3' and reverse 5'-ACCACGCGGCCGCTTACACGGGTAGAGAATCCACAA-3' (restriction sites for BamHI and NotI underlined). cDNA amplification for the construction of expression plasmids was performed using the Phusion DNA polymerase. The full length of TpCarS was also cloned into pACYC-DUET-1 (Novagen) using primers forward 5' ACTACGGATCCGTCTGCTAAAGAAGAGAAAGTA-3' and reverse 5' ACCACGCGGCCGCTTATATAGGTATAGGATGAACGAG-3'. For functional characterization the two sesquiterpene synthases ORFs (cloned into the pACYC-DUET-1 (Novagen) expression vector with an aminoterminal histidine tag) were expressed in *Escherichia coli* BL-21 under an isopropylthio-β-galactoside and arabinose inducible promoter. For the functional assay, 1mL of transformed bacteria was cultured overnight at 250 rpm at 37 °C in LB supplemented with chloramphenicol. Subsequently, 500 µL of the bacteria were added to 50 ml 2xYT supplemented with chloramphenicol for 1.5 h on shaker incubator at 250 rpm and 37 °C. Then 50 µL 20% L-arabinose was added to induce the bacteria and the culture was incubated overnight on a shaker at 18 °C at 250 rpm. The bacteria were centrifuged for 10 min at 2500 rpm. The resulting pellet was resuspend in 1 mL buffer A (50 mM Tris, pH 8; 300 mM

NaCl, 1.4 mM β -mercaptoethanol) followed by sonication on ice. The sample was centrifuged for 10 min at 13,000xg at 4 °C and the supernatant transferred to a Qiagen Nickel column which was then centrifuged for 2 min at 3000 rpm. The column was washed two times with 600 μ L buffer A and then eluted with 200 μ L buffer A containing 175 mM imidazole. 100 μ L of this purified enzyme was diluted into 800 μ L assay buffer (15 mM MOPSO, pH 7.5; 12.5% (v/v) glycerol, 1 mM ascorbic acid, 0.001% (v/v) Tween-20, 1 mM MgCl₂, 2 mM DTT). To the assay a final concentration of 50 μ M farnesyl diphosphate was added after which the assay was overlaid with 1mL of pentane and incubated at 30 °C with mild agitation for 2h. Subsequently, the pentane phase was collected and the assay extracted with 1 mL ethylacetate. The ethylacetate and pentane phases were combined, centrifuged at 1200xg and then dried using anhydrous Na₂SO₄ packed in a small glass column and used for GC-MS analysis.

GC-MS analysis

Volatiles produced in the enzyme assays were analyzed by an Agilent Technologies 7890A GC, equipped with a 5975C inert MSD with Triple Axis Detector using helium as carrier gas at a flow rate of 1ml.min⁻¹. The injector was used in splitless mode with the inlet temperature set to 250 °C. The initial temperature of 45 °C was gradually increased after 1 min to 300 °C by a ramp of 10°C min⁻¹ held for 5 min at 300 °C. Peaks were identified by comparison of mass spectra to the Wiley mass spectra library. Kovats Indices (KI) were calculated for each peak according to the retention time relative to alkane standards (Sekiwa-Iijima, 2001).

Gene expression analysis

First-strand cDNA was synthesized using the iScript cDNA Synthesis kit (BioRad) according to the manufacturer's instructions. Gene expression analysis was done by real-time quantitative PCR (qPCR) with the iCycler iQ5 system (BioRad) (Spinsanti G, 2006) using the iQ™ SYBR® Green Supermix master mix (Biorad) in three independent biological and two technical replicates. Actin was used as a housekeeping gene. The Δ Ct was calculated as follows: Δ Ct = Ct(TpGAS) – Ct(TpActin) and the RGE as: RGE= POWER(2; - δ Ct) (Livak & Schmittgen, 2001). A two step program was used as follows: 3 min at 95 °C; 40 cycles of 10 s at 95 °C, 30 s at 55 °C followed by melting curve analysis. The following primer pairs were used: forward actin 5'-CCTCTTAATCCTAAGGCTAATC-3' : reverse actin 5'-CCAGGAATCCAGCA-CAATACC-3' ; forward TpGAS 5'-TTCTCCTCTTATTCTCAACTGTGG-3; reverse TpGAS 5'-TGCTATCTCGGGTACTTCAAGG-3'; forward TpCarS 5'-GCATCCAGTGTGAAA-GTTAC-3'; reverse TpCarS 5'-GGTCATCAGAGGCATCGG -3'.

Data analysis

Sequence comparison was performed by Blast Search in GenBank (<http://www.ncbi.nih.gov>). Phylogenetic tree analysis and sesquiterpene alignment analysis were performed using ClustalW (<http://www.ebi.ac.uk/Tools/clustalw2/index.html>) and Bio-edit software, respectively.

A completely randomized design with 3 replications was used for the comparison of the parthenolide concentration and RGE in different tissues, within flower parts and in different developmental stages of the flower. Mean comparison was conducted using Duncan's test.

Student's t-test was conducted to compare parthenolide concentration in disc florets and chloroform dipped disc florets and for the comparison of the RGE for *TpGAS* and *TpCarS* in glandular trichomes. All the data were statistically analysed using SPSS statistical software.

Acknowledgements

MM acknowledges the Ministry of Sciences, Research and Technology of Iran for awarding a fellowship. LQ, RdV, ST, AS and HB acknowledge funding by the European Commission (EU-project TerpMed, 227448). JB and KC were funded by IBOS-ACTS 053.63.305. We acknowledge Francel Verstappen, Benyamin Houshyani, Aldana Ramirez, Miriam Goedbloed, Liping Gao, and Jos Molthoff for their helpful suggestions.

References

- Arsenault PR, Vail D, Wobbe KK, Erickson K, Weathers PJ. 2010. Reproductive development modulates gene expression and metabolite levels with possible feedback inhibition of artemisinin in *Artemisia annua*. *Plant Physiology* 154(2): 958-968.
- Awang DVCD, B. A.; Kindack, D. G.; Crompton, C. W.; Heptinstall, S. . 1991. Parthenolide content of feverfew (*Tanacetum parthenium*) assessed by HPLC and ¹H-NMR spectroscopy. *Journal of Natural Products* 54: 1516-1521.
- Berteaux CM, Voster A, Verstappen FWA, Maffei M, Beekwilder J, Bouwmeester HJ. 2006. Isoprenoid biosynthesis in *Artemisia annua*: Cloning and heterologous expression of a germacrene A synthase from a glandular trichome cDNA library. *Archives of Biochemistry and Biophysics* 448(1-2): 3-12.
- Bouwmeester HJ, Kodde J, Verstappen FWA, Altug IG, de Kraker JW, Wallaart TE. 2002. Isolation and characterization of two germacrene A synthase cDNA clones from chicory. *Plant Physiology* 129(1): 134-144.
- Brown AMG, Edwards CM, Davey MR, Power JB, Lowe KC. 1997. Effects of extracts of *Tanacetum* species on human polymorphonuclear leucocyte activity *in vitro*. *Phytotherapy Research* 11(7): 479-484.
- Cankar K, Houwelingen Av, Bosch D, Sonke T, Bouwmeester H, Beekwilder J. 2011. A chicory cytochrome P450 mono-oxygenase CYP71AV8 for the oxidation of (+)-valencene. *FEBS Letters* 585(1): 178-182.
- Chappell J, Coates RM, Lew M, Hung-Wen L. 2010. Sesquiterpenes. *Comprehensive natural products II*. Oxford: Elsevier, 609-641.
- Cheng AX, Lou YG, Mao YB, Lu S, Wang LJ, Chen XY. 2007. Plant terpenoids: Biosynthesis and ecological functions. *Journal of Integrative Plant Biology* 49(2): 179-186.
- Covello PS, Teoh KH, Polichuk DR, Reed DW, Nowak G. 2007. Functional genomics and the biosynthesis of artemisinin. *Phytochemistry* 68(14): 1864-1871.
- Cretnik L, Skerget M, Knez Z. 2005. Separation of parthenolide from feverfew: performance of conventional and high-pressure extraction techniques. *Separation and Purification Technology* 41(1): 13-20.
- Curtis JD. 1988. Secretory reservoirs (ducts) of two kinds in giant ragweed, *Ambrosia trifida* (Asteraceae). *American Journal of Botany* 75: 1313-1323.
- Curtis JD, Lersten NR. 1990. Oil-reservoirs in stem, rhizome, and root of *Solidago canadensis* (Asteraceae, tribe Astereae). *Nordic Journal of Botany* 10(4): 443-449.
- Cury G, Appezzato-da-Gloria B. 2009. Internal secretory spaces in thickened underground systems of Asteraceae species. *Australian Journal of Botany* 57(3): 229-239.
- Davis EM, Croteau R. 2000. Cyclization enzymes in the biosynthesis of monoterpenes, sesquiterpenes, and diterpenes. *Biosynthesis: Aromatic Polyketides, Isoprenoids, Alkaloids* 209: 53-95.
- de Kraker JW, Franssen MCR, de Groot A, Konig WA, Bouwmeester HJ. 1998. (+)-Germacrene A biosynthesis - The committed step in the biosynthesis of bitter sesquiterpene lactones in chicory. *Plant Physiology* 117(4): 1381-1392.
- de Kraker JW, Franssen MCR, Joerink M, de Groot A, Bouwmeester HJ. 2002. Biosynthesis of costunolide, dihydrocostunolide, and leucodin. Demonstration of cytochrome P450-catalyzed formation of the lactone ring present in sesquiterpene lactones of chicory. *Plant Physiology* 129(1): 257-268.
- De Vos RCH, Moco S, Lommen A, Keurentjes JJB, Bino RJ, Hall RD. 2007. Untargeted large-scale plant metabolomics using liquid chromatography coupled to mass spectrometry. *Nature Protocols* 2(4): 778-791.

- Duke MV, Paul RN, Elsohly HN, Sturtz G, Duke SO. 1994. Localization of artemisinin and artemisitene in foliar tissues of glanded and glandless biotypes of *Artemisia annua* L. *International Journal of Plant Sciences* 155(3): 365-372.
- Elisa Saranitzky CMW, Erica L. Baker, William L. Baker, Craig I. Coleman. 2009. Feverfew for migraine prophylaxis: A systematic review. *Journal of Dietary Supplements* 6: 91-103.
- Esau K. 1965. *Plant Anatomy*. New York: John Wiley & Sons, .
- Fonseca JM, Rushing JW, Rajapakse NC, Thomas RL, Riley MB. 2005. Parthenolide and abscisic acid synthesis in feverfew are associated but environmental factors affect them dissimilarly. *Journal of Plant Physiology* 162(5): 485-494.
- Fonseca JM, Rushing JW, Rajapakse NC, Thomas RL, Riley MB. 2006. Potential implications of medicinal plant production in controlled environments: The case of feverfew (*Tanacetum parthenium*). *Hortscience* 41(3): 531-535.
- Gershenzon J. 1994. Metabolic costs of terpenoid accumulation in higher-plants. *Journal of Chemical Ecology* 20(6): 1281-1328.
- Gianfagna TJ CC, and Sacalis JN 1992. Temperature and photoperiod influence trichome density and sesquiterpene content of *Lycopersicon hirsutum*. *Plant Physiology* 100: 1403-1405.
- Gopfert JC, Heil N, Conrad J, Spring O. 2005. Cytological development and sesquiterpene lactone secretion in capitate glandular trichomes of sunflower. *Plant Biology* 7(2): 148-155.
- Gopfert JC, MacNevin G, Ro DK, Spring O. 2009. Identification, functional characterization and developmental regulation of sesquiterpene synthases from sunflower capitate glandular trichomes. *BMC Plant Biology* 9(86): 1-18.
- Head SW. 1966. A study of the insecticidal constituents in *Chrysanthemum cinerariaefolium*. (1) Their development in the flower head. (2) Their distribution in the plant. *Pyrrhtrum Post* 8(4): 32-37.
- Hristozov D, Da Costa FB, Gasteiger J. 2007. Sesquiterpene lactones-based classification of the family Asteraceae using neural networks and k-nearest neighbors. *Journal of Chemical Information and Modeling* 47(1): 9-19.
- Kelsey RG, and F. Shafizadeh. 1980. Glandular trichomes and sesquiterpene lactones of *Artemisia ova* (Asteraceae). *Biochemical Systematics and Ecology* 8: 371-377.
- Kim SH, Chang YJ, Kim SU. 2008. Tissue specificity and developmental pattern of amorpha-4,11-diene synthase (ADS) proved by ADS promoter-driven GUS expression in the heterologous plant, *Arabidopsis thaliana*. *Planta Medica* 74(2): 188-193.
- Knight DW. 1995. Feverfew - chemistry and biological activity. *Natural Product Reports* 12(3): 271-276.
- Lesiak K KK, Zalesna I, Nejc D, Döchler M, Czyz M. 2010. Parthenolide, a sesquiterpene lactone from the medical herb feverfew, shows anticancer activity against human melanoma cells *in vitro*. *Melanoma Research* 20: 21-34.
- Lies Maes FCWVN, Yansheng Zhang, Darwin W. Reed, Jacob Pollier, Sofie R. F. Vande Castele, Dirk Inzé, Patrick S. Covello, Dieter L. D. Deforce, Alain Goossens. 2010. Dissection of the phytohormonal regulation of trichome formation and biosynthesis of the antimalarial compound artemisinin in *Artemisia annua* plants. *New Phytologist* 189(1): 176-189.
- Livak KJ, Schmittgen TD. 2001. Analysis of relative gene expression data using real-time quantitative PCR and the 2(T)(-ΔΔC) method. *Methods* 25(4): 402-408.
- Lommen WJM, Schenk E, Bouwmeester HJ, Verstappen FWA. 2006. Trichome dynamics and artemisinin accumulation during development and senescence of *Artemisia annua* leaves. *Planta Medica* 72(4): 336-345.
- Maffei M, Chialva F, Sacco T. 1989. Glandular trichomes and essential oils in developing peppermint leaves. *New Phytologist* 111(4): 707-716.
- Majdi M, Karimzadeh G, Malboobi MA, Omidbaigi R, Mirzaghaderi G. 2010. Induction of tetraploidy to feverfew (*Tanacetum parthenium* Schulz-Bip.): Morphological, physiological, cytological, and phytochemical changes. *Hortscience* 45(1): 16-21.
- McCaskill D, Croteau R. 1995. Monoterpene and sesquiterpene biosynthesis in glandular trichomes of peppermint (*mentha x piperita*) rely exclusively on plastid-derived isopentenyl diphosphate. *Planta* 197(1): 49-56.
- McCaskill D, Croteau R. 1999. Strategies for bioengineering the development and metabolism of glandular tissues in plants. *Nature Biotechnology* 17(1): 31-36.
- McConkey ME, Gershenzon J, Croteau RB. 2000. Developmental regulation of monoterpene biosynthesis in the glandular trichomes of peppermint. *Plant Physiology* 122(1): 215-223.
- Mín Li-Weber MG, Monika K. Treiber, Peter H. Kramer. 2002. The anti-inflammatory sesquiterpene lactone parthenolide suppresses IL-4 gene expression in peripheral blood T cells. *European Journal of Immunology* 32(12): 3587-3597.
- Nagegowda DA. 2010. Plant volatile terpenoid metabolism: Biosynthetic genes, transcriptional regulation and sub-cellular compartmentation. *FEBS Letters* 584(14): 2965-2973.

- Nagel J, Culley LK, Lu YP, Liu EW, Matthews PD, Stevens JF, Page JE. 2008. EST analysis of hop glandular trichomes identifies an O-methyltransferase that catalyzes the biosynthesis of xanthohumol. *Plant Cell* 20(1): 186-200.
- Nguyen DT, Gopfert JC, Ikezawa N, MacNevin G, Kathiresan M, Conrad J, Spring O, Ro DK. 2010. Biochemical conservation and evolution of germacrene A Oxidase in Asteraceae. *Journal of Biological Chemistry* 285(22): 16588-16598.
- Olsson ME, Olofsson LM, Lindahl AL, Lundgren A, Brodelius M, Brodelius PE. 2009. Localization of enzymes of artemisinin biosynthesis to the apical cells of glandular secretory trichomes of *Artemisia annua* L. *Phytochemistry* 70(9): 1123-1128.
- Omidbaigi R, Dadman B, Yavari S. 2007. Various harvest times of *Tanacetum parthenium* cv. Zardband flowers affecting its oil content and compositions. *Journal of Essential Oil Bearing Plants* 10(4): 287-291.
- Palevitch D, Earon G, Carasso R. 1997. Feverfew (*Tanacetum parthenium*) as a prophylactic treatment for migraine: A double-blind placebo-controlled study. *Phytotherapy Research* 11(7): 508-511.
- Pfaffenrath V, Diener HC, Fischer M, Friede M, Henneicke-von Zepelin HH. 2002. The efficacy and safety of *Tanacetum parthenium* (feverfew) in migraine prophylaxis - a double-blind, multicentre, randomized placebo-controlled dose-response study. *Cephalalgia* 22(7): 523-532.
- Schillmiller AL, Miner DP, Larson M, McDowell E, Gang DR, Wilkerson C, Last RL. 2010. Studies of a biochemical factory: tomato trichome deep expressed sequence tag sequencing and proteomics. *Plant Physiology* 153(3): 1212-1223.
- Sekiwa-Iijima Y, Aizawa, Yoko., and Kikue Kubota. 2001. Geraniol dehydrogenase activity related to aroma formation in Ginger (*Zingiber officinale* Roscoe). *Journal of Agricultural and Food Chemistry* 49: 5902-5906.
- Sessa RA, Bennett MH, Lewis MJ, Mansfield JW, Beale MH. 2000. Metabolite profiling of sesquiterpene lactones from *Lactuca* species - Major latex components are novel oxalate and sulfate conjugates of lactucin and its derivatives. *Journal of Biological Chemistry* 275(35): 26877-26884.
- Spinsanti G PC, Lazzeri E, Marsili L, Casini S, Frati F, Fossi CM. . 2006. Selection of reference genes for quantitative RT-PCR studies in striped dolphin (*Stenella coeruleoalba*) skin biopsies. *BMC Molecular Biology* 7: 32.
- Teoh KH, Polichuk DR, Reed DW, Nowak G, Covello PS. 2006. *Artemisia annua* L. (Asteraceae) trichome-specific cDNAs reveal CYP71AV1, a cytochrome P450 with a key role in the biosynthesis of the antimalarial sesquiterpene lactone artemisinin. *Febs Letters* 580(5): 1411-1416.
- Trusheva B, Todorov I, Ninova M, Najdenski H, Daneshmand A, Bankova V. 2010. Antibacterial mono- and sesquiterpene esters of benzoic acids from Iranian propolis. *Chemistry Central Journal* 4: 8.
- van Klink J, Becker H, Andersson S, Boland W. 2003. Biosynthesis of antheכותולoide, an irregular sesquiterpene lactone from *Anthemis cotula* L. (Asteraceae) via a non-farnesyl diphosphate route. *Organic & Biomolecular Chemistry* 1(9): 1503-1508.
- Vogler BK, Pittler MH, Ernst E. 1998. Feverfew as a preventive treatment for migraine: a systematic review. *Cephalalgia* 18(10): 704-708.
- Wagner GJ. 1991. Secreting glandular trichomes: More than just hairs. *Plant Physiology* 96: 675-679.
- Wallaart TE, Bouwmeester HJ, Hille J, Poppinga L, Maijers NCA. 2001. Amorpha-4,11-diene synthase: cloning and functional expression of a key enzyme in the biosynthetic pathway of the novel antimalarial drug artemisinin. *Planta* 212(3): 460-465.
- Werker E. 2000. Trichome diversity and development. *Advances in Botanical Research Incorporating Advances in Plant Pathology, Vol 31 2000* 31: 1-35.
- Williams CA, Hoult JRS, Harborne JB, Greenham J, Eagles J. 1995. Biologically-active lipophilic flavonol from *Tanacetum parthenium*. *Phytochemistry* 38(1): 267-270.

Chapter 3

Reconstitution of the costunolide biosynthetic pathway in yeast and *Nicotiana benthamiana*

Qing Liu¹, Mohammad Majdi¹, Katarina Cankar, Miriam Goedbloed, Tatsiana Charnikhova, Francel W.A. Verstappen, Ric C.H. de Vos, Jules Beekwilder, Sander van der Krol, Harro J. Bouwmeester

¹These two authors contributed equally to this work.

Published as Liu et al., (2011) PLoS ONE 6(8): e23255.

Abstract

The sesquiterpene costunolide has a broad range of biological activities and is the parent compound for many other biologically active sesquiterpenes such as parthenolide. Two enzymes of the pathway leading to costunolide have been previously characterized: germacrene A synthase (GAS) and germacrene A oxidase (GAO) which together catalyse the biosynthesis of germacra-1(10),4,11(13)-trien-12-oic acid. However, the gene responsible for the last step towards costunolide has not been characterized until now. Here we show that chicory costunolide synthase (CiCOS), CYP71BL3, can catalyse the oxidation of germacra-1(10),4,11(13)-trien-12-oic acid to yield costunolide. Co-expression of feverfew GAS (*TpGAS*), chicory GAO (*CiGAO*), and chicory COS (*CiCOS*) in yeast resulted in the biosynthesis of costunolide. The catalytic activity of *TpGAS*, *CiGAO* and *CiCOS* was also verified in planta by transient expression in *Nicotiana benthamiana*. Mitochondrial targeting of *TpGAS* resulted in a significant increase in the production of germacrene A compared with the native cytosolic targeting. When the *N. benthamiana* leaves were co-infiltrated with *TpGAS* and *CiGAO*, germacrene A almost completely disappeared as a result of the presence of *CiGAO*. Transient expression of *TpGAS*, *CiGAO* and *CiCOS* in *N. benthamiana* leaves resulted in costunolide production of up to 60 ng.g⁻¹ FW. In addition, two new compounds were formed that were identified as costunolide-glutathione and costunolide-cysteine conjugates.

Introduction

Sesquiterpene lactones (SLs) are a major class of plant secondary metabolites. These bitter tasting, lipophilic molecules form the active constituents of a variety of medicinal plants used in traditional medicine (Rodriguez et al., 1976; Zhang et al., 2005). Some SLs show bioactivities which are beneficial to human health, such as anti-inflammatory (e.g. helenalin) (Lyss et al., 1998), anti-cancer (e.g. costunolide) (Koo et al., 2001), and anti-malarial (artemisinin) (Klayman, 1985). The majority of SLs have been reported from the Asteraceae family, with over 4000 different SLs that have been identified (de Kraker et al., 2002). While the detailed structure of those SLs varies, their backbones are constrained to a limited set of core skeletons, such as germacranolide, eudesmanolide and guaianolide (Seto et al., 1988; Fischer, 1990; Van Beek et al., 1990). For all these three types of sesquiterpene lactones costunolide is generally considered the common precursor (de Kraker et al., 2002). Costunolide has been detected in many medicinal plants and several biological activities were ascribed to it including anti-carcinogenic, anti-viral, anti-fungal, and immunosuppressive activities (Mori et al., 1994; Chen et al., 1995; Taniguchi et al., 1995; Barrero et al., 2000; Wedge et al., 2000). Synthetic derivatives of costunolide such as 13-amino costunolide derivatives have anti-cancer activity (Srivastava et al., 2006) and also biosynthetic downstream products derived from costunolide have been reported to have interesting biological properties. For example, parthenolide has been reported to have anti-inflammatory and anti-cancer activity (Bedoya et al., 2008; Zhang et al., 2009).

Despite the importance of costunolide-derived SLs, the biosynthesis pathway of costunolide has not been fully elucidated. The pathway from FPP to costunolide was first proposed by de Kraker et al. based on the presence of enzymes in chicory roots that convert FPP to costunolide (de Kraker et al., 1998; de Kraker, JW et al., 2001; de Kraker et al., 2002) (Figure 1). First, farnesyl diphosphate is converted to germacrene A by germacrene A synthase (GAS) (de Kraker et al., 1998). GAS genes have been isolated and characterized from several members of the Asteraceae family, such as chicory (Bouwmeester et al., 2002), lettuce (Bennett et al., 2002), *Artemisia annua* (Berthea et al., 2006), and feverfew (Majdi et al., 2011).

In the next step of the pathway, germacrene A is oxidized at its C13 methyl by germacrene A oxidase (GAO) to form germacra-1(10),4,11(13)-trien-12-ol, which is then further oxidised to germacra-1(10),4,11(13)-trien-12-al and germacra-1(10),4,11(13)-trien-12-oic acid (de Kraker, J-W et al., 2001; de Kraker et al., 2002). The C6 position of germacra-1(10),4,11(13)-trien-12-oic acid is subsequently hydroxylated by a putative cytochrome P450 mono-oxygenase, after which presumably spontaneous cyclization of the C6 hydroxyl and C12 carboxylic group leads to the formation of costunolide (de Kraker et al., 2002).

Although biosynthesis of costunolide from germacra-1(10),4,11(13)-trien-12-oic acid has been demonstrated in chicory biochemically (de Kraker et al., 2002), the corresponding gene responsible for this step has not been identified to date. It was shown that both germacrene A oxidase and costunolide synthase are cytochrome P450 enzymes. Recently, genes that encode germacrene A oxidase were cloned from a number of Asteraceae species (Nguyen et al.,

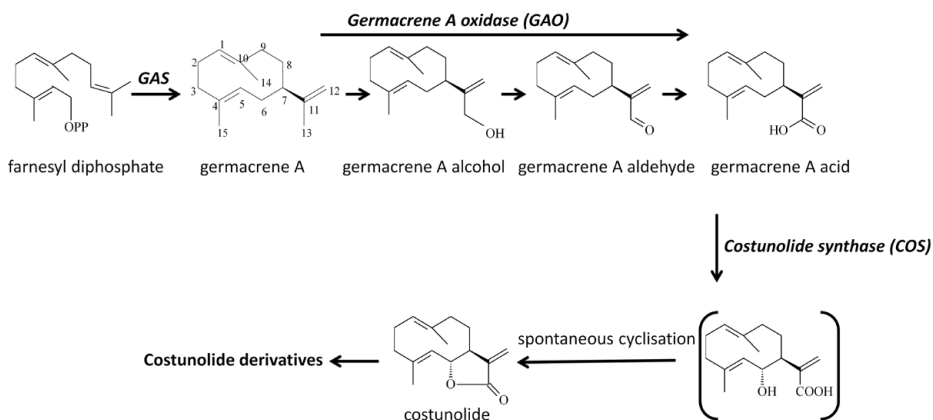


Figure 1. Biosynthetic pathway of costunolide in Asteraceae. GAS, germacrene A synthase.

2010). A valencene oxidase gene (*CYP71AV8*) was also reported to have the germacrene A oxidase activity (Cankar et al., 2011). All these genes belong to the CYP71 group of cytochrome P450s. In the present study, we investigated 5 candidate CYP71 P450 genes from a chicory cDNA library for costunolide synthase activity. The putative *CiCOS* gene was characterised by reconstitution of the costunolide biosynthetic pathway in yeast as well as in *Nicotiana benthamiana*, and the products formed were analysed using GC-MS and LC-MS metabolic profiling.

Results

Optimizing germacrene A production *in planta*

To produce germacrene A we used the *GAS* gene isolated from feverfew (*Tanacetum parthenium*), *TpGAS* (Majdi et al., 2011). After cloning of the full length coding sequence into a yeast expression vector, the *TpGAS* activity was compared with the previously characterized *GAS* genes from chicory (*CiGAS-l* and *CiGAS-s*) (Bouwmeester et al., 2002). Results showed that yeast culture expressing *TpGAS* had an approximately three fold higher activity than that of the *CiGAS* gene(s) (Figure 2). Subsequently, the *TpGAS* cDNA - using its native targeting to the cytosol (*cTpGAS*) or equipped with a mitochondrial targeting

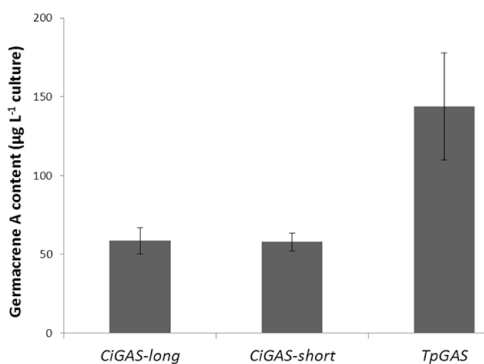


Figure 2. Germacrene A production in yeast. A yeast culture transformed by either *CiGAS-long*, *CiGAS-short* (Bouwmeester et al., 2002), or *TpGAS* (Majdi et al., 2011). Induced yeast culture medium was extracted and analysed by GC-MS.

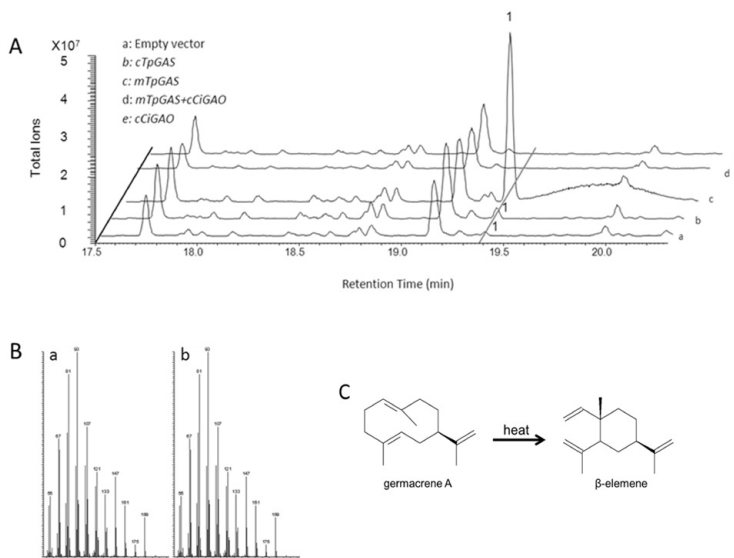


Figure 3. Headspace analysis of volatiles emitted from agro-infiltrated *Nicotiana benthamiana* leaves. A, GC-MS chromatograms are shown for the volatiles emitted from *N. benthamiana* leaves infiltrated with the indicated genes. Line a is a negative control, line b and c display the different amount of compound 1 (germacrene A) produced by *N. benthamiana* leaves infiltrated with *TpGAS* with different targeting signals: *mTpGAS*, mitochondrial targeting; *cTpGAS*, cytosolic targeting. Line d shows that compound 1 which is produced upon *mTpGAS* agro-infiltration disappears upon agro-infiltration with *CiGAO*. Agro-infiltration with *CiGAO* alone does not induce any volatile formation (Line e). B, the mass fragmentation patterns of compound 1 (a) and a β -elemene from the Wiley library (b). C, cope rearrangement of germacrene A to β -elemene by heat.

signal (*mTpGAS*) - was cloned into a binary expression vector under control of the Rubisco promoter and introduced into *Agrobacterium tumefaciens*. For analysis of in planta activity, *N. benthamiana* leaves were agro-infiltrated with the *cTpGAS* or *mTpGAS* containing *A. tumefaciens* strain and were analysed after 3 days. In the headspace of *cTpGAS* agro-infiltrated *N. benthamiana*, germacrene A was detected while no germacrene A was detected in leaves infiltrated with the empty vector (Figure 3A, line a and b). It has been shown for several terpene synthases that targeting to the mitochondria rather than to the cytosol which is the native compartment for sesquiterpene synthases results in higher production, presumably because of higher substrate availability in the mitochondria (Kappers et al., 2005; van Herpen et al., 2010). The *TpGAS* coding sequences was therefore fused to the CoxIV mitochondrial targeting sequence (*mTpGAS*). In *N. benthamiana* leaves infiltrated with *A. tumefaciens* carrying *mTpGAS*, the germacrene A production was approximately 15-fold higher than obtained by expression of *cTpGAS* (Figure 3A, line b and line c). Therefore, *mTpGAS* was used for the reconstruction of the costunolide pathway in *N. benthamiana*.

Functional characterization of *GAO* in planta

Previously the chicory *germacrene A oxidase* (*CiGAO*, GenBank: GU256644) was character-

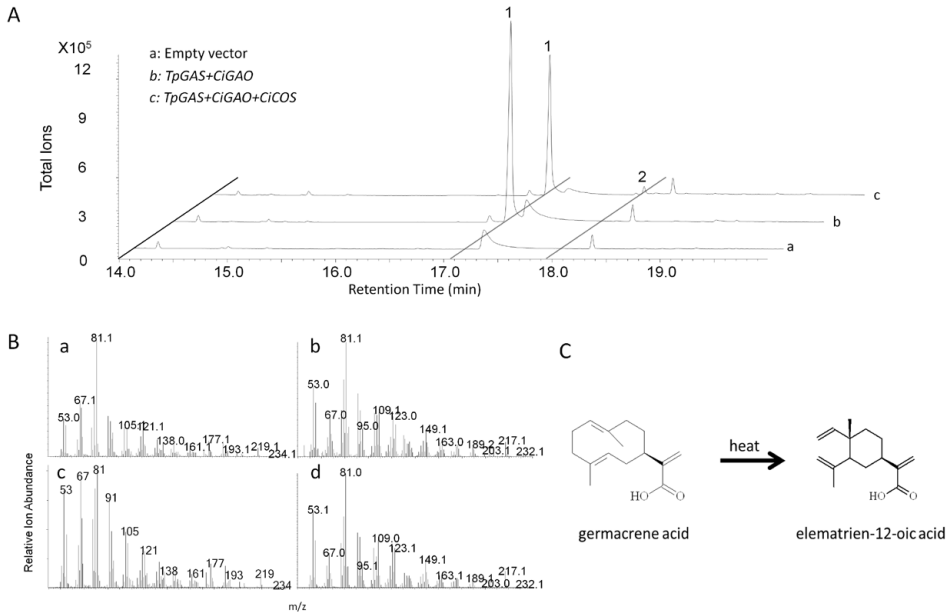


Figure 4. Costunolide production in yeast. A, GC-MS chromatograms are shown for the metabolites from yeast transformed with the indicated genes. Line a is a negative control, line b displays the metabolites in the yeast transformed with two genes (*TpGAS*, *CiGAO*), and line c displays the metabolites in the yeast transformed with three genes (*TpGAS*, *CiGAO*, and *CiCOS*). B, the mass spectra of compound 1 (a) and compound 2 (b) produced by yeast and elematrien-12-oic acid (c) and costunolide standards (d) are shown. C, cope rearrangement of germacrene acid to elematrien-12-oic acid by heat is shown. 1 = germacra-1(10),4,11(13)-trien-12-oic acid; 2 = costunolide.

ized by expression in yeast (Nguyen et al., 2010). We amplified the same gene (*CiGAO*) from a chicory cDNA library and the enzymatic activity was confirmed in our yeast system by co-expression of *TpGAS* and *CiGAO* (Figure 4A, line b). To test the activity of *CiGAO* *in planta*, an expression vector containing *CiGAO* was co-infiltrated with the *mTpGAS* expression vector into *N. benthamiana* leaves. In the headspace of *mTpGAS*+*CiGAO* agro-infiltrated *N. benthamiana* leaves, the germacrene A peak was no longer detected (compare Figure 3A line c with line d), suggesting that *CiGAO* can efficiently catalyse the conversion of the product of *mTpGAS*, germacrene A, into one or more other products. However, new peaks were visible neither in the headspace (Figure 3), nor in dichloromethane (DCM) extracts (data not shown) of *mTpGAS*+*CiGAO* agro-infiltrated *N. benthamiana* leaves compared with those of *mTpGAS*. Agro-infiltrated with *CiGAO* alone in *N. benthamiana* leaves, used as negative control, does not induce any volatile formation (compare Figure 3A line e and line d).

To investigate whether any non-volatile products were formed, the infiltrated leaves were extracted with aqueous methanol and the extracts analysed by accurate mass LC-QTOF-MS analysis. Metabolite profiles of the *pBIN* (empty vector), *mTpGAS*, and *mTpGAS*+*CiGAO* samples were recorded and the mass signals extracted in an untargeted manner using Metalign software (www.metAlign.nl), followed by clustering of extracted mass features into recon-

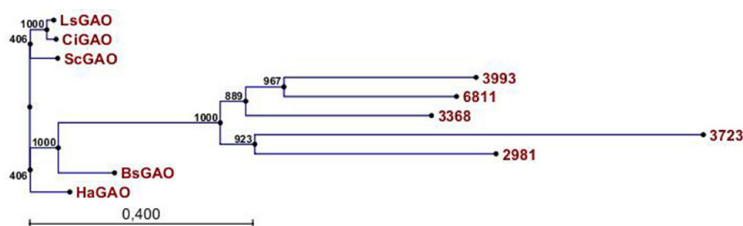


Figure 5. Phylogenetic analysis of Asteraceae GAO genes and five chicory CYP71 P450 ESTs. Chicory candidate 3368 was later identified as *Cichorium intybus costunolide synthase* (*CiCOS*). Amino acid sequences of GAOs were obtained from cDNAs deposited at the NCBI. *LsGAO* germacrene A oxidase from *Lactuca sativa* (GU198171) or from *Cichorium intybus* (*Ci*; GU256644), *Helianthus annuus* (*Ha*; GU256646), *Saussurea costus* (*Sc*; GU256645) and *Barnadesia. spinosa* (*Bs*; GU256647). Bootstrap values are shown in frequency values from 1000 replicates.

structed metabolites (Tikunov et al., 2005). The comparison of the *mTpGAS*+*CiGAO* co-infiltrated leaves and the *mTpGAS* infiltrated leaves revealed that, of the 2023 individual mass peaks with a signal-to-noise ratio higher than 3, none differed more than 2-fold ($p < 0.01$, $n = 3$; student T-test) between the two sample groups. This result could be explained by conjugation of the expected products of GAO oxidation of germacrene A (germacra-1(10),4,11(13)-trien-12-ol, germacra-1(10),4,11(13)-trien-12-al and germacra-1(10),4,11(13)-trien-12-oic acid) to multiple compounds, resulting in a distribution of the product signal over multiple masses that apparently remain below the 2-fold threshold or the level of detection.

Characterisation of a costunolide synthase gene from chicory

Chicory (*Cichorium intybus* L.) accumulates costunolide in roots (Van Beek et al., 1990). We assumed costunolide synthase to be a cytochrome P450 enzyme (as demonstrated by de Kraker et al. (2002)) which evolved from the GAO gene and therefore should show close homology to the *CiGAO* amino acid sequences. A root-specific cDNA library from chicory was available (Cankar et al., 2011), the sequences from the library were combined with chicory ESTs from GenBank (<http://www.ncbi.nlm.nih.gov>) and UC Davis database (http://compgenomics.ucdavis.edu/compositae_index.php), and these were searched for sequences with homology to the cytochrome P450 sequences of germacrene A oxidase from *Cichorium intybus* (Nguyen et al., 2010; Cankar et al., 2011) and *Lactuca sativa* (Nguyen et al., 2010). Five P450 sequences were identified which clustered into class CYP71 and had high similarity to the GAO genes mentioned above. Figure 5 shows the phylogenetic relationship of the candidate chicory CYP71 P450 sequences and GAO genes from different plant species. Each of these candidate cDNA sequences was then cloned into a yeast expression vector and tested in the yeast expression system by co-transformation with *TpGAS* and *CiGAO*. One of the isolated cDNAs (3368) encodes an enzymatic activity which was able to produce costunolide (Figure 4) in the presence of *TpGAS* and *CiGAO*, and therefore was designated as *costunolide synthase* (*CiCOS*) (*CYP71BL3*).

As the conversion of the germacra-1(10),4,11(13)-trien-12-oic acid to costunolide was quite low in HEPES buffer (Figure 4), we tested the effect of another buffer, MOPS, on cos-

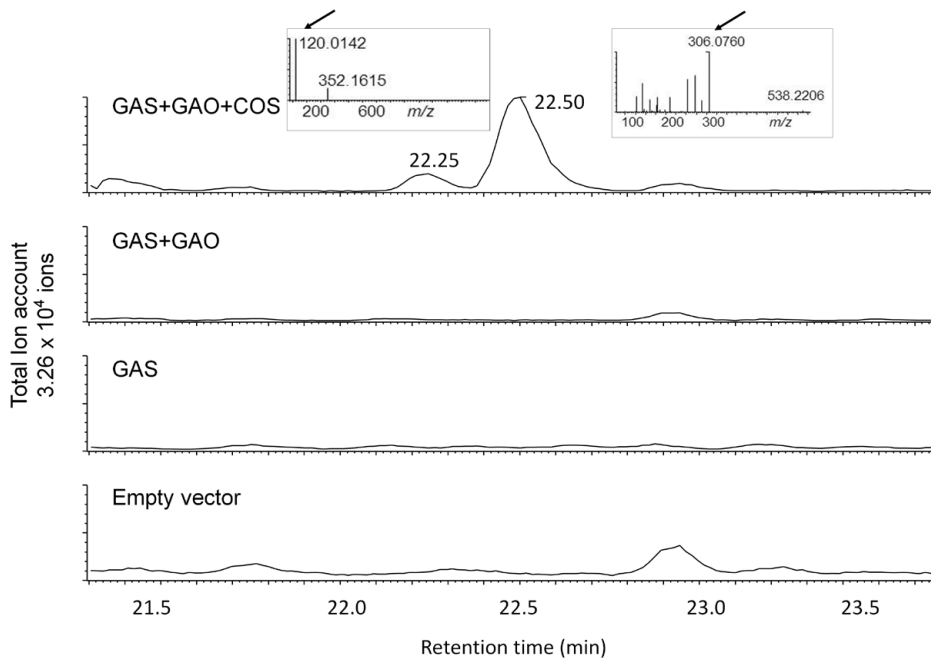


Figure 6. LC-MS/MS analysis of non-volatile metabolites in *N. benthamiana* leaves agro-infiltrated with empty vector, *TpGAS*, *TpGAS+CiGAO* and *TpGAS+CiGAO+CiCOS*. The two new peaks in *TpGAS+CiGAO+CiCOS* agro-infiltrated leaves were further fragmented by MS/MS. The $[m/z]$ for the parent ion of peak 22.30 is 352.1615. The $[m/z]$ for the parent ion of peak 22.50 is 538.2206. Inserted figures show MS/MS spectrum of peak 22.30 and peak 22.50 at 25 eV. Arrows indicate characteristic Cys and GSH MS/MS fragments, respectively. The Y-axis scale is identical in all chromatograms.

tunolide production in yeast, using UPLC-MRM-MS to quantify costunolide production. For *TpGAS+CiGAO+CiCOS* transformed yeast cultured in HEPES buffer (pH 7.5) the costunolide production was $9 \mu\text{g mL}^{-1}$ culture, while in MOPS buffer (pH 7.5) production was about 3-fold higher ($28 \mu\text{g mL}^{-1}$ culture).

To test the activity of the newly identified *CiCOS* in *planta*, the cDNA was cloned into a binary expression vector under control of the Rubisco promoter. *N. benthamiana* leaves were co-infiltrated with agrobacterium cultures with *RBC::mTpGAS*, *RBC::CiGAO* and *RBC::CiCOS* and after 3 days leaves were extracted with methanol and extracts were analysed by UPLC-MRM-MS for quantification of free costunolide. Results show that average production of costunolide from eight infiltration experiments was $48.6 \pm 13.4 \text{ ng g}^{-1}$ FW. No costunolide was detected in extracts from leaves infiltrated with either *pBIN* (empty vector), *RBC::mTpGAS*, *RBC::mTpGAS+RBC::CiGAO* or *RBC::mTpGAS+RBC::CiCOS* (data not shown), indicating that the production of costunolide by *CiCOS* in *N. benthamiana* leaves is dependent on the presence of both *TpGAS* and *CiGAO*.

To investigate whether there were any other metabolic changes caused by co-infiltration of *RBC::mTpGAS*, *RBC::CiGAO* and *RBC::CiCOS*, an untargeted LC-QTOF-MS analysis of aqueous methanol extracts from leaves was carried out. Comparison of the chromatograms

of extracts from co-infiltrated leaves showed two new compounds, eluting at 22.30 and 22.48 min, in the leaves infiltrated with *mTpGAS+CiGAO+CiCOS* compared to leaves infiltrated with *mTpGAS+CiGAO* (Figure 6)

Identification of costunolide conjugates

In order to identify the two new compounds in the leaves infiltrated with *mTpGAS+CiGAO+CiCOS*, the apparent parent masses of the peaks at 22.30 and 22.48 min were fragmented by LC-MS/MS in negative mode. Within the MS/MS fragments of 352.1615 (parent ion of peak at 22.30 min, a 9.2 ppm deviation from the elemental formula $C_{18}H_{27}NO_4S$), we detected an ion with mass 120.0142, a 19 ppm deviation from the elemental formula of cysteine ($C_3H_7NO_2S$). This MS/MS experiment therefore suggests that the peak at 22.30 min is a costunolide ($C_{15}H_{20}O_2$)-cysteine ($C_3H_7NO_2S$) conjugate. Within the MS/MS fragments of 538.2206 (parent ion of peak at 22.48 min, a -19.9 ppm deviation from the elemental formula $C_{25}H_{37}N_3O_8S$), we detected an ion with mass 306.0760, a -2.9 ppm deviation from the elemental formula of glutathione ($C_{10}H_{17}N_3O_6S$). This MS/MS experiment therefore suggests that the peak at 22.48 min is a costunolide ($C_{15}H_{20}O_2$)-glutathione ($C_{10}H_{17}N_3O_6S$) conjugate (Figure 6).

To further confirm the identity of these putative costunolide glutathione and cysteine conjugates, we tested the activity of a glutathione-S-transferase (GST) enzyme on costunolide in an in vitro enzyme assay. Analysis of the reaction mix of costunolide with glutathione and GST by LC-QTOF-MS showed that costunolide was efficiently converted into a costunolide-glutathione conjugate (Figure 7) that had the same retention time and exact mass and MS fragments as the postulated costunolide conjugate detected in the extract of the *mTpGAS+CiGAO+CiCOS* agro-infiltrated leaf sample (Figure 7A and 7C). When costunolide and glutathione were incubated without GST enzyme, the same costunolide-glutathione conjugate was formed indicating that the conjugation of costunolide and glutathione can occur spontaneously. Similarly, when costunolide was incubated with cysteine a costunolide-cysteine conjugate was spontaneously formed (Figure 7B). The cysteine conjugate that was spontaneously formed by the in vitro reaction had the same mass spectrum and retention time as the compound produced in *mTpGAS+CiGAO+CiCOS* agro-infiltrated *N. benthamiana* leaves (Figure 7B and 7D). Thus the two new peaks in *mTpGAS+CiGAO+CiCOS* agro-infiltrated *N. benthamiana* leaf were confirmed to be a costunolide-glutathione and a costunolide-cysteine conjugate. The presumed structure of these two compounds is shown in Figure 7E.

Discussion

Reconstitution of the costunolide biosynthesis pathway in yeast

Costunolide is the precursor of many biologically active SLs, and reconstitution of its biosynthetic pathway in heterologous hosts could form an attractive option for commercial production of these compounds. Partial reconstruction of the sesquiterpene biosynthesis pathways in yeast has been demonstrated for the antimalarial drug artemisinin (Ro et al., 2006) and for germacra-1(10),4,11(13)-trien-12-oic acid (Nguyen et al., 2010; Cankar et al., 2011). Here we

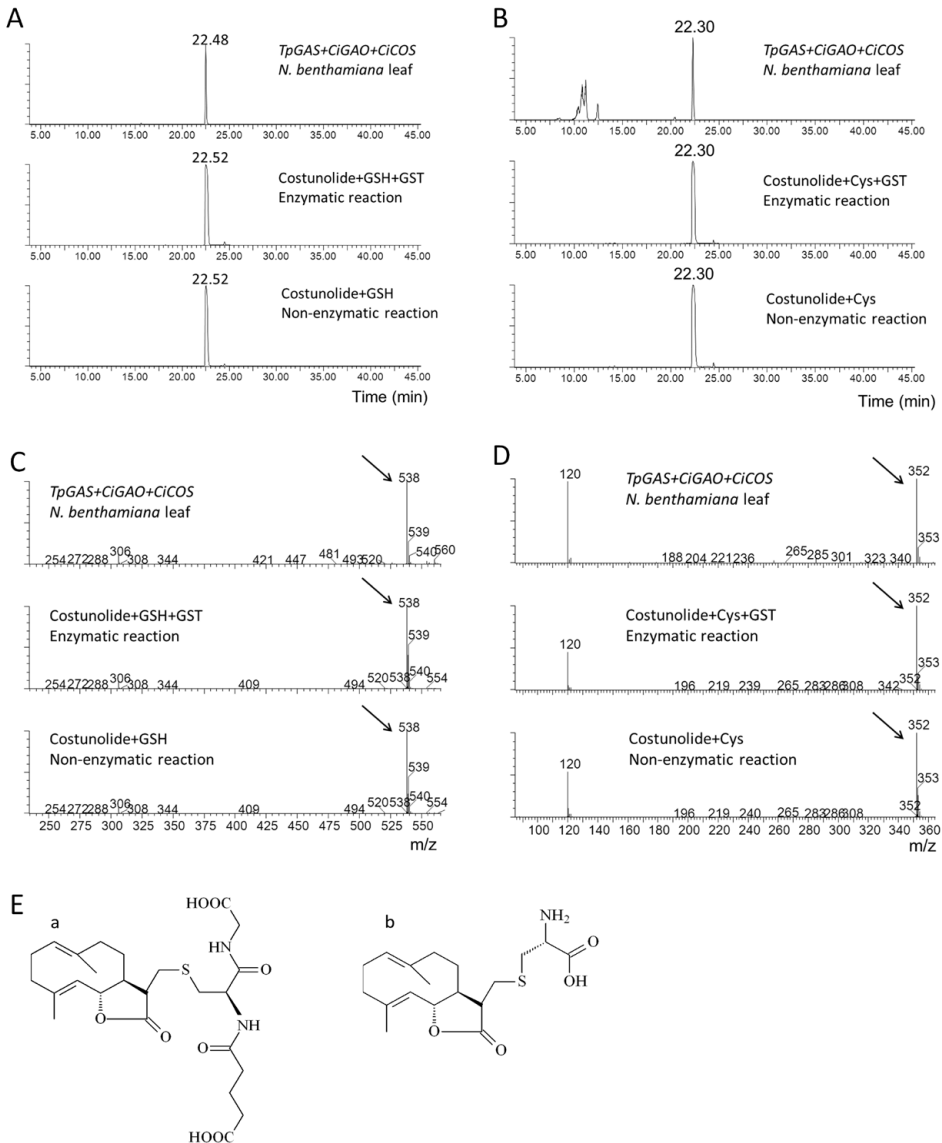


Figure 7. Costunolide-glutathione and costunolide-cysteine conjugate identification by GST enzyme assay and LC-MS analysis. A. LC-MS chromatograms of $[m/z]=538$ of extracts of *N. benthamiana* leaves agro-infiltrated with *TpGAS+CiGAO+CiCOS*, costunolide-GSH conjugate formed in an enzyme assay of costunolide and GSH with GST, costunolide-GSH conjugate formed by non-enzymatic conjugation of costunolide and GSH. B. LC-MS chromatograms of $[m/z]=352$ of extracts of *N. benthamiana* leaves agro-infiltrated with *TpGAS+CiGAO+CiCOS*, costunolide-cysteine (Cys) conjugate formed in an enzyme assay of costunolide and Cys with GST, costunolide-Cys conjugate formed non enzymatically from costunolide and Cys. C. $[m/z]$ spectrum of peak 22.48 and costunolide-GSH conjugate (RT=22.52). Arrows indicate parent ions of GSH-glutathione. D. $[m/z]$ spectrum of peak 22.30 and costunolide-Cys conjugate (RT=22.30). Arrows indicate parent ions of GSH-cysteine. E. Presumed molecular structure of costunolide-GSH (a) and costunolide-Cys (b) conjugates. GSH, glutathione; Cys, cysteine; GST, glutathione S-transferase. RT, retention time. Y-axis scale is identical in all chromatograms.

reconstituted the biosynthetic pathway of costunolide in yeast and in planta. To achieve this we screened five candidate CYP71 P450 genes from chicory for costunolide synthase activity, which yielded one gene which had this activity, *CiCOS*. This novel gene was combined with a new *GAS* gene from feverfew (*TpGAS*) and the previously identified chicory *GAO* (Nguyen et al., 2010; Cankar et al., 2011). Co-expression of *TpGAS* together with *CiGAO* and *CiCOS* in yeast yielded just low levels of costunolide, so it was of interest to see if production in yeast could be boosted. We showed that using *GAS* from different sources may have a strong effect on germacrene A production (Figure 2).

Also the culture buffer conditions strongly affect costunolide production. We showed that germacra-1(10),4,11(13)-trien-12-oic acid can be more efficiently converted by *CiCOS* into costunolide when the yeast is cultured in MOPS (pH7.5) buffer instead of HEPES buffer (pH 7.5). The pH of the buffered yeast culture decreased from 7.5 to 6.8 for both MOPS and HEPES buffered culture after 48 hours of cultivation. Therefore, the difference in costunolide production was not due to the buffering capacity of the buffer. We presume that the increased costunolide production results from improved growth of yeast in the presence of MOPS, compared to the HEPES-buffered yeast culture.

Reconstitution of the costunolide biosynthesis pathway in *N. benthamiana*

Reconstruction of pathways in the transient *Nicotiana* spp. plant expression system was demonstrated for many medically relevant proteins (Tremblay et al., 2010) and has been shown to be a good model to study the production of sesquiterpenoid pharmaceutical compounds (van Herpen et al., 2010). A marked peak of germacrene A was detected in the headspace of *mTpGAS* agro-infiltrated *N. benthamiana* leaves. The targeting of sesquiterpene synthases in metabolic engineering seems to have a great effect on its performance in plants. It has been shown in *Arabidopsis* that fusion of nerolidol synthase from strawberry to a mitochondrial targeting sequence leads to the biosynthesis of nerolidol, whereas this was not the case when using a cytosol targeting sequence (Kappers et al., 2005). This is in line with our observation that the germacrene A emitted from *N. benthamiana* leaves infiltrated with mitochondrial targeted germacrene A synthase is much higher than that from leaves infiltrated with the cytosolic germacrene A synthase (Figure. 3).

The disappearance of germacrene A observed upon co-expression of mitochondrial *TpGAS* and *CiGAO* suggests that germacrene A is efficiently transferred from the mitochondrial compartment to the cytosol/ER, where it is presumably converted into germacrene A acid by *CiGAO*. The activity of mitochondrial *TpGAS* might produce a concentration gradient sufficient to drive diffusion of germacrene A into the cytosol. Or, as suggested by Turner and Croteau (2004), some type of terpenoid carrier protein, mitochondrial membrane pump, or transient contacts between ER and mitochondrial membranes might facilitate germacrene A movement from mitochondria to cytosol/ER. Germacrene A could not be detected in the headspace or solvent extracts of *mTpGAS*+*CiGAO* agro-infiltrated *N. benthamiana* leaves. We suppose that this is due to an efficient conversion of germacrene A into germacra-1(10),4,11(13)-trien-12-oic acid by the expressed *CiGAO* enzyme. The fact that we were

not able to detect germacra-1(10),4,11(13)-trien-12-oic acid may be explained by assuming that the compounds produced by CiGAO subsequently react with endogenous metabolites to form conjugates that were either not detected by our GC-MS and LC-QTOF-MS (ESI negative mode) profiling approaches, or were converted and diluted out into many new metabolites of which the signals were below our detection levels. The disappearance of germacrene A after introduction of CiGAO suggests an efficient transfer of substrate between GAS and GAO. Similar results have been reported by van Herpen et al. (2010): co-infiltration of *N. benthamiana* with the cDNA encoding amorphadiene synthase plus CYP71AV1, also a sesquiterpene oxidizing P450, leads to an almost complete conversion of amorphadiene. Also in the latter paper, the product of this conversion, artemisinic acid was efficiently further converted to a diglucose conjugate (2010).

Co-expression of *TpGAS* together with *CiGAO* and *CiCOS* in *N. benthamiana* leaves yielded up to 60 ng.g⁻¹ FW of costunolide. In addition, two novel costunolide conjugates were detected.

Costunolide glutathione conjugates are present *in planta* but not in yeast

Most glutathione conjugations are catalysed by glutathione S-transferase (GST), which may be constitutively active or be induced upon oxidative stress or exogenous heterocyclic compounds, such as herbicides (Marrs, 1996). The expression of two glutathione S-transferases (*NbGSTU1* and *NbGSTU3*) in *N. benthamiana* was up-regulated progressively during infection by the fungus *Colletotrichum destructivum* (Dean et al., 2005). Here we show that glutathione conjugates may be formed spontaneously from costunolide and GSH in an in vitro enzyme assay (Figure 7). S-glutathionylated metabolites are likely tagged for vacuolar import by ATP binding cassette (ABC) transporters, which selectively transport GSH conjugates, as has been shown for other glutathione S-conjugates (Rea, 1999). Storage of target metabolites as glutathione S-conjugates may have the advantage that the storage capacity of the vacuole is used and that high concentrations can be reached without phytotoxic effects. Marrs et al. (1995) reported that anthocyanin pigments require GSH conjugation for transport into the vacuole. If conjugation is inhibited, this leads to inappropriate cytoplasmic retention of the pigment which is toxic for the cells.

In addition to costunolide-GSH, costunolide-cysteine was also found to accumulate in agro-infiltrated *N. benthamiana* leaves. This cysteine conjugate may be a breakdown product of costunolide-glutathione (Ohkama-Ohtsu et al., 2007). However, we showed that the costunolide-cysteine conjugate may also be formed spontaneously from costunolide and cysteine (Figure 7).

Remarkably, no costunolide-glutathione or costunolide-cysteine conjugates were detected in medium of yeast transformed by *TpGAS*+*CiGAO*+*CiCOS* (data not shown), even though GSH is present in yeast (Shimizu et al., 1991) and some transporter genes, such as Bpt1p (Klein et al., 2002), have been reported to mediate vacuolar sequestration of glutathione conjugates in yeast. It could be that free costunolide is excreted out of the yeast cells and that any costunolide-glutathione conjugate formed inside the cell has a short half-life.

Spontaneous conjugation to glutathione related to bioactivity of costunolide?

It has been shown that the effect of costunolide treatment of cancer cells is based on a rapid depletion of the intracellular reduced glutathione and protein thiols, which precedes apoptosis. Indeed, the effect of costunolide can be blocked by pretreatment with sulfhydryl compounds such as GSH, N-acetyl-L-cysteine, dithiothreitol and 2-mercaptoethanol (Choi et al., 2002). The apoptosis-inducing activity of costunolide likely depends on the exomethylene moiety because derivatives in which this group was reduced, such as dihydrocostunolide and saussurea lactone, did not deplete the cellular thiols and showed no apoptotic activity (Choi et al., 2002; Park et al., 2006). If the biological activity of costunolide depends on the ability to conjugate glutathione and thiols, then the costunolide-glutathione conjugate produced in *N. benthamiana* may not exhibit biological activity. On the other hand, the poor water-solubility of costunolide may also limit its potential as a promising clinical agent (Ma et al., 2007) and conjugation could improve this property. Regulation of conjugation in heterologous plant hosts and secretion into cell compartments that allow accumulation of free costunolide could therefore be an important target for further optimization of a costunolide production platform.

In conclusion

We describe here the discovery of a new gene, *CiCOS*, and its functional characterization in yeast as well as *in planta*. *CiCOS* encodes the enzyme catalyzing the formation of a sesquiterpene lactone, costunolide, a promising anti-cancer medicine, and a crucial intermediate in the biosynthesis of many other sesquiterpene lactones with important biological activities, such as parthenolide. The cloning of this gene allows for the development of platforms – in microbial as well as in plant hosts – for the production of sesquiterpene lactones that can potentially be developed into new drugs. The conjugation of costunolide to glutathione and cysteine detected upon *in planta* expression has never been reported before in plants and could present new opportunities for high production because of better storability as well as for the development of drugs with better water solubility.

Materials and methods

Isolation and cloning of costunolide synthase candidate gene from chicory

A previously reported chicory cDNA taproot library (Cankar et al., 2011) was used for gene isolation. Five candidate cytochrome P450 contigs belonging to the CYP71 family were identified by sequence homology to known sesquiterpene monooxygenases. RACE PCR (Clontech) was used to obtain the sequence of the 5' - and 3' -region of the candidate contigs. Full length cDNAs of candidate genes were amplified from chicory cDNA with the addition of NotI/PacI restriction sites. They were subsequently cloned to the yeast expression vector pYEDP60 (Pompon et al., 1996), which was modified to contain PacI/ NotI sites at the polylinker, and sequenced. The DNA sequence for the chicory *costunolide synthase (CiCOS)*, has been deposited in GenBank under the accession number JF816041. The sequence was also submitted

to David Nelson's cytochrome P450 homepage (<http://drnelson.uthsc.edu/cytochromeP450.html>) and was assigned the name CYP71BL3 (Nelson, 2009).

Plasmid construction for gene expression in yeast

For the production of germacra-1(10),4,11(13)-trien-12-oic acid in yeast, *CiGAO* and *TpGAS* genes were both cloned into the pESC-Trp yeast expression vector (Agilent technologies) with the TRP1 auxotrophic selection marker. *CiGAO* (Cankar et al., 2011) was subcloned from the yeast vector PYEDP60 (Pompon et al., 1996) to the pESC-Trp vector using NotI/PacI restriction sites. The obtained construct was named *CiGAO* pESC-Trp. Subsequently, *TpGAS* was amplified from the pACYCDuet™-1 vector (Majdi et al., 2011) using high fidelity Phusion polymerase (Finnzymes) with the addition of BamHI/KpnI restriction sites. The amplified product was digested by BamHI/KpnI and ligated into the *CiGAO* pESC-Trp plasmid, yielding the final plasmid *TpGAS+CiGAO* pESC-Trp. No terminal tags were added in these constructs. This plasmid was transformed into the WAT11 (Urban et al., 1997) yeast strain and the clones were selected on Synthetic Dextrose (SD) minimal medium (0.67% Difco yeast nitrogen base medium without amino acids, 2% D-glucose, 2% agar) supplemented with amino acids, but omitting L-tryptophane for auxotrophic selection of transformants. *TpGAS+CiGAO* pESC-Trp and pYEDP60 plasmids containing costunolide synthase candidates were co-transformed into the WAT11 yeast strain. After transformation yeast clones containing both plasmids were selected on SD minimal medium supplemented with amino acids, but omitting uracil, adenine sulphate and L-tryptophane for auxotrophic selection of transformants.

Gene induction in yeast and metabolite extraction

For the induction of gene expression in yeast, the transformed WAT11 yeast strain with *TpGAS+CiGAO* pESC-Trp or co-transformed with *TpGAS+CiGAO* pESC-Trp and costunolide synthase candidate-PYED60-Ura-Ade were inoculated in 3 mL Synthetic Galactose (SG) minimal medium (0.67% Difco yeast nitrogen base medium without amino acids, 2% D-galactose, 2% agar) but omitting TRP or Trp-Ura-Ade amino acids, respectively. The yeast was cultured overnight at 30 °C and 300 rpm. The start culture was diluted to OD 0.05 in SG minimal medium omitting Trp or Trp-Ura-Ade amino acids, respectively. All yeast induction experiments were performed in triplicates in 50 mL of culture volume. Cultures were buffered at pH 7.5 using 100 mM HEPES or 100 mM MOPS. After fermentation for 48h at 30 °C and 300 rpm, the medium was extracted with 20 mL ethyl acetate. From this, a 10 mL sample was taken and the ethyl acetate evaporated with a stream of N₂ to a final volume of 1 mL which was analyzed by GC-MS. For UPLC-MRM-MS analysis the ethyl acetate in a 10 mL subsample was completely evaporated and the residue redissolved in 300 µl of 25% acetonitrile in water.

Plasmid construction for expression in *Nicotiana benthamiana*

For expression in *N. benthamiana*, *TpGAS*, *CiGAO* and *CiCOS* were cloned into ImpactVector1.1 (<http://www.impactvector.com/>) to express them under the control of the Rubisco (RBC) promoter (Outchkourov et al., 2003). *TpGAS* was also cloned into ImpactVector1.5

to fuse it with the RBC promoter and the CoxIV mitochondrial targeting sequence. An LR reaction (Gateway-LR Clonase TM II) was carried out to clone each gene into pBinPlus binary (Vanengelen et al., 1995) vector between the right and left borders of the T-DNA for plant transformation.

Transient expression in *N. benthamiana*

A. tumefaciens infiltration (agro-infiltration) was performed according to the description of van Herpen et al. (2010). *A. tumefaciens* batches were grown at 28 °C at 220 rpm for 24 hours in YEP media with kanamycin (50 mg L⁻¹) and rifampicillin (34 mg L⁻¹). Cells were harvested by centrifugation for 20 min at 4000xg and 20 °C and then resuspended in 10 mM MES buffer containing 10 mM MgCl₂ and 100 µM acetosyringone (4'-hydroxy-3',5'-dimethoxyacetophenone, Sigma) to a final OD₆₀₀ of ~ 0.5, followed by incubation at room temperature under gentle shaking at 50 rpm for 150 min. For co-infiltration, equal volumes of the *Agrobacterium* batches were mixed. Batch mixtures were infiltrated into leaves of three-week-old *N. benthamiana* plants by pressing a 1 mL syringe without metal needle against the abaxial side of the leaf and slowly injecting the bacterium suspension into the leaf. *N. benthamiana* plants were grown from seeds on soil in the greenhouse with a minimum of 16 hour light. Day temperatures were approximately 28 °C, night temperatures 25 °C. After agro-infiltration the plants were grown under greenhouse conditions for another 3 days and then harvested for analysis.

Headspace analysis and GC-MS thermodesorption

Volatile collection from agro-infiltrated *N. benthamiana* leaves and GC-MS analysis were performed according to van Herpen et al. (2010). Steel sorbent cartridges (89 mm × 6.4 mm O.D.; Markes) containing Tenax were used for volatile collection. Cartridges were conditioned at 280 °C for 40 min under a nitrogen flow of 20 psi in a TC-20 multi-tube conditioner and were capped airtight until use. *N. benthamiana* leaves were sampled and placed on water in a small vial and were enclosed in a glass container. To trap the leaf-produced volatiles, air was sucked through the containers with a flow rate of 90 mL min⁻¹ for 24 hours and released through one cartridge. A second cartridge was used to purify the incoming air. Sample cartridges were dried for 15 min at room temperature with a nitrogen flow of 20 psi before GC-MS analysis on a Thermo Trace GC Ultra connected to a Thermo Trace DSQ quadruple mass spectrometer (Thermo Fisher Scientific, USA).

Cartridges were placed in an automated thermodesorption unit (Ultra; Markes, Llantrisant) in which they were flushed with helium at 50 mL min⁻¹ for 2 min to remove moisture and oxygen just before thermodesorption. The volatiles were desorbed by heating of the cartridges at 220 °C for 5 min with a helium flow of 50 mL min⁻¹. The compounds released were trapped on an electrically cooled sorbent trap (Unity; Markes, Llantrisant) at a temperature of 5 °C. Subsequently, the trapped volatiles were injected on the analytical column (ZB-5MSI, 30 m × 0.25 mm ID, 1.0 µm – film thickness, Zebron, Phenomenex) in splitless mode by ballistic heating of the cold trap to 250 °C for 3 min. The temperature program of the GC started at 40 °C (3 min hold) and rose 10°C min⁻¹ to 280 °C (2 min hold). The column effluent was ionised by electron impact (EI) ionisation at 70 eV. Mass scanning was done from 33 to 280 m/z with

a scan time of 4.2 scans s^{-1} . Xcalibur software (Thermo, USA) was used to identify the eluted compounds by comparing the mass spectra with those of authentic reference standards.

GC-MS analysis of solvent extracts

Seven mL yeast culture was extracted three times with 2 mL ethyl acetate, which was concentrated, dried using anhydrous Na_2SO_4 and used for GC-MS analysis. Agro-infiltrated leaves (100 mg) were ground in liquid nitrogen and extracted with 800 μ l dichloromethane. The extracts were prepared by brief vortexing and sonication for 10 min. Then the extracts were centrifuged for 15 min at 3000 rpm, dehydrated using Na_2SO_4 , and then used for GC-MS analysis. A gas chromatograph (7809A, Agilent, USA) equipped with a 30 m \times 0.25 mm, 0.25 mm film thickness column (ZB-5, Phenomenex) using helium as carrier gas at flow rate of 1 mL min^{-1} was used for GC-MS analysis. Splitless mode was used for the injector with the inlet temperature set to 250°C. The initial oven temperature was 45 °C for 1 min, and was increased to 300 °C after 1 min at a rate of 10 °C min^{-1} and held for 5 min at 300 °C. The GC was coupled to a Triple-Axis detector (5975C, Agilent). Compounds were identified by comparison of mass spectra and retention times (RT) with those of the following authentic standards: germacrene A, germacra-1(10),4,11(13)-trien-12-ol, germacra-1(10),4,11 (13)-trien-12-ol (Cankar et al., 2011) and costunolide (TOCRIS bioscience). Quantification of sesquiterpenoids was conducted by determination of total ion count (TIC) peak area of the sesquiterpenoid peaks from three independent fermentation experiments. An absolute concentration of sesquiterpenoids was calculated from the peak area by comparison with calibration curves of the authentic standards. At the routine injection port temperature of 250 °C germacrene A, germacra-1(10),4,11(13)-trien-12-oic acid and costunolide are thermally converted into β -elemene, elematrien-12-oic acid, and saussurea lactone, respectively as discussed by de Kraker et al. (de Kraker et al., 1998; de Kraker et al., 2002; de Kraker et al., 2003; Yang et al., 2011). We also regularly injected samples with an injection port temperature of 150 °C to confirm the presence of non-rearranged germacrene A, germacra-1(10),4,11(13)-trien-12-oic acid and costunolide.

LC-QTOF MS and MS/MS analysis

Non-volatile metabolites were analysed by LC-QTOF-MS (liquid chromatography, coupled to quadrupole time-of-flight mass spectrometry) according to a protocol for untargeted metabolomics of plant tissues (De Vos et al., 2007). A Waters Alliance 2795 HPLC connected to a Waters 2996 PDA detector and subsequently a QTOF Ultima V4.00.00 mass spectrometer (Waters, MS technologies, UK) operating in negative ionization mode was used. An analytical column (Luna 3 μ C18/2 100A; 2.0 \times 150 mm; Phenomenex, USA) attached to a C18 pre-column (2.0 \times 4 mm; Phenomenex, USA) was used. Degassed eluent A [ultra-pure water: formic acid (1000:1, v/v)] and eluent B [acetonitril:formic acid (1000:1, v/v)] were used at a flow rate of 0.19 mL min^{-1} . Masses were recorded between m/z X and m/z Y; leucine enkephalin ($[M-H]^- = 554.2620$) was used as a lock mass for on-line accurate mass correction.

For agro-infiltrated *N. benthamiana*, 100 mg infiltrated leaf from each treatment was ground in liquid nitrogen and extracted with 300 μ l methanol:formic acid (1000:1, v/v). After

brief vortexing and sonication for 15 min, the extracts were centrifuged for 5 min at 13,000 rpm and filtered through a 0.2 µm inorganic membrane filter (RC4, Sartorius, Germany). The gradient of the HPLC started at 5% eluent B and increased linearly to 75% eluent B in 45 min, after which the column was washed and equilibrated for 15 min before the next injection. The injection volume was 5 µl. Data-directed MS-MS measurements were done at collision energies of 10, 15, 25, 35 and 50 eV.

Costunolide detection and quantification by UPLC- MRM- MS

Targeted analysis of costunolide in yeast extract and agro-infiltrated *N. benthamiana* leaves was performed with a Waters Xevo tandem quadrupole mass spectrometer equipped with an electrospray ionization source and coupled to an Acquity UPLC system (Waters) as described by Kohlen et al. (2011) with some modifications. Chromatographic separation was obtained on an Acquity UPLC BEH C18 column (100 × 2.1 mm, 1.7 µm; Waters) by applying a water/acetonitrile gradient to the column, starting from 5% (v/v) acetonitrile in water for 1.25 min and rising to 50% (v/v) acetonitrile in water in 2.35 min, followed by an increase to 90% (v/v) acetonitrile in water in 3.65 min, which was maintained for 0.75 min before returning to 5% acetonitrile in water using a 0.15 min gradient. Finally, the column was equilibrated for 1.85 min using this solvent composition. Operation temperature and flow rate of the column were 50°C and 0.5 mL min⁻¹, respectively. Injection volume was 5 µL. The mass spectrometer was operated in positive electrospray ionization mode. Cone and desolvation gas flows were set to 50 and 1000 L h⁻¹, respectively. The capillary voltage was set at 3.0 kV, the source temperature at 150°C, and the desolvation temperature at 650°C. The cone voltage was optimized for costunolide using the Waters IntelliStart MS Console. Argon was used for fragmentation by collision-induced dissociation in the ScanWave collision cell. MRM method was used for identification of costunolide in yeast extract and agro-infiltrated *N. benthamiana* leaves by comparing retention times and MRM mass transitions with that of a costunolide standard. MRM transitions for costunolide m/z 233.16>131.01 and 233.16>187.23 were optimized using the Waters IntelliStart MS Console.

GC-MS and LC-MS data processing

GC-MS and LC-MS data analysis was done according to the description by Yang et al. (2011) with minor modifications. GC-MS data were acquired using Xcalibur 1.4 (Thermo Electron Corporation) and LC-MS data using MassLynx 4.0 (Waters). The data were processed using MetAlign version 1.0 (www.metAlign.nl) for baseline correction, noise elimination and subsequent spectral data alignment (De Vos et al., 2007). The processing parameters of MetAlign for GC-MS data were set to analyse scan numbers 1,340–16,000 (corresponding to retention times 2.32 to 28.05 min) with maximum amplitude of 1.4×10⁸. The processing parameters for LC-MS data were set to analyse scan numbers 60–2300 (corresponding to retention time 1.4 to 49.73 min) with a signal-to-noise ratio higher than 3.

To combine mass signals belonging to the same metabolite, all the detected masses were clustered by an in-house developed script called Multivariate Mass Spectra Reconstruction (MMSR) (Tikunov et al., 2005). The mass signal intensities (expressed as peak height using

MetAlign) obtained from agro-infiltrated plants and empty vector control plants were compared using the Student's t-test. Masses with a significant ($p < 0.05$) intensity change of at least 2-fold were verified manually in the original chromatograms.

To annotate significantly different compounds in LC-QTOF-MS, accurate masses were manually calculated, taking into account only those scans with the proper intensity ratios of analyte and lock mass (between 0.25- and 2 (Moco et al., 2006)) and elemental formulae generated within 5 ppm deviation from the observed mass. In addition, data-directed LC-MS/MS experiments were performed on differential compounds. To obtain proper MS/MS spectra only molecular ions with signal intensities higher than 500 ion counts per scan were selected.

Costunolide conjugation enzyme assay

This enzyme assay was performed according to the method of Habig et al. (1974) with modifications. In brief, glutathione (150 mM) or cysteine (150 mM) in 7 μ l potassium buffer (100 mM; pH 6.5), and costunolide (30 mM) in 7 μ l ethanol were added to 200 μ l potassium buffer (100 mM; pH 6.5). The reaction was initiated by adding 7 μ l of GST (1g L⁻¹, in 100mM potassium buffer; pH 6.5) into the mixture. Complete assay mixtures without GST enzyme or either of the substrates were used as controls. After incubation for 15 min at room temperature, samples were kept at -20°C until analysis by LC-QTOF-MS.

Acknowledgements

We thank Bert Schipper for assistance in LC-MS analysis, Ting Yang for her help in MS data analysis, and Benyamin Houshyani for technical support in headspace analysis.

Note added in submission: During submission of this manuscript, a paper by Ikezawa et al. (2011) was published online (22 April 2011), in which a lettuce *costunolide synthase* (*CYP71BL2*) is reported. The amino acid sequence of chicory *costunolide synthase* (*CYP71BL3*) is 97% identical to that of *CYP71BL2* according to the alignment made by David Nelson (<http://drnelson.uthsc.edu/cytochromeP450.html>).

References

- Barrero AF, Oltra JE, Álvarez M, Raslan DS, Saúde DA, Akssira M. 2000. New sources and antifungal activity of sesquiterpene lactones. *Fitoterapia* 71(1): 60-64.
- Bedoya LM, Abad MJ, Bermejo P. 2008. The role of parthenolide in intracellular signalling processes: Review of current knowledge. *Current Signal Transduction Therapy* 3(2): 82-87.
- Bennett MH, Mansfield JW, Lewis MJ, Beale MH. 2002. Cloning and expression of sesquiterpene synthase genes from lettuce (*Lactuca sativa* L.). *Phytochemistry* 60(3): 255-261.
- Berteau CM, Voster A, Verstappen FWA, Maffei M, Beekwilder J, Bouwmeester HJ. 2006. Isoprenoid biosynthesis in *Artemisia annua*: Cloning and heterologous expression of a germacrene A synthase from a glandular trichome cDNA library. *Archives of Biochemistry and Biophysics* 448(1-2): 3-12.
- Bouwmeester HJ, Kodde J, Verstappen FWA, Altug IG, de Kraker JW, Wallaart TE. 2002. Isolation and characterization of two germacrene A synthase cDNA clones from chicory. *Plant Physiology* 129(1): 134-144.
- Cankar K, Houwelingen Av, Bosch D, Sonke T, Bouwmeester H, Beekwilder J. 2011. A chicory cytochrome P450 mono-oxygenase CYP71AV8 for the oxidation of (+)-valencene. *FEBS Letters* 585(1): 178-182.
- Chen H-C, Chou C-K, Lee S-D, Wang J-C, Yeh S-F. 1995. Active compounds from *Saussurea lappa* Clarks that suppress hepatitis B virus surface antigen gene expression in human hepatoma cells. *Antiviral Research* 27(1-2):

99-109.

- Choi JH, Ha J, Park JH, Lee JY, Lee YS, Park HJ, Choi JW, Masuda Y, Nakaya K, Lee KT. 2002. Costunolide triggers apoptosis in human leukemia U937 cells by depleting intracellular thiols. *Japanese Journal of Cancer Research* 93(12): 1327-1333.
- de Kraker J-W, Franssen MCR, de Groot A, Shibata T, Bouwmeester HJ. 2001. Germacrenes from fresh costus roots. *Phytochemistry* 58(3): 481-487.
- de Kraker J-W, Schurink M, Franssen MCR, König WA, de Groot A, Bouwmeester HJ. 2003. Hydroxylation of sesquiterpenes by enzymes from chicory (*Cichorium intybus* L.) roots. *Tetrahedron* 59(3): 409-418.
- de Kraker JW, Franssen MCR, Dalm MCF, de Groot A, Bouwmeester HJ. 2001. Biosynthesis of germacrene A carboxylic acid in chicory roots. Demonstration of a cytochrome P450 (+)-germacrene A hydroxylase and NADP(+)-dependent sesquiterpenoid dehydrogenase(s) involved in sesquiterpene lactone biosynthesis. *Plant Physiology* 125(4): 1930-1940.
- de Kraker JW, Franssen MCR, de Groot A, König WA, Bouwmeester HJ. 1998. (+)-Germacrene A biosynthesis - The committed step in the biosynthesis of bitter sesquiterpene lactones in chicory. *Plant Physiology* 117(4): 1381-1392.
- de Kraker JW, Franssen MCR, Joerink M, de Groot A, Bouwmeester HJ. 2002. Biosynthesis of costunolide, dihydrocostunolide, and leucodin. Demonstration of cytochrome P450-catalyzed formation of the lactone ring present in sesquiterpene lactones of chicory. *Plant Physiology* 129(1): 257-268.
- De Vos RCH, Moco S, Lommen A, Keurentjes JJB, Bino RJ, Hall RD. 2007. Untargeted large-scale plant metabolomics using liquid chromatography coupled to mass spectrometry. *Nature Protocols* 2(4): 778-791.
- Dean JD, Goodwin PH, Hsiang T. 2005. Induction of glutathione S-transferase genes of *Nicotiana benthamiana* following infection by *Colletotrichum destructivum* and *C. orbiculare* and involvement of one in resistance. *Journal of Experimental Botany* 56(416): 1525-1533.
- Fischer NH. 1990. *Biochemistry of the mevalonic acid pathway to terpenoids*. New York: Plenum Press.
- Habig WH, Pabst MJ, Jakoby WB. 1974. Glutathione s-transferases - First enzymatic step in mercapturic acid formation. *Journal of Biological Chemistry* 249(22): 7130-7139.
- Ikezawa N, Goepfert JC, Nguyen DT, Kim S-U, O'Maille PE, Spring O, Ro D-K. 2011. Lettuce costunolide synthase (CYP71BL2) and its homolog (CYP71BL1) from sunflower catalyze distinct regio- and stereo-selective hydroxylations in sesquiterpene lactone metabolism. *Journal of Biological Chemistry* 286(24): 21601-21611.
- Kappers IF, Aharoni A, van Herpen TWJM, Luckerhoff LL, Dicke M, Bouwmeester HJ. 2005. Genetic engineering of terpenoid metabolism attracts bodyguards to *Arabidopsis*. *Science* 309(5743): 2070-2072.
- Klayman DL. 1985. Qinghaosu (Artemisinin) - an antimalarial drug from China. *Science* 228(4703): 1049-1055.
- Klein M, Mannun YM, Eggmann T, Schuller C, Wolfger H, Martinoia E, Kuchler K. 2002. The ATP-binding cassette (ABC) transporter Bpt1p mediates vacuolar sequestration of glutathione conjugates in yeast. *FEBS Letters* 520(1-3): 63-67.
- Kohlen W, Charnikhova T, Liu Q, Bours R, Domagalska MA, Beguerie S, Verstappen F, Leyser O, Bouwmeester HJ, Ruyter-Spira C. 2011. Strigolactones are transported through the xylem and play a key role in shoot architectural response to phosphate deficiency in non-AM host *Arabidopsis thaliana*. *Plant Physiology*(155): 974-987.
- Koo TH, Lee J-H, Park YJ, Hong Y-S, Kim HS, Kim K-W, Lee JJ. 2001. A sesquiterpene lactone, costunolide, from *Magnolia grandiflora* inhibits NF- κ B by targeting I κ B phosphorylation. *Planta Medica* 67(02): 103,107.
- Lyss G, Knorre A, Schmidt TJ, Pahl HL, Merfort I. 1998. The anti-inflammatory sesquiterpene lactone Helenalin inhibits the transcription factor NF- κ B by directly targeting p65. *Journal of Biological Chemistry* 273(50): 33508-33516.
- Ma X-C, Zheng J, Guo D-A. 2007. Microbial transformation of dehydrocostuslactone and costunolide by *Mucor polymorphosporus* and *Aspergillus candidus*. *Enzyme and Microbial Technology* 40(5): 1013-1019.
- Majdi M, Liu Q, Karimzadeh G, Malboobi MA, Beekwilder J, Cankar K, Vos Rd, Todorovic S, Simonovic A, Bouwmeester H. 2011. Biosynthesis and localization of parthenolide in glandular trichomes of feverfew (*Tanacetum parthenium* L. Schulz Bip.). *Phytochemistry* 72 (14-15): 1739-1750
- Marrs KA. 1996. The functions and regulation of glutathione s-transferases in plants. *Annual Review of Plant Physiology and Plant Molecular Biology* 47(1): 127-158.
- Marrs KA, Alfenito MR, Lloyd AM, Walbot V. 1995. A glutathione-s-transferase involved in vacuolar transfer encoded by the maize gene *Bronze-2*. *Nature* 375(6530): 397-400.
- Moco S, Bino RJ, Vorst O, Verhoeven HA, de Groot J, van Beek TA, Vervoort J, de Vos CHR. 2006. A liquid chromatography-mass spectrometry-based metabolome database for tomato. *Plant Physiology* 141(4): 1205-1218.
- Mori H, Kawamori T, Tanaka T, Ohnishi M, Yamahara J. 1994. Chemopreventive effect of costunolide, a constituent of oriental medicine, on azoxymethane-induced intestinal carcinogenesis in rats. *Cancer Letters* 83(1-2): 171-175.

- Nelson DR.** 2009. The cytochrome P450 homepage. *Human Genomics* 4(1): 59-65.
- Nguyen DT, Gopfert JC, Ikezawa N, Macnevin G, Kathiresan M, Conrad J, Spring O, Ro DK.** 2010. Biochemical conservation and evolution of germacrene A oxidase in asteraceae. *Journal of Biological Chemistry* 285(22): 16588-16598.
- Ohkama-Ohtsu N, Zhao P, Xiang CB, Oliver DJ.** 2007. Glutathione conjugates in the vacuole are degraded by γ -glutamyl transpeptidase GGT3 in Arabidopsis. *Plant Journal* 49(5): 878-888.
- Outchkourov NS, Peters J, de Jong J, Rademakers W, Jongsma MA.** 2003. The promoter-terminator of chrysanthemum *rbcS1* directs very high expression levels in plants. *Planta* 216(6): 1003-1012.
- Park HJ, Jung HJ, Lee KT, Choi J.** 2006. Biological characterization of the chemical structures of naturally occurring substances with cytotoxicity. *Natural Product Science, Korea* 12(4): 175-192.
- Pompon D, Louerat B, Bronine A, Urban P.** 1996. Yeast expression of animal and plant P450s in optimized redox environments. *Methods in Enzymology* 272: 51-64.
- Rea PA.** 1999. MRP subfamily ABC transporters from plants and yeast. *Journal of Experimental Botany* 50: 895-913.
- Ro DK, Paradise EM, Ouellet M, Fisher KJ, Newman KL, Ndungu JM, Ho KA, Eachus RA, Ham TS, Kirby J, Chang MCY, Withers ST, Shiba Y, Sarpong R, Keasling JD.** 2006. Production of the antimalarial drug precursor artemisinic acid in engineered yeast. *Nature* 440(7086): 940-943.
- Rodriguez E, Towers GHN, Mitchell JC.** 1976. Biological activities of sesquiterpene lactones. *Phytochemistry* 15(11): 1573-1580.
- Seto M, Miyase T, Umehara K, Ueno A, Hirano Y, Otani N.** 1988. Sesquiterpene lactones from *Cichorium endivia* L. and *C. intybus* L. and cytotoxic activity. *Chemical & pharmaceutical Bulletin* 36(7): 2423-2429.
- Shimizu H, Araki K, Shioya S, Suga K.** 1991. Optimal production of glutathione by controlling the specific growth-rate of yeast in fed-batch culture. *Biotechnology and Bioengineering* 38(2): 196-205.
- Srivastava SK, Abraham A, Bhat B, Jaggi M, Singh AT, Sanna VK, Singh G, Agarwal SK, Mukherjee R, Burman AC.** 2006. Synthesis of 13-amino costunolide derivatives as anticancer agents. *Bioorganic & Medicinal Chemistry Letters* 16(16): 4195-4199.
- Taniguchi M, Kataoka T, Suzuki H, Uramoto M, Ando M, Arai K, Magae JJ, Nishimura T, Otake N, Nagai K.** 1995. Costunolide and dehydrocostus lactone as inhibitors of killing function of cytotoxic T-Lymphocytes. *Bio-science Biotechnology and Biochemistry* 59(11): 2064-2067.
- Tikunov Y, Lommen A, de Vos CHR, Verhoeven HA, Bino RJ, Hall RD, Bovy AG.** 2005. A novel approach for non-targeted data analysis for metabolomics. Large-scale profiling of tomato fruit volatiles. *Plant Physiology* 139(3): 1125-1137.
- Tremblay R, Wang D, Jevnikar AM, Ma SW.** 2010. Tobacco, a highly efficient green bioreactor for production of therapeutic proteins. *Biotechnology Advances* 28(2): 214-221.
- Turner GW, Croteau R.** 2004. Organization of monoterpene biosynthesis in mentha. Immunocytochemical localizations of geranyl diphosphate synthase, limonene-6-hydroxylase, isopiperitenol dehydrogenase, and pulegone reductase. *Plant Physiology* 136(4): 4215-4227.
- Urban P, Mignotte C, Kazmaier M, Delorme F, Pompon D.** 1997. Cloning, yeast expression, and characterization of the coupling of two distantly related *Arabidopsis thaliana* NADPH-Cytochrome P450 reductases with P450 CYP73A5. *Journal of Biological Chemistry* 272(31): 19176-19186.
- Van Beek TA, Maas P, King BM, Leclercq E, Voragen AGJ, De Groot A.** 1990. Bitter sesquiterpene lactones from chicory roots. *Journal of Agricultural and Food Chemistry* 38(4): 1035-1038.
- van Herpen TWJM, Cankar K, Nogueira M, Bosch D, Bouwmeester HJ, Beekwilder J.** 2010. *Nicotiana benthamiana* as a production platform for Artemisinin precursors. *PLoS ONE* 5(12): e14222.
- Vanengelen FA, Molthoff JW, Conner AJ, Nap JP, Pereira A, Stiekema WJ.** 1995. Pbinplus - an improved plant transformation vector based on Pbin19. *Transgenic Research* 4(4): 288-290.
- Wedge DE, Galindo JCG, Macias FA.** 2000. Fungicidal activity of natural and synthetic sesquiterpene lactone analogs. *Phytochemistry* 53(7): 747-757.
- Yang T, Stoopen G, Yalpani N, Vervoort J, de Vos R, Voster A, Verstappen FWA, Bouwmeester HJ, Jongsma MA.** 2011. Metabolic engineering of geranic acid in maize to achieve fungal resistance is compromised by novel glycosylation patterns. *Metabolic Engineering* 13(4): 414-425.
- Zhang DL, Qiu L, Jin XQ, Guo ZH, Guo CB.** 2009. Nuclear factor- κ B inhibition by parthenolide potentiates the efficacy of taxol in non-small cell lung cancer *in vitro* and *in vivo*. *Molecular Cancer Research* 7(7): 1139-1149.
- Zhang S, Won YK, Ong CN, Shen HM.** 2005. Anti-cancer potential of sesquiterpene lactones: bioactivity and molecular mechanisms. *Current Medicinal Chemistry - Anti-Cancer Agents* 5(3): 239-249.

Chapter 4

In planta reconstitution of the parthenolide biosynthetic pathway

Qing Liu, David Manzano, Nikola Tanić, Milica Pesic, Jasna Bankovic, Irini Pateraki, Lea Ricard, Albert Ferrer, Ric de Vos, Sander van de Krol, Harro Bouwmeester

Submitted

Abstract

Parthenolide, the main bioactive compound of the medicinal plant feverfew (*Tanacetum parthenium*), is a promising anti-cancer drug. Here we report on the isolation and characterization of all the genes from feverfew that are required for the biosynthesis of parthenolide, using a combination of 454 sequencing of a feverfew glandular trichome cDNA library, co-expression analysis and metabolomics. When parthenolide biosynthesis was reconstituted by transient co-expression of all pathway genes in *Nicotiana benthamiana*, up to 1.4 mg.g⁻¹ parthenolide was produced, mostly present as cysteine and glutathione conjugates. These relatively polar conjugates were highly active against colon cancer cells, with only slightly lower activity than free parthenolide. In addition to these biosynthetic genes, another gene encoding a costunolide and parthenolide 3 β -hydroxylase was identified opening up further options to improve the water solubility of parthenolide and therefore its potential as a drug.

Introduction

Sesquiterpene lactones are a major class of plant secondary metabolites and over 4000 different structures have been elucidated (de Kraker et al., 2002). Many of these colourless, frequently bitter tasting, semi-polar molecules are the bioactive constituents of a variety of medicinal plants used in (traditional) medicine (Rodriguez et al., 1976; Zhang et al., 2005). Feverfew (*Tanacetum parthenium*) is one of the most prominent medicinal species in the Asteraceae family and a well-known remedy for the treatment of various diseases (Bedoya et al., 2008). It has been used for at least two millennia for the treatment of fever, as well as headache, menstrual irregularities, stomach-ache and to relieve arthritis and inflammation (Pareek et al., 2011). Parthenolide is the principal bioactive sesquiterpene lactone component in feverfew (Bork et al., 1997). The nucleophilic nature of the methylene- γ -lactone ring and epoxide group of parthenolide enables rapid interactions with different biological targets (Mathema et al., 2012). For instance, parthenolide can promote apoptosis by inhibiting the activity of the NF- κ B transcription factor complex, and thereby down-regulating anti-apoptotic genes under NF- κ B control (Bork et al., 1997; Wen, J. et al., 2002; Kishida et al., 2007; Parada-Turska et al., 2007; Zhang et al., 2009). Parthenolide has been reported to selectively target human leukaemia stem cells, while sparing normal stem or progenitor cells (Guzman et al., 2005). Despite these promising activities, application of this potent natural product is limited by its poor water-solubility (Sweeney et al., 2005). A number of chemically synthesized parthenolide derivatives with increased water solubility –hence allowing oral application – have been shown to retain bioactivity (Guzman et al., 2007; Neelakantan et al., 2009). Very recently, parthenolide and its cyclopropyl analogue have been synthesized chemically from costunolide (Long et al., 2013).

Parthenolide, a germacranolide type sesquiterpene lactone, is presumably derived from costunolide, in line with the proposed precursor role of costunolide for germacranolide-, eudesmanolide- and guaianolide-type sesquiterpene lactones (de Kraker et al., 2002). The initial committed step towards the formation of costunolide is the formation of germacrene A from farnesyl diphosphate (FDP), catalysed by the enzyme (+)-germacrene A synthase (GAS, Fig. 1) (de Kraker et al., 1998). Genes encoding GAS have been cloned from chicory (*Cichorium intybus*) (Bouwmeester et al., 2002), lettuce (*Lactuca sativa*) (Bennett et al., 2002), artemisia (*Artemisia annua*) (Bertea et al., 2006) and feverfew (Liu et al., 2011). In a number of oxidation steps, germacrene A is subsequently converted into germacra-1(10),4,11(13)-trien-12-oic acid by a cytochrome P450 enzyme, germacrene A oxidase (GAO) (de Kraker et al., 2001). Genes encoding GAO have previously been isolated from several Asteraceae species (Nguyen et al., 2010; Cankar et al., 2011). Germacra-1(10),4,11(13)-trien-12-oic acid is subsequently oxidised by costunolide synthase (COS) to 6 α -hydroxy-germacra-1(10),4,11(13)-trien-12-oic acid, which undergoes spontaneous lactone ring formation to yield costunolide (de Kraker et al., 2002; Ikezawa et al., 2011; Liu et al., 2011). Finally, presumably a P450 monooxygenase catalyses the epoxidation of the C4-C5 double bond of costunolide, yielding parthenolide (Liu et al., 2011). The gene encoding the enzyme responsible for that epoxidation, *parthenolide*

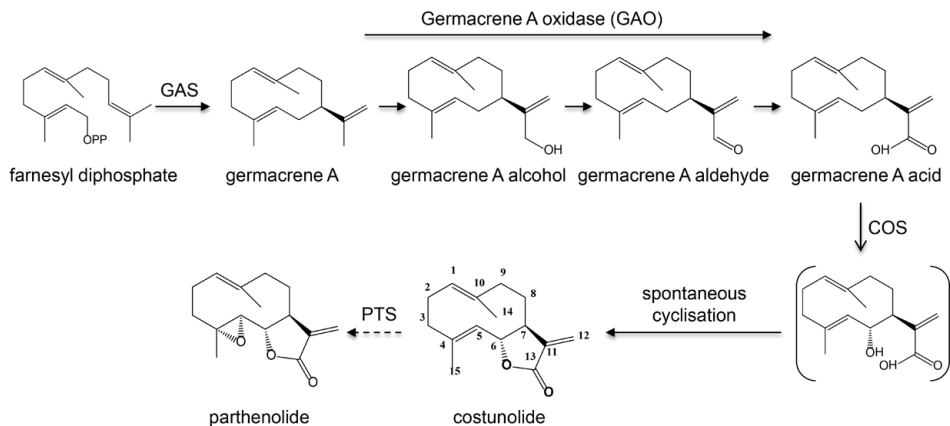


Figure 1. Biosynthetic pathway of parthenolide in feverfew. GAS, germacrene A synthase; COS, costunolide synthase; PTS, parthenolide synthase.

ynthase (PTS), has not been reported yet.

Elucidation of all parthenolide biosynthetic pathway and cloning of the structural genes may enable the production of parthenolide in heterologous systems. Therefore, we set out to identify and isolate all the genes of the parthenolide biosynthetic pathway in feverfew. We have previously reported on the *TpGAS* gene from feverfew (Majdi et al., 2011). Here we report on the isolation and characterisation of the remaining genes required for parthenolide biosynthesis in feverfew (*TpGAO*, *TpCOS* and *TpPTS*). Enzyme activities were characterized by expression of genes in yeast and subsequently the complete parthenolide biosynthetic pathway was reconstituted in *Nicotiana benthamiana*, by co-expression of *TpGAS* with the newly identified *TpGAO*, *TpCOS* and *TpPTS*. Extracts of *N. benthamiana* leaves co-expressing these genes contained free parthenolide, as well as cysteine and glutathione (GSH) conjugates of parthenolide. Because the conjugation to cysteine and GSH affects water solubility, we assessed the biological activity of these parthenolide derivatives in can cell lines. The parthenolide conjugates were less effective than free parthenolide but still displayed considerable anti-cancer activity, particularly in colon cancer cells. In addition to the parthenolide biosynthetic genes, another candidate gene was identified to encode a β -hydroxylase that uses costunolide as well as parthenolide as substrate. This may give additional possibilities to improve the water solubility of parthenolide. The production of parthenolide and more water-soluble conjugates through metabolic engineering of heterologous hosts may provide a sustainable alternative source for the further development of parthenolide as an anti-cancer drug.

Results

Identification of parthenolide biosynthesis candidate genes

Previously we have shown that parthenolide accumulates to high levels in floral glandular trichomes of feverfew (*Tanacetum parthenium*) (Majdi et al., 2011). To identify the genes in-

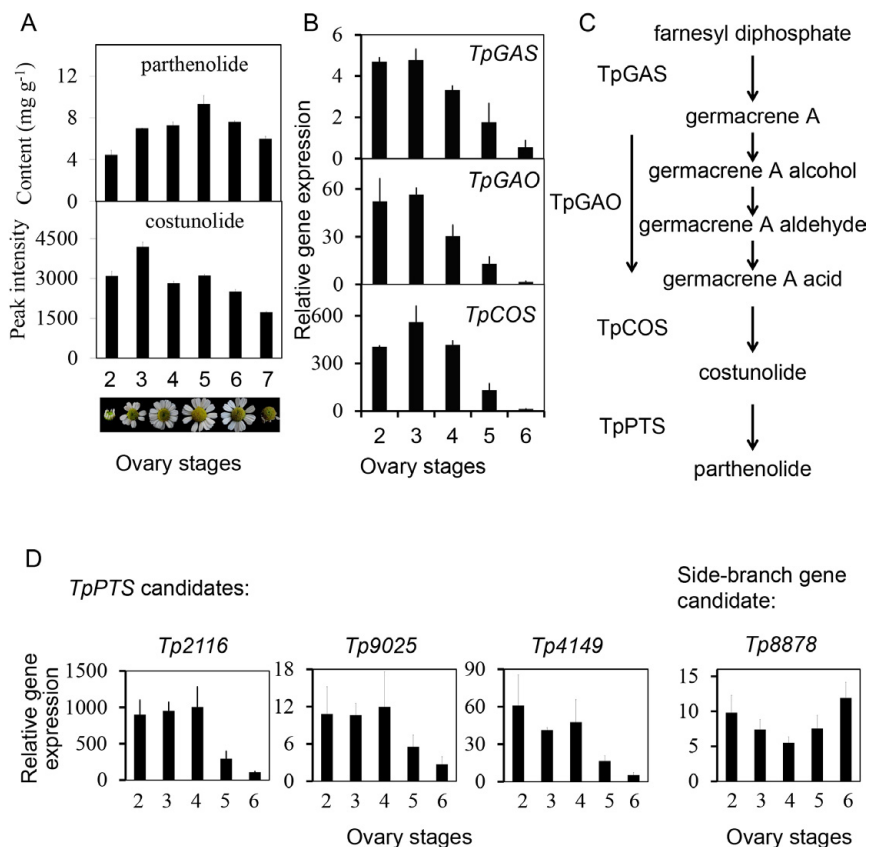


Figure 2. Parthenolide and costunolide content, and expression profile of parthenolide synthase candidates genes during ovary development. (A) Costunolide and parthenolide content in different developmental stages of feverfew ovaries. Bars represent means ($n = 3$) \pm S.E. (B) Gene expression profile of feverfew *germacrene A synthase* (*TpGAS*), *germacrene A oxidase* (*TpGAO*), and *costunolide synthase* (*TpCOS*) during ovary development. (C) Simplified biosynthetic pathway of parthenolide in feverfew. (D) Gene expression profile of *parthenolide synthase* (*TpPTS*) candidates and side-branch gene candidate during ovary development

involved in this parthenolide biosynthesis, mRNA was extracted from isolated flower trichomes and used for deep-sequencing to obtain a feverfew trichome EST database (Majdi et al., 2011). Subsequently, sequences of reported Asteraceae GAOs and COSs were used to blast against the feverfew EST database. Two sets of EST sequences with the highest homology to chicory GAO and chicory COS were assembled into two contigs from which full length open reading frames (ORF) were obtained. The expression of *TpGAS*, putative *TpGAO*, and putative *TpCOS* was profiled in feverfew during ovary development with real time RT-PCR. Those three genes showed similar patterns of expression, which was highest in stage 2 and stage 3 ovaries, and then decreased from stage 4 until virtually zero in stage 6 (Fig. 2B). Moreover, the expression pattern of *TpGAS*, the putative *TpGAO*, and the putative *TpCOS* is consistent

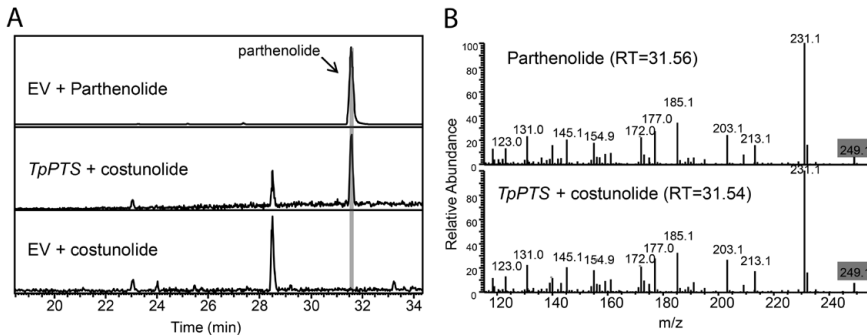


Figure 3. Identification of *parthenolide synthase* (*TpPTS*) using a yeast microsomal assay. (A) LC-Orbitrap-FTMS chromatogram at $m/z=249.14852$ (10 ppm, positive ionization mode) demonstrating that the compound produced by *TpPTS* from costunolide has identical retention time and mass as a parthenolide standard. EV, empty vector. (B) A parthenolide standard and the *TpPTS* product have an identical fragmentation pattern. Grey boxes indicate the parent ion at $[M+H]^+=249.14852$.

with the accumulation profile of parthenolide in ovaries during flower development (Fig. 2): the parthenolide content increased from stage 2 to stage 5, and then decreased slightly. The content of its precursor, costunolide, increased in stage 2 and 3 and then decreased.

Most sesquiterpene-modifying P450s belong to the CYP71 subfamily (Ikezawa et al., 2011). Indeed, the putative feverfew *TpGAO* and *TpCOS* belong to this CYP71 subfamily. Identification of the expected *parthenolide synthase* (*TpPTS*) gene therefore was focussed on P450 sequences showing closest homology to the CYP71 class. Screening of the feverfew EST sequence database for putative *TpPTS* candidates identified twenty eight P450 contigs that belong to the CYP71 family and all have relatively high amino acid sequence similarity with *TpCOS*. To limit the number of candidate genes to be characterized for enzymatic activity, we compared the expression profiles of the candidate genes with *TpGAS*, and the putative *TpGAO* and *TpCOS*, assuming that *TpPTS* will have a similar expression pattern as the upstream genes. Three out of the twenty eight candidate genes - *Tp2116*, *Tp4149*, and *Tp9025* - showed maximum expression in ovary development stage 2-4, similar as *TpGAS*, putative *TpGAO* and *TpCOS* and were therefore considered as *TpPTS* candidate genes (Fig. 2D). Costunolide and parthenolide levels decreased slightly after stage 4 (Fig. 2A), which suggests further metabolism of costunolide and parthenolide in these late stages. Indeed, one of the candidate genes (*Tp8878*) displayed increased expression after ovary development stage 4 (Fig. 2D) and was therefore considered as pathway-side branch candidate gene for costunolide and/or parthenolide conversion. The ORFs of putative *TpGAO* and *TpCOS*, three *TpPTS* candidates (*Tp2116*, *Tp4149*, *Tp9025*), and one pathway side branch candidate (*Tp8878*) were cloned into yeast expression vector pYED60 for expression and characterization.

Functional characterization of parthenolide biosynthesis genes in yeast

***TpGAO* and *TpCOS* candidates:** To test the enzymatic function of the putative *TpGAO*, this gene was expressed in yeast together with the previously characterized gene *TpGAS* (Majdi et al., 2011), and crude yeast extracts were subsequently prepared and analyzed by GC-MS

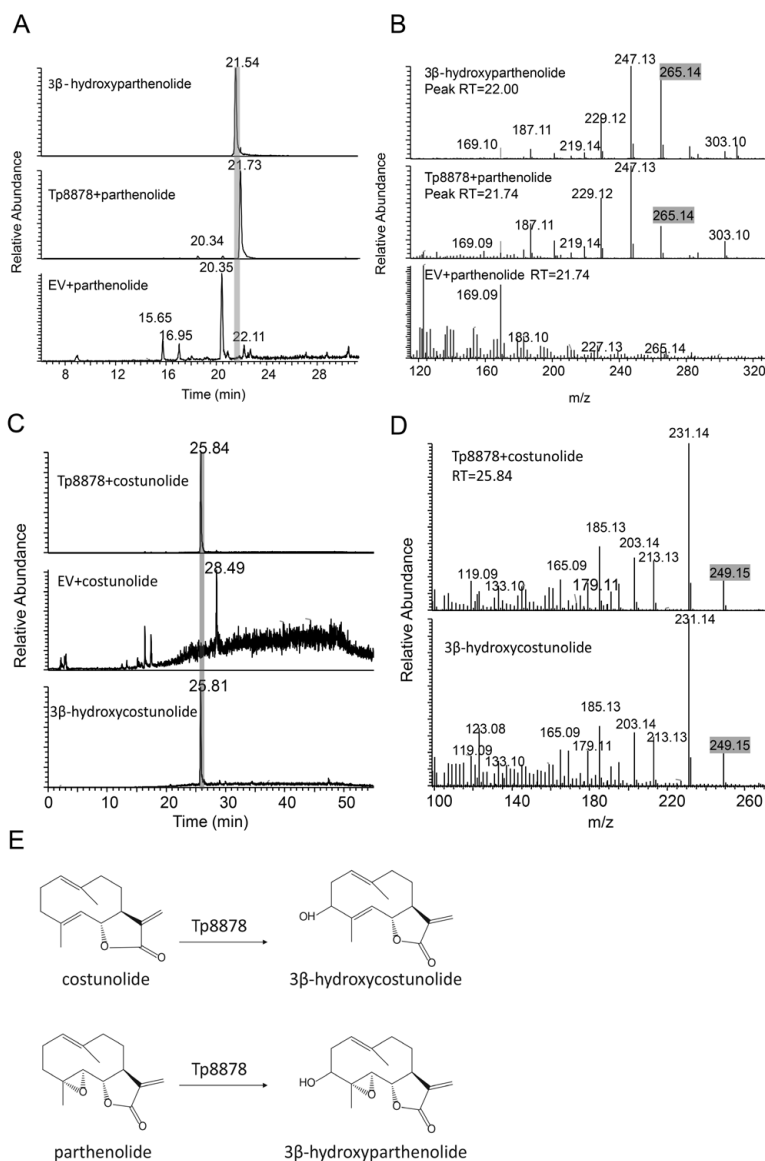


Figure 4. Functional identification of *Tp8878* using a yeast microsomal assay. (A) LC-Orbitrap-FTMS chromatogram at $m/z=265.14344$ (10 ppm, positive ionization mode) demonstrating that the compound produced by *Tp8878* from parthenolide has identical retention time as a 3β-hydroxyparthenolide standard. EV, empty vector. (B) A 3β-hydroxyparthenolide standard and *Tp8878* product have an identical fragmentation pattern. Grey boxes indicate the parent ion at $[M+H]^+=265.14344$. (C) LC-Orbitrap-FTMS chromatogram at $m/z=249.14852$ (10 ppm, positive ionization mode) demonstrating that the compound produced by *Tp8878* from costunolide has identical retention time as a 3β-hydroxycostunolide standard. EV, empty vector. (D) A 3β-hydroxycostunolide standard and the *Tp8878* product have an identical fragmentation pattern. Grey boxes indicate the parent ion at $[M+H]^+=249.14852$. (E) Molecular structures of costunolide, 3β-hydroxycostunolide, parthenolide, and 3β-hydroxyparthenolide.

for the presence of sesquiterpene lactones. Cells expressing *TpGAS+TpGAO* showed a clear GC-MS peak of elementrien-12-oic acid, which is missing in cells expressing *TpGAS* alone. This compound is a cope-rearrangement product of germacra-1(10),4,11(13)-trien-12-oic acid (Supplementary Fig. 3), showing that the protein encoded by *TpGAO* is able to catalyze oxidation of germacrene A to germacra-1(10),4,11(13)-trien-12-oic acid (Fig. 1). To test the catalytic function of the putative *TpCOS*, the gene was co-expressed with *TpGAS* and *TpGAO* in yeast. Compared to the products produced by yeast cells expressing both *TpGAS* and *CiGAO*, the extracts of yeast cells expressing *TpGAS+TpGAO+TpCOS* showed a new GC-MS peak which was identified as costunolide, while the peak for germacra-1(10),4,11(13)-trien-12-oic acid was strongly reduced (Supplementary Fig. 3). Thus, it is confirmed that the protein encoded by the putative *TpCOS* gene is able to catalyze the conversion of germacra-1(10),4,11(13)-trien-12-oic acid to costunolide.

Characterization of parthenolide synthase candidates

To test the catalytic activity of *TpPTS* candidates, microsomes of yeast expressing *Tp2116*, *Tp4149*, and *Tp9025* were isolated and incubated with costunolide. Compared to the microsomes from yeast transformed with the control construct, the microsomes from yeast expressing *Tp2116* induced a new LC-MS peak that was unambiguously identified as parthenolide ($[M+H]^+=249$, retention time and mass spectrum match with that of the parthenolide standard) (Fig. 3). An official name CYP71CA1 was assigned to this *parthenolide synthase* (*TpPTS*). No new peaks were detected in the assays with microsomes isolated from yeast expressing *Tp4149* or *Tp9025*.

To test the catalytic activity of *Tp8878*, a candidate assumed to be involved in a side branch of parthenolide biosynthesis, microsomes of yeast transformed with *Tp8878* were isolated and incubated with costunolide or parthenolide. With parthenolide as a substrate, a new LC-MS peak was detected which was identified as 3 β -hydroxyparthenolide ($[M+H]^+=265$, retention time and mass spectrum matches that of the 3 β -hydroxyparthenolide standard) (Fig. 4A and 4B). With costunolide as a substrate, also a new product peak was detected, which was identified as 3 β -hydroxycostunolide ($[M+H]^+=249$, retention time and mass spectrum matches that of a 3 β -hydroxycostunolide standard) (Fig. 4C and 4D). An official name CYP71CB1 was assigned to this 3 β -hydroxylase.

Reconstitution of the parthenolide biosynthetic pathway in *Nicotiana benthamiana*

With all the genes for the production of parthenolide available, we aimed to reconstitute the parthenolide biosynthetic pathway in the plant host *N. benthamiana* through transient heterologous gene expression. In addition, we tested the effect on product accumulation of the co-expression of the pathway genes together with a soluble *Arabidopsis thaliana* HMG-CoA reductase (*AtHMGR*) which can increase FDP substrate availability needed for the pathway. Hereto, the *AtHMGR*, *TpGAS*, *TpGAO*, *TpCOS* and *TpPTS* (*CYP71CA1*) coding sequences were cloned into the binary expression vector pBIN under the control of the Rubisco promoter (RBC). *Agrobacterium tumefaciens* was transformed with the various binary expression vectors and leaves were co-infiltrated with different combinations of the transformed A. tu-

Table 1. New metabolites detected in *N. benthamiana* leaves agro-infiltrated by different combinations of genes

Metabolites	Combinations of genes transiently expressed in <i>N. benthamiana</i> leaves ^a					
	<i>GAS</i>	<i>GAS+GAO</i>	<i>GAS+GAO+COS</i>	<i>GAS+GAO+COS+PTS</i>	<i>AtHMGR+GAS+GAO+COS+PTS</i>	<i>AtHMGR+GAS+GAO+COS+PTS+8878</i>
germacrene A	†† ^b	†	- ^c	-	-	-
germacra-1(10),4,11(13)-trien-12-oic acid	-	-	-	-	-	-
costunolide	-	-	††	†	††	††
costunolide-GSH	-	-	†††	††	†††	†††
costunolide-cysteine	-	-	††††	†††	††††	††††
parthenolide	-	-	-	-	†	†
parthenolide-GSH	-	-	-	†	††	††
parthenolide-cysteine	-	-	-	††	†††	†††
3β-hydroxycostunolide	-	-	-	-	-	-
3β-hydroxycostunolide-GSH	-	-	-	-	-	†
3β-hydroxycostunolide-cysteine	-	-	-	-	-	††
3β-hydroxyparthenolide	-	-	-	-	-	-
3β-hydroxyparthenolide-GSH	-	-	-	-	-	-
3β-hydroxyparthenolide-cysteine	-	-	-	-	-	-

^a *GAS*, germacrene A synthase; *GAO*, germacrene A oxidase; *COS*, costunolide synthase; *PTS*, parthenolide synthase; 8878, 3β-hydroxylase.

^b †: metabolites detected by LC-MS. The number of † indicates their relative level.

^c - means metabolites not detected by LC-MS.

tumefaciens strains to reconstitute the parthenolide biosynthetic pathway in *N. benthamiana* step by step.

***TpGAS* and *TpGAS+TpGAO*:** Four days after infiltration with the *A. tumefaciens* strain carrying the RBC:*TpGAS* construct, the *N. benthamiana* leaves emitted the volatile compound germacrene A into their headspace (Table 1 and Supplementary Fig. 4). When leaves were co-infiltrated with two *A. tumefaciens* strains carrying the *TpGAS* and *TpGAO* constructs, respectively, germacrene A levels in the headspace were reduced by 90% compared to infiltration with *TpGAS* alone, suggesting that *TpGAO* can efficiently utilise germacrene A. However, no new product peaks were detected neither in the headspace nor in dichloromethane (DCM) extracts of the infiltrated leaves, indicating that the expected products of the *TpGAO* enzyme, germacra-1(10),4,11(13)-trien-12-ol, germacra-1(10),4,11(13)-trien-12-al and germacra-1(10),4,11(13)-trien-12-oic acid, are not stable *in planta* or are further metabolized into other products, analogous to our previous results obtained with the heterologous expressed *CiGAO* gene (Liu et al., 2011). Using high mass resolution LC-QTOF-MS in negative ionization mode, we checked whether any germacra-1(10),4,11(13)-trien-12-oic acid produced was possibly glycosylated within the *N. benthamiana* leaves, but accurate mass signals corresponding to the elemental formulae of the acid conjugated to either a hexose, a deoxyhexose or a pentose, or to combinations thereof, were not detected. We nevertheless decided to infiltrate the next gene of the pathway to see if the anticipated product and hence the substrate of the next enzyme was produced or not.

***TpGAS+TpGAO+TpCOS*:** Co-infiltration of *A. tumefaciens* strains carrying the *TpGAS*, *TpGAO* and *TpCOS* expression constructs did result in the production of costunolide at four days post-infiltration (Table 1 and Supplementary Fig. 5A). The average production of costunolide was $9.6 \pm 0.8 \mu\text{g.g}^{-1}$ FW (n=8). No costunolide was detected in extracts from leaves upon transient expression of the empty vector (pBIN), neither in those of *TpGAS* alone, *TpGAS+TpGAO* or *TpGAS+TpCOS*, indicating that the production of costunolide in *N. benthamiana*

Table 2. IC 50 values (μM) of parthenolide and its conjugates acquired by sulforhodamine B viability test

	NCI-H460 ^a	NCI-H460/R ^b	U87 ^c	U87-TxR ^d	DLD1 ^e	DLD1-TxR ^f	HT-29 ^e	HaCaT ^g
Parthenolide	2.1	6.8	40.5	26.7	2.1	1.8	3.6	10.6
Parthenolide-Cysteine	76.8	46.9	107.7	105.0	37.0	33.1	17.3	65.7
Parthenolide-Glutathione	71.4	44.7	120.8	83.3	29.2	23.1	10.7	57.9

^a Sensitive non-small cell lung carcinoma cell line

^b Multi-drug resistant non-small cell lung carcinoma cell line derived from its sensitive counterpart

^c Sensitive glioblastoma cell line

^d Multi-drug resistant glioblastoma cell line derived from its sensitive counterpart

^e Sensitive colon carcinoma cell lines

^f Multi-drug resistant colon carcinoma cell line derived from its sensitive counterpart DLD1

^g Normal human keratinocyte

amiana leaves is dependent on the presence of three genes: *TpGAS*, *TpGAO* and *TpCOS*.

To investigate whether there were any other unexpected products formed in the infiltrated leaves, we performed untargeted LC-QTOF-MS analysis of leaf extracts. This resulted in the detection of two chromatographic peaks eluting at 22.24 and 22.48 min in leaves infiltrated with *TpGAS*+*TpGAO*+*TpCOS* that were absent in leaves infiltrated with *TpGAS*+*TpGAO* (Supplementary Fig. 5B-E). These two *TpCOS*-induced products were identified as the cysteine and glutathione (GSH) conjugates of costunolide, respectively.

***TpGAS* +*TpGAO*+*TpCOS*+*TpPTS* with boosting by *AtHMGR*:** No free parthenolide was detected in leaf extracts transiently expressing the four genes *TpGAS*+*TpGAO*+*TpCOS*+*TpPTS* (Table 1). In an attempt to boost the availability of substrate for the parthenolide pathway, we also co-expressed *AtHMGR*. In combination with *TpGAS*+*TpGAO*+*TpCOS*, this resulted in 4-fold increased costunolide production (Supplementary Fig. 6B). When *AtHMGR* was co-expressed with *TpGAS*+*TpGAO*+*TpCOS*+*TpPTS*, free parthenolide was detected (2.05 ng.g⁻¹ FW) four days after infiltration by MRM-LC-MS (Supplementary Fig. 6A). Moreover, two new LC-QTOF-MS peaks eluting at 17.74 and 18.53 min were detected, which were absent in leaves infiltrated with *TpGAS*+*TpGAO*+*TpCOS*+*pBIN* as control. The exact mass and comparison with standards identified these products as the cysteine and GSH conjugates of parthenolide (Supplementary Fig. 6C-F). Total parthenolide yield (including the conjugates) was about 1.4 mg.g⁻¹ FW.

***TpGAS* +*TpGAO*+*TpCOS*+*TpTPS*+*Tp8878* with boosting by *AtHMGR*:** To verify the function of *Tp8878* (*CYP71CB1*) in *planta*, *A. tumefaciens* strains with the parthenolide pathway constructs plus *AtHMGR* were infiltrated into *N. benthamiana* together with *A. tumefaciens* with the *Tp8878* expression construct. Compared with the control (parthenolide pathway without *Tp8878*) one new peak (RT=14.68 min) was detected that was identified as 3 β -hydroxycostunolide-GSH (both retention time and mass spectrum match that of a 3 β -hydroxycostunolide-GSH standard) (Table 1 and Supplementary Fig. 7A-B). A second new peak was identified as 3 β -hydroxycostunolide-cysteine. GSH or cysteine conjugates of 3 β -hydroxyparthenolide was not detectable in these samples. Compared with leaves infiltrated with only the costunolide pathway, about 50% of the original costunolide conjugates were converted into

parthenolide when *TpPTS* was added to the infiltration mix. When *Tp8878* was co-infiltrated with the costunolide pathway together with *TpPTS*, about 40% of the costunolide conjugates were converted, yet the amount of parthenolide conjugates was decreased by 71% (Supplementary Fig. 7C). This is possibly the result of 3-hydroxylation of parthenolide by *Tp8878*, as we showed to occur in yeast microsomes (Fig. 4), but we were unable to detect any parthenolide-derived compounds.

Anti-cancer activity of parthenolide conjugates in cell lines

The anti-cancer effect of parthenolide GSH and cysteine conjugates was examined in 8 different human cell lines: both sensitive and multi-drug resistant lines of non-small cell lung carcinoma, glioblastoma and colon carcinoma cells as well as normal human keratinocytes (Table 2). Parthenolide-cysteine and parthenolide-GSH conjugates were less potent than free parthenolide: the concentrations necessary to inhibit cell growth by 50% (IC50 values) for conjugates were significantly higher than for free parthenolide in all tested cancer cell lines and normal human keratinocytes. Nevertheless, IC50 values of the conjugates for colon cancer cells are substantially lower than those for normal cells (HaCaT), indicating selectivity of both parthenolide conjugates towards colon carcinoma cells. The parthenolide-cysteine and parthenolide-GSH conjugates exerted the highest bioactivity in HT-29 cells (colon adenocarcinoma) with IC50s of 17.3 and 10.7 μM , respectively. The sensitivity to free or conjugated parthenolide was not affected by multi-drug resistance as the inhibitory profiles of the compounds were similar in both sensitive (DLD1) and resistant (DLD1-TxR) colon carcinoma cell lines (Table 2, Supplementary Fig. 8). Cysteine and GSH, when applied alone, had no influence on cell growth (Supplementary Fig. 8).

Discussion

The sesquiterpene lactone parthenolide from feverfew is a promising anti-cancer drug. The identification of feverfew *parthenolide synthase* (*TpPTS*) which uses costunolide as substrate confirms the hypothesis that parthenolide is derived from costunolide through epoxidation of the C4-C5 double bond (Liu et al., 2011). With the identified *germacrene A synthase* (*TpGAS*) (Majdi et al., 2011), *germacrene A oxidase* (*TpGAO*), costunolide synthase (*TpCOS*) and *TpPTS* we have isolated all structural genes of the biosynthetic pathway from the universal sesquiterpene precursor farnesyl diphosphate (FDP) (Majdi et al., 2011) up to parthenolide. Expression of these genes in the heterologous hosts *Nicotiana benthamiana* results in the formation of parthenolide plus a number of parthenolide conjugates, which may provide an attractive option for a more efficient and controlled production of this compound. The successful identification of the *TpPTS* gene shows that gene mining based on sequence similarity to related enzymes in combination with gene expression profiling is a good strategy to identify candidate genes involved in plant secondary metabolite pathways.

In the present study we showed that the production of parthenolide in a heterologous host plant species is feasible. No free parthenolide was detected in *N. benthamiana* leaves infiltrated with *TpGAS+TpGAO+TpCOS+TpPTS* by sensitive UPLC-MRM-MS, but when

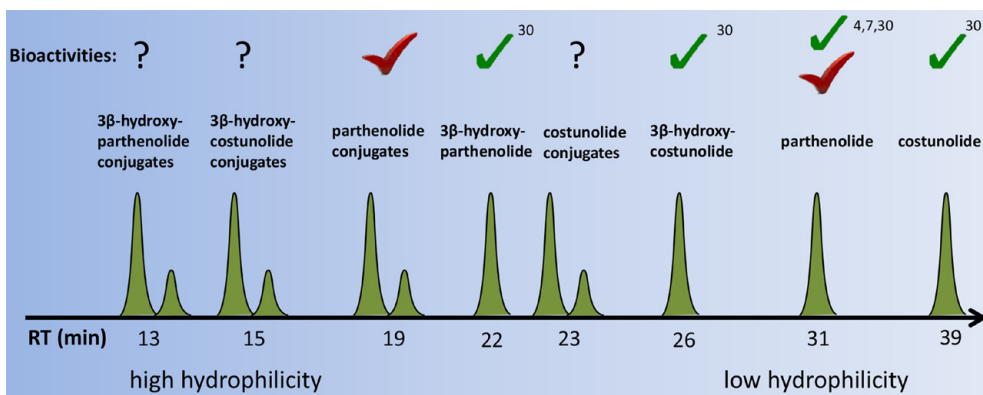


Figure 5. Relative hydrophilicity and bioactivity of compounds identified during the reconstitution of the parthenolide biosynthetic pathway in *N. benthamiana*. The x-axis indicates the retention time of compounds using C18 reverse phase HPLC. The higher the retention time, the lower the hydrophilicity of the molecule. Green-check marks indicate that bioactivities of the corresponding compounds have been reported; the numbers after the green-check marks indicating the corresponding references; question marks indicate that the bioactivities of corresponding compounds are unknown; red-check mark indicates that the bioactivity of the corresponding compound has been identified in the present study.

AtHMGR was added to boost the supply of the precursor FDP, indeed a trace amount of free parthenolide ($2.05 \text{ ng.g}^{-1} \text{ FW}$) was detected. This low amount of free parthenolide was caused by the conjugation of the parthenolide produced towards both parthenolide-cysteine ($1368.4 \text{ ng.g}^{-1} \text{ FW}$) and parthenolide-GSH ($87.5 \text{ ng.g}^{-1} \text{ FW}$) conjugates. As costunolide, parthenolide and the hydroxylated products are cytotoxic, conjugation to GSH or cysteine may be part of a detoxification reaction of the *N. benthamiana* host cells. The cysteine-conjugates may be produced from the GSH-conjugate through the actions of peptidases (Marrs, 1996). As the conjugation to GSH is reversible (Heilmann et al., 2001) at physiological pH and the conjugation to cysteine is not, this would explain the relatively high levels of cysteine-conjugated products.

More than 90% of the total parthenolide produced in *N. benthamiana* was conjugated to either cysteine or GSH, while more than 95% of the parthenolide detected in the trichomes of feverfew was present as free parthenolide. *TpGAS* was found to be expressed much higher in the trichomes compared in the other tissues (Majdi et al., 2011). Trichome specific expression of a diterpene synthase in transgenic tobacco was recently reported (Ennajdaoui et al., 2010). To obtain higher production of free parthenolide in heterologous plants host, it would be a good option to try tissue specific expression in trichomes to prevent conjugation. An alternative host could be lettuce (*Lactuca sativa*) or chicory (*Cichorium intybus*). Both can produce costunolide and its derivatives, that are accumulating in specialized structures called laticifers throughout the plant (Hagel et al., 2008). Thus lettuce and chicory could potentially be used as a production platform for the heterologous production of parthenolide.

As water solubility is one of the major limiting factors for parthenolide being used as an

anti-cancer drug (Shanmugam et al., 2006), obtaining more water-soluble parthenolide derivatives or analogues can be of interest. We have isolated *Tp8878* and showed that it encodes a cytochrome P450 enzyme that can oxidise both costunolide and parthenolide to produce the more polar derivatives 3 β -hydroxycostunolide and 3 β -hydroxyparthenolide respectively (Fig. 4). Indeed, both compounds have also been detected in feverfew extracts (Fischedick et al., 2012). Hydroxylation makes these compounds more polar and may also allow additional enzymatic or chemical modifications to further improve water solubility. 3 β -Hydroxyparthenolide has been shown to be active in the treatment of neurodegenerative disease (Fischedick et al., 2012), suggesting the additional hydroxyl group does not compromise its biological activity.

Previous studies have demonstrated the anti-cancer property of parthenolide *in vitro*, through induction of apoptotic cell death in a number of human cancer cell lines (Mathema et al., 2012). The depletion of intracellular GSH by parthenolide probably contributes to its apoptotic activity (Wen, Jing et al., 2002; Zhang et al., 2004), indicating that the anti-cancer effect of parthenolide involves interaction with GSH. Indeed, in our study, the parthenolide-GSH and parthenolide-cysteine conjugates showed less biological activity than free parthenolide in the cancer cell lines investigated. However, even though less effective in most cell lines, these conjugates showed quite high and selective activity against colon carcinoma cells and this feature could be an advantage in colon cancer treatment. Perhaps they act as a pro-drug in these cells, requiring biotransformation into free parthenolide to exert the anti-cancer effect.

The relative polarity (hydrophilicity) of the sesquiterpene lactones identified in this study can be deduced from their relative retention times in the C18 reverse phase LC-MS chromatograms (Fig. 5). Considering that poor water-solubility of parthenolide (and its oxidised derivatives) is a significant limitation for its application in cancer treatment (Sweeney et al., 2005) and that parthenolide-conjugates are selectively active against colon cancer cells, the conjugation of parthenolide and its oxidised derivatives could be a new strategic tool in drug development for cancer treatment.

In conclusion, the isolation of the genes encoding the entire parthenolide biosynthetic pathway will enable the industrial scale production of parthenolide in heterologous systems such as plants, yeast or other micro-organisms. The success of that will improve the availability of parthenolide - and parthenolide derivatives with improved chemical properties - and hence speed up the development of parthenolide-based anti-cancer drugs.

Experimental Procedures

Detailed description of the Gene expression analysis, Headspace analysis and Thermodesorption GC-MS, LC-QTOF-MS LC-Orbitrap-FTMS analysis of leaf extracts, parthenolide detection and quantification by LC-MRM-MS and Cysteine and glutathione (GSH) conjugation can be found in the supplementary data.

Isolation and cloning of full length candidate genes from feverfew

An EST library constructed from mRNA isolated from feverfew (*Tanacetum parthenium*) trichomes as reported before (Majdi et al., 2011) was used for gene isolation. For *TpGAO* and *TpCOS* candidates, one contig was identified for each gene by sequence homology to known GAOs (*LsGAO*, GU198171; *CiGAO*, GU256644; *SiGAO*, GU256646; *HaGAO*, GU256645; *BsGAO*, GU256647) and COSs (*LsCOS*, AEI59780; and *CiCOS*, AEG79727). Twenty-eight parthenolide synthase candidate cytochrome P450 contigs were identified by sequence homology to known sesquiterpene monooxygenases of the CYP71 subfamily. Four of them, *Tp2116*, *Tp4149*, *Tp9025* and *Tp8878*, were selected for functional characterization based on their expression profile during ovary development. RACE PCR (Clontech) was used to obtain the sequence of the 5'- and 3'-region of all candidate contigs. Full length cDNAs of candidate genes were amplified from feverfew cDNA with the addition of NotI/PacI restriction sites. The cDNAs were subsequently cloned into the yeast expression vector pYEDP60 (Pompon et al., 1996) and sequenced. The cDNA sequences of all candidates genes have been deposited in GenBank: *TpGAO*, KC964544; *TpCOS*, KC964545, *Tp8878*, KC954153; *Tp9025*, KC954154; *Tp2116* (*TpPTS*), KC954155; *Tp4149*, KC954156. The sequences were also submitted to David Nelson's cytochrome P450 homepage (<http://drnelson.uthsc.edu/cytochromeP450.html>), *Tp2116* and *Tp8878* were assigned the name as CYP71CA1 and CYP71CB1, respectively (Nelson, 2009).

Plasmid construction for gene expression in yeast

TpGAO, *TpCOS* and three parthenolide synthase candidates (*Tp2116*, *Tp4149*, *Tp9025*) were cloned into pYED60 vector using NotI/PacI restriction sites. The obtained constructs were named *TpGAO::pYED60*, *TpCOS::pYED60*, *Tp2116::pYED60*, *Tp4149::pYED60*, and *Tp9025::pYED60*. *TpGAS::pYES3* (Liu et al., 2011) plus *TpGAO::pYED60* and *TpGAS/TpGAO::pESC-Trp* plus *TpCOS::pYEDP60* were co-transformed into the WAT11 (Urban et al., 1997) yeast strain. After transformation yeast clones containing both plasmids were selected on SD minimal medium supplemented with amino acids, but omitting uracil, adenine sulphate and L-tryptophane for auxotrophic selection of transformants.

Yeast in vitro microsomal assay

The procedure of the yeast microsomal isolation is described in detail in the supplementary data. For in vitro microsomal assays, 72 µl isolated microsomal fractions, 10 µl substrate (of a 10mM stock in DMSO), 100 µl NADPH (of a 10mM stock in 100mM potassium buffer), 20 µl potassium buffer (1M, pH7.5), and 288 µl water were mixed and incubated for 2.5 h at 25 °C with shaking (200 rpm). Then the mixture was centrifuged at 12000 rpm for 10 min. The supernatant was filtered through an 0.22 µm filter before analysis of the products by LC-Orbitrap-FTMS (for details see supplementary data).

Plasmid construction and transient expression in *N. benthamiana*

For transient expression in *N. benthamiana*, *TpGAS*, *TpGAO*, *TpCOS*, *Tp8878*, and 3 parthenolide synthase candidates (*Tp2116*, *Tp4149*, *Tp9025*) were cloned into ImpactVector1.1 (<http://www.wageningenur.nl/en/show/Productie-van-farmaceutische-en-industriele-eiwit>

ten-door-planten.htm) to express them under the control of the Rubisco (RBC) promoter (Outchkourov et al., 2003). *TpGAS* was also cloned into ImpactVector1.5 to fuse it with the RBC promoter and the CoxIV mitochondrial targeting sequence as we have demonstrated before that mitochondrial targeting of sesquiterpene synthases results in improved sesquiterpene production (2011). An LR reaction (Gateway-LR Clonase TM II) was carried out to clone each gene into the pBinPlus binary vector (Vanengelen et al., 1995) between the right and left borders of the T-DNA for plant transformation. *A. tumefaciens* infiltration (agro-infiltration) for transient expression in *N. benthamiana* was performed as described by Liu et al. (2011). After infiltration the plants were grown for another four and half days and then harvested for analysis.

Acknowledgements

We thank Francel Verstappen for assistance with MRM-LC-MS analysis, Bert Schipper for assistance with LC-QTOF-MS and LC-Orbitrap-MS analysis, Miriam Goedbloed for assistance with making expression constructs, Justin T. Fishedick for providing standards isolated from feverfew. This project was funded by the European Commission (EU-project TerpMed, Plant Terpenoids for Human Health: a chemical and genomic approach to identify and produce bioactive compounds, Grant agreement no.: 227448). Ric C.H. de Vos acknowledges additional funding by the Netherlands Metabolomics Centre and the Centre for BioSystems Genomics, both of which are part of the Netherlands Genomics Initiative / Netherlands Organization for Scientific Research.

References

- Bedoya LM, Abad MJ, Bermejo P. 2008.** The role of parthenolide in intracellular signalling processes: Review of current knowledge. *Current Signal Transduction Therapy* 3(2): 82-87.
- Bennett MH, Mansfield JW, Lewis MJ, Beale MH. 2002.** Cloning and expression of sesquiterpene synthase genes from lettuce (*Lactuca sativa* L.). *Phytochemistry* 60(3): 255-261.
- Berteau CM, Voster A, Verstappen FWA, Maffei M, Beekwilder J, Bouwmeester HJ. 2006.** Isoprenoid biosynthesis in *Artemisia annua*: Cloning and heterologous expression of a germacrene A synthase from a glandular trichome cDNA library. *Archives of Biochemistry and Biophysics* 448(1-2): 3-12.
- Bork PM, Schmitz ML, Kuhnt M, Escher C, Heinrich M. 1997.** Sesquiterpene lactone containing Mexican Indian medicinal plants and pure sesquiterpene lactones as potent inhibitors of transcription factor NF- κ B. *FEBS Letters* 402(1): 85-90.
- Bouwmeester HJ, Kodde J, Verstappen FWA, Altug IG, de Kraker JW, Wallaart TE. 2002.** Isolation and characterization of two germacrene A synthase cDNA clones from chicory. *Plant Physiology* 129(1): 134-144.
- Cankar K, Houwelingen Av, Bosch D, Sonke T, Bouwmeester H, Beekwilder J. 2011.** A chicory cytochrome P450 mono-oxygenase CYP71AV8 for the oxidation of (+)-valencene. *FEBS Letters* 585(1): 178-182.
- de Kraker JW, Franssen MCR, Dalm MCF, de Groot A, Bouwmeester HJ. 2001.** Biosynthesis of germacrene A carboxylic acid in chicory roots. Demonstration of a cytochrome P450 (+)-germacrene A hydroxylase and NADP(+)-dependent sesquiterpenoid dehydrogenase(s) involved in sesquiterpene lactone biosynthesis. *Plant Physiology* 125(4): 1930-1940.
- de Kraker JW, Franssen MCR, de Groot A, König WA, Bouwmeester HJ. 1998.** (+)-Germacrene A biosynthesis - The committed step in the biosynthesis of bitter sesquiterpene lactones in chicory. *Plant Physiology* 117(4): 1381-1392.
- de Kraker JW, Franssen MCR, Joerink M, de Groot A, Bouwmeester HJ. 2002.** Biosynthesis of costunolide, dihydrocostunolide, and leucodin. Demonstration of cytochrome P450-catalyzed formation of the lactone ring

- present in sesquiterpene lactones of chicory. *Plant Physiology* **129**(1): 257-268.
- Ennajdaoui H, Vachon G, Giacalone C, Besse I, Sallaud C, Herzog M, Tissier A. 2010.** Trichome specific expression of the tobacco (*Nicotiana glauca*) cembratrien-ol synthase genes is controlled by both activating and repressing cis-regions. *Plant Molecular Biology* **73**(6): 673-685.
- Fischedick JT, Standiford M, Johnson DA, De Vos RCH, Todorović S, Banjanac T, Verpoorte R, Johnson JA. 2012.** Activation of antioxidant response element in mouse primary cortical cultures with sesquiterpene lactones isolated from *Tanacetum parthenium*. *Planta Medica*(EFirst).
- Guzman ML, Rossi RM, Karnischky L, Li X, Peterson DR, Howard DS, Jordan CT. 2005.** The sesquiterpene lactone parthenolide induces apoptosis of human acute myelogenous leukemia stem and progenitor cells. *Blood* **105**(11): 4163-4169.
- Guzman ML, Rossi RM, Neelakantan S, Li XJ, Corbett CA, Hassane DC, Becker MW, Bennett JM, Sullivan E, Lachowicz JL, Vaughan A, Sweeney CJ, Matthews W, Carroll M, Liesveld JL, Crooks PA, Jordan CT. 2007.** An orally bioavailable parthenolide analog selectively eradicates acute myelogenous leukemia stem and progenitor cells. *Blood* **110**(13): 4427-4435.
- Hagel JM, Yeung EC, Facchini PJ. 2008.** Got milk? The secret life of laticifers. *Trends in Plant Science* **13**(12): 631-639.
- Heilmann J, Wasescha MR, Schmidt TJ. 2001.** The influence of glutathione and cysteine levels on the cytotoxicity of helenanolide type sesquiterpene lactones against KB cells. *Bioorganic & Medicinal Chemistry* **9**(8): 2189-2194.
- Ikezawa N, Goepfert JC, Nguyen DT, Kim S-U, O'Maille PE, Spring O, Ro D-K. 2011.** Lettuce costunolide synthase (CYP71BL2) and its homolog (CYP71BL1) from sunflower catalyze distinct regio- and stereo-selective hydroxylations in sesquiterpene lactone metabolism. *Journal of Biological Chemistry* **286**(24): 21601-21611.
- Kishida Y, Yoshikawa H, Myoui A. 2007.** Parthenolide, a natural inhibitor of Nuclear Factor- κ B, inhibits lung colonization of murine osteosarcoma cells. *Clinical Cancer Research* **13**(1): 59-67.
- Liu Q, Majdi M, Cankar K, Goedbloed M, Charnikhova T, Verstappen FWA, de Vos RCH, Beekwilder J, van der Krol S, Bouwmeester HJ. 2011.** Reconstitution of the costunolide biosynthetic pathway in yeast and *Nicotiana glauca*. *PLoS ONE* **6**(8): e23255.
- Long J, Ding Y-H, Wang P-P, Zhang Q, Chen Y. 2013.** Protection-group-free semisyntheses of parthenolide and its cyclopropyl analogue. *Journal of Organic Chemistry* DOI: 10.1021/jo401606q.
- Majdi M, Liu Q, Karimzadeh G, Malboobi MA, Beekwilder J, Cankar K, Vos Rd, Todorović S, Simonović A, Bouwmeester H. 2011.** Biosynthesis and localization of parthenolide in glandular trichomes of feverfew (*Tanacetum parthenium* L. Schulz Bip.). *Phytochemistry* **72**(14-15): 1739-1750.
- Marrs KA. 1996.** The functions and regulation of glutathione S-transferases in plants. *Annual Review of Plant Physiology and Plant Molecular Biology* **47**(1): 127-158.
- Mathema V, Koh Y-S, Thakuri B, Sillanpää M. 2012.** Parthenolide, a sesquiterpene lactone, expresses multiple anti-cancer and anti-inflammatory activities. *Inflammation* **35**(2): 560-565.
- Neelakantan S, Nasim S, Guzman ML, Jordan CT, Crooks PA. 2009.** Aminoparthenolides as novel anti-leukemic agents: Discovery of the NF- κ B inhibitor, DMAPT (LC-1). *Bioorganic & Medicinal Chemistry Letters* **19**(15): 4346-4349.
- Nelson DR. 2009.** The cytochrome P450 homepage. *Human Genomics* **4**(1): 59-65.
- Nguyen DT, Gopfert JC, Ikezawa N, Macnevin G, Kathiresan M, Conrad J, Spring O, Ro DK. 2010.** Biochemical conservation and evolution of germacrene A oxidase in asteraceae. *Journal of Biological Chemistry* **285**(22): 16588-16598.
- Outchkourov N, Peters J, De Jong J, Rademakers W, Jongasma M. 2003.** The promoter-terminator of chrysanthemum rbcS1 directs very high expression levels in plants. *Planta* **216**(6): 1003-1012.
- Parada-Turska J, Paduch R, Majdan M, Kandefer-Szerszen M, Rzeski W. 2007.** Antiproliferative activity of parthenolide against three human cancer cell lines and human umbilical vein endothelial cells. *Pharmacological Report* **59**(2): 233-237.
- Pareek A, Suthar M, Rathore SG, Bansal V. 2011.** Feverfew (*Tanacetum parthenium* L.): A systematic review. *Pharmacognosy Review* **5**(9): 103-110.
- Pompon D, Louerat B, Bronin A, Urban P. 1996.** Yeast expression of animal and plant P450s in optimized redox environments. *Methods in Enzymology* **272**: 51-64.
- Rodriguez E, Towers GHN, Mitchell JC. 1976.** Biological activities of sesquiterpene lactones. *Phytochemistry* **15**(11): 1573-1580.
- Shanmugam R, Jayaprakasan V, Gokmen-Polar Y, Kelich S, Miller KD, Yip-Schneider M, Cheng L, Bhat-Nakshatri P, Sledge GW, Nakshatri H, Zheng QH, Miller MA, DeGrado T, Hutchins GD, Sweeney CJ. 2006.** Restoring chemotherapy and hormone therapy sensitivity by parthenolide in a xenograft hormone refractory prostate cancer.

- cer model. *Prostate* **66**(14): 1498-1511.
- Sweeney CJ, Mehrotra S, Sadaria MR, Kumar S, Shortle NH, Roman Y, Sheridan C, Campbell RA, Murry DJ, Badve S, Nakshatri H. 2005.** The sesquiterpene lactone parthenolide in combination with docetaxel reduces metastasis and improves survival in a xenograft model of breast cancer. *Molecular Cancer Therapeutics* **4**(6): 1004-1012.
- Urban P, Mignotte C, Kazmaier M, Delorme F, Pompon D. 1997.** Cloning, yeast expression, and characterization of the coupling of two distantly related *Arabidopsis thaliana* NADPH-Cytochrome P450 reductases with P450 CYP73A5. *Journal of Biological Chemistry* **272**(31): 19176-19186.
- Vanengelen FA, Molthoff JW, Conner AJ, Nap JP, Pereira A, Stiekema WJ. 1995.** Pbinplus - an improved plant transformation vector based on Pbin19. *Transgenic Research* **4**(4): 288-290.
- Wen J, You K-R, Lee S-Y, Song C-H, Kim D-G. 2002.** Oxidative stress-mediated apoptosis the anticancer effect of the sesquiterpene lactone parthenolide. *Journal of Biological Chemistry* **277**(41): 38954-38964.
- Wen J, You KR, Lee SY, Song CH, Kim DG. 2002.** Oxidative stress-mediated apoptosis - The anticancer effect of the sesquiterpene lactone parthenolide. *Journal of Biological Chemistry* **277**(41): 38954-38964.
- Zhang DL, Qiu L, Jin XQ, Guo ZH, Guo CB. 2009.** Nuclear factor-kappa B inhibition by parthenolide potentiates the efficacy of taxol in non-small cell lung cancer *in vitro* and *in vivo*. *Molecular Cancer Research* **7**(7): 1139-1149.
- Zhang S, Ong C-N, Shen H-M. 2004.** Critical roles of intracellular thiols and calcium in parthenolide-induced apoptosis in human colorectal cancer cells. *Cancer Letters* **208**(2): 143-153.
- Zhang S, Won YK, Ong CN, Shen HM. 2005.** Anti-cancer potential of sesquiterpene lactones: bioactivity and molecular mechanisms. *Current Medicinal Chemistry - Anti-Cancer Agents* **5**(3): 239-249.

SUPPLEMENTARY INFORMATION

Supplementary methods

Gene expression analysis

mRNA levels of candidate genes were measured by quantitative real time RT-PCR. Total RNA was extracted from ovaries of feverfew flowers collected at developmental stages 2 to 6 and the corresponding cDNAs were obtained as previously reported (Majdi et al., 2011). Real time RT-PCR was performed using a LightCycler 480 (Roche Diagnostics). All real time RT-PCR reactions were carried out in a total volume of 20 μ l mastermix containing 10 μ l LightCycler 480 SYBR Green I Master (Roche Diagnostics), 0.6 μ l forward primer (0.3 μ M), 0.6 μ l reverse primer (0.3 μ M), 6.8 μ l water and 2 μ l cDNA (50 ng). The LightCycler experimental run protocol used was: 95°C for 10 min, 95°C for 10s, 60°C for 30s for 40 cycles and finally a cooling step to 40°C. LightCycler Software 1.5.0 was used for data analysis. For efficiency determination, a standard curve of six serial dilution points (ranging from 200 to 6.25 ng) was made in triplicate. Primer pairs for *TpGAS* and *TpActin* were described previously (Majdi et al., 2011). The following primer pairs were used for *TpGAO*, *TpCOS* and *TpPTS* amplification: forward *TpGAO* 5'-TGCAGCTCCCCTTGCTAATATAC-3', reverse *TpGAO* 5'-AGTCTTTCTTTGAACCGTGGCTCC-3', forward *TpCOS* 5'-TAGCTTCATCCCGGAGCGATTTGA-3', reverse *TpCOS* 5'-AAATTCTTCGGCCCGCACCAAATG-3', forward *TpPTS* 5'-AGACATTACGTTTACACCCTCCCG-3', reverse *TpPTS* 5'-ATCACGACACAA-GTCCCAGGAAA-3'. Quantification of transcript levels was done in three independent biological replicates and for each biological replicate three technical replicates were run. Actin was used as a housekeeping gene. The Δ CT was calculated as follows: Δ CT = CT (Target) - CT (Actin). The fold change value was calculated using the expression $2^{-\Delta$ CT} (Schmittgen & Livak, 2008).

Headspace analysis and thermodesorption GC-MS

Volatile collection and GC-MS analysis were performed as described before (2011). Steel sorbent cartridges (89 mm \times 6.4 mm O.D.; Markes) containing Tenax were used for volatile collection. *N. benthamiana* leaves were cut from the plant and their petioles placed in water in a small vial and were enclosed in a glass cuvette. To trap the leaf-produced volatiles, air was sucked through the cuvettes at a flow rate of 90 mL min⁻¹ for 2 h through a Tenax containing cartridge. A second cartridge was used to purify the incoming air. Sample cartridges were dried for 15 min at room temperature with a nitrogen flow of 20 psi before GC-MS analysis.

For GC-MS analysis, cartridges were placed in an automated thermodesorption unit (Ultra; Markes, Llantrisant, UK) and were flushed with helium at 50 mL min⁻¹ for 2 min to remove moisture and oxygen before thermodesorption. Volatiles in the cartridges were desorbed by heating at 220 °C for 5 min with a helium flow of 50 mL min⁻¹. The compounds released were trapped on an electrically cooled sorbent trap (Unity; Markes, Llantrisant) at a temperature of 5 °C. The trapped volatiles were injected on the analytical column (ZB-5MSI,

30 m × 0.25 mm ID, 1.0 μm – film thickness, Zebtron, Phenomenex) by ballistic heating of the cold trap to 250 °C for 3 min. The temperature program of the GC started at 40 °C (3 min hold) and rose 10 °C min⁻¹ to 280 °C (2 min hold). The column effluent was ionised by electron impact (EI) ionisation at 70 eV. Mass scanning was done from 33 to 280 m/z with a scan time of 4.2 scans s⁻¹. Data analysis was done using Xcalibur (Thermo, USA) to identify compounds by comparing mass spectra with those of MS libraries such as NICT and the mass spectra and retention times of authentic reference standards.

LC-QTOF-MS analysis of leaf extracts

For LC-QTOF-MS analysis of leaf extracts, a Waters Alliance 2795 HPLC connected to a Waters 2996 PDA detector and subsequently a QTOF Ultima V4.00.00 mass spectrometer (Waters, MS technologies, UK) operating in negative ionization mode was used. An analytical column (Luna 3 μ C18/2 100A; 2.0 × 150 mm; Phenomenex, USA) attached to a C18 pre-column (2.0 × 4 mm; Phenomenex, USA) was used. Degassed eluent A [ultra-pure water: formic acid (1000:1, v/v)] and eluent B [acetonitril:formic acid (1000:1, v/v)] were used at a flow rate of 0.19 mL min⁻¹. Masses were recorded between m/z 80 and m/z 1500; leucine enkaphalin ([M-H]⁻=554.2620) was used as a lock mass for on-line accurate mass correction. The gradient of the HPLC started at 5% eluent B and increased linearly to 75% eluent B in 45 min, after which the column was washed and equilibrated for 15 min before next injection. Injection volume was 5 μL.

LC-Orbitrap-FTMS analysis of yeast microsomal assay products

To analyse microsomal assay mixtures, a LC-LTQ-Orbitrap FTMS system (Thermo Scientific) consisting of an Accela HPLC, an Accela photodiode array detector, connected to an LTQ/Orbitrap hybrid mass spectrometer equipped with an ESI source was used. Chromatographic separation took place on an analytical column (Luna 3 μ C18/2 100A; 2.0 × 150 mm; Phenomenex, USA). Degassed eluent A [ultra-pure water: formic acid (1000:1, v/v)] and eluent B [acetonitril:formic acid (1000:1, v/v)] were used at a flow rate of 0.19 mL min⁻¹. A linear gradient from 5 to 75% acetonitrile in 45 min was applied, which was followed by 15 min of washing and equilibration. FTMS full scans (m/z 100–1200) were recorded with a resolution of 60000, whereas for MSⁿ scans a resolution of 15000 was used. The FTMS was externally calibrated in negative mode using sodium formate clusters in the range m/z 150–1200, and automatic tuning was performed on m/z 384.93. Injection volume was 5 μL.

Parthenolide detection and quantification by LC-MRM-MS

Targeted analysis of parthenolide and costunolide was performed with a Waters Xevo tandem quadrupole mass spectrometer equipped with an electrospray ionization source and coupled to an Acquity UPLC system (Waters) as described before (2011). Chromatographic separation was obtained on an Acquity UPLC BEH C18 column (100 × 2.1 mm, 1.7 μm; Waters) by applying a water/acetonitrile gradient to the column, starting from 5% (v/v) acetonitrile in water for 1.25 min and rising to 50% (v/v) acetonitrile in water in 2.35 min, followed by an increase to 90% (v/v) acetonitrile in water in 3.65 min, which was maintained for 0.75 min

before returning to 5% acetonitrile in water using a 0.15 min gradient. Finally, the column was equilibrated for 1.85 min using this solvent composition. Operation temperature and flow rate of the column were 50 °C and 0.5 mL min⁻¹, respectively. Injection volume was 5 µL. The mass spectrometer was operated in positive electrospray ionization mode. Cone and desolvation gas flows were set to 50 and 1000 L h⁻¹, respectively. The capillary voltage was 3.0 kV, the source temperature 150 °C, and the desolvation temperature 650 °C. The cone voltage was optimized for parthenolide or costunolide using the Waters IntelliStart MS Console. Argon was used for fragmentation by collision-induced dissociation in the ScanWave collision cell. Multiple Reaction Monitoring (MRM) was used for identification and quantification of costunolide in yeast extract and agro-infiltrated *N. benthamiana* leaves by comparing retention times and MRM mass transitions with that of a costunolide standard. MRM transitions for costunolide [M+H]⁺=233.16>131.01 and [M+H]⁺=233.16>187.23, and for parthenolide [M+H]⁺=249.16>231.229 and [M+H]⁺= 249.16>185.224 were optimized using the Waters IntelliStart MS Console.

Yeast microsome isolation

Microsomes of yeast transformed with parthenolide synthase candidates were isolated as described by Pompon et al.(1996) with modifications. Yeast cell cultures were grown in 50mL SGI medium for 36 hours at 30 °C. After adding 250 mL YPL medium containing 2% galactose, induction was allowed to proceed for 24 hours at 30 °C. Cells were collected and chilled on ice for 20 min. After centrifugation at 4,900 x g for 10 min, pellets were re-suspended in 100 mL extraction buffer (50 mM Tris-HCl pH 7.5, 1 mM EDTA, 0.6 M sorbitol and 10 mM β-mercaptoethanol) and incubated for 10 min at room temperature. Following centrifugation at 4,900 x g for 10 min, the pellet was washed three times with extraction buffer (without resuspending the pellet). Cells were re-suspended in 3 mL extraction buffer (without β-mercaptoethanol) and transferred into a 50 mL Falcon tube. About 25 mL of glass beads (450-500 µm) were used to lyse the cells by shaking for 10 min in a cold room. The lysed cells were transferred to a 25 mL centrifuge tube and centrifuged at 10,500 x g for 10 min. The supernatant was centrifuged at 195,000 x g for 2 h. The pelleted microsomal fractions were re-suspended in 4 mL chilled 50 mM Tris-HCl buffer pH 7.5 containing 1 mM EDTA and 20% (v/v) glycerol using a chilled glass Tenbroeck homogenizer. Yeast microsomes were then aliquoted in pre-cooled 1.5 mL eppendorf tubes and stored at -80 °C until use.

Cysteine and glutathione (GSH) conjugation

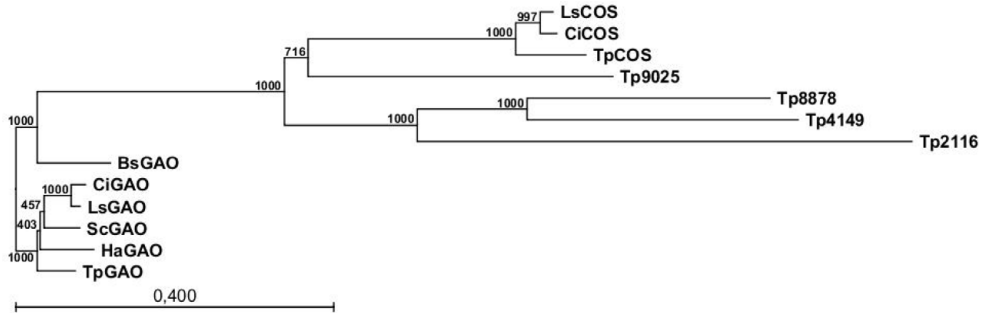
Cysteine and GSH conjugation was performed as described by Liu et al.(2011). The reaction mixture contains GSH (1 mM) or cysteine (1 mM), substrates (0.2 mM), and GST (0.7 mg L⁻¹; Sigma, USA) in 1000 µl potassium buffer (100 mM; pH 6.5). Complete assay mixtures without GST enzyme or either of the substrates were used as controls. After incubation for 30 min at room temperature, samples were kept at -20 °C until analysis. Costunolide was purchased from TOCRIS Bioscience (United Kingdom). Parthenolide, 3β-hydroxycostunolide, and 3β-hydroxyparthenolide, isolated from dried aerial parts of feverfew plants, were provided by Justin T. Fishedick of PRISNA (Leiden, the Netherlands)(Fishedick et al., 2012).

Cytotoxicity assay

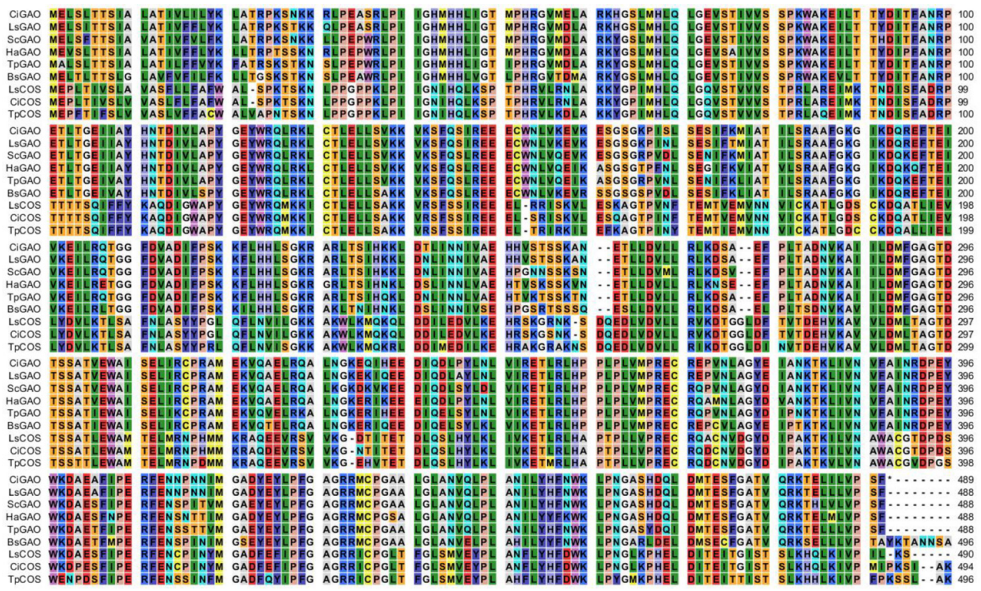
The NCI-H460, U87, DLD1 and HT-29 cell lines were purchased from the American Type Culture Collection (ATCC). Human normal keratinocytes (HaCaT) were obtained from Cell Lines Service (CLS). NCI-H460/R cells were selected originally from NCI-H460 cells and cultured in a medium containing 100 nM doxorubicin. U87-TxR and DLD1-T/R cells were selected from U87 and DLD1 cells, respectively, and cultured in a medium containing 300 nM paclitaxel (Urban et al., 1997). All cell lines were sub-cultured at 72 h intervals using 0.25% trypsin/EDTA and seeded into a fresh medium at the following densities: 8,000 cells/cm² for NCI-H460, DLD1, DLD1-T/R and HT-29, 16,000 cells/cm² for U87 and NCI-H460xR, and 32,000 cells/cm² for U87-T/R and HaCaT.

Cells grown in 25 cm² tissue flasks were trypsinized, seeded into flat-bottomed 96-well tissue culture plates, and incubated overnight. Treatment with all compounds (1-100 μ M) lasted 72 h. The cellular proteins were stained with Sulforhodamine B (SRB), following a slightly modified protocol (Outchkourov et al., 2003). The absorbance after SRB staining was measured at 540 nm using an automatic microplate reader (LKB5060-006-Micro-PlateReader-Vienna-Austria).

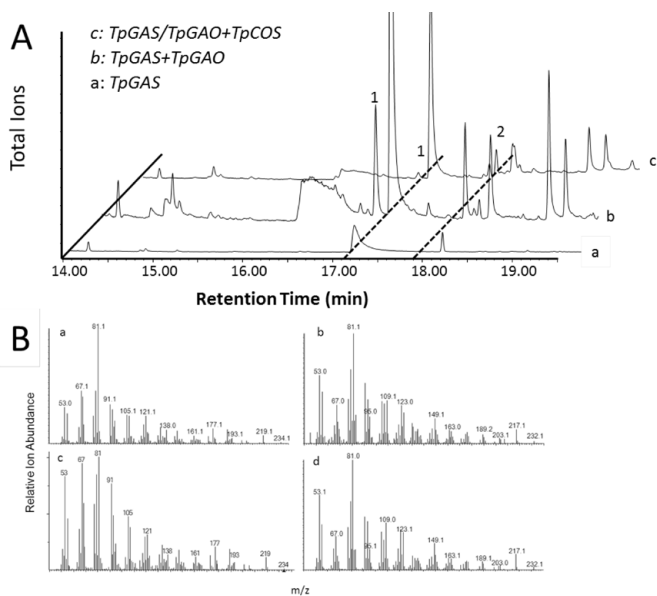
Supplementary figures



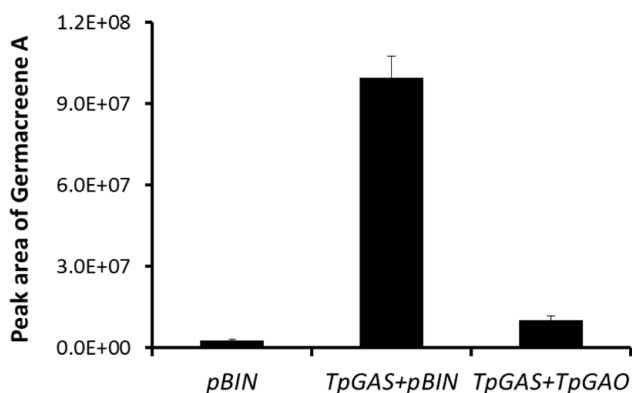
Supplementary Figure 1. Phylogenetic tree of *TpGAO*, *TpCOS*, parthenolide synthase candidates (*Tp2116*, *Tp4149*, *Tp9025*, *Tp8878*) and other GAOs and COSs of the Asteraceae. Bootstrap values are shown as percentage from 1,000 replicates.



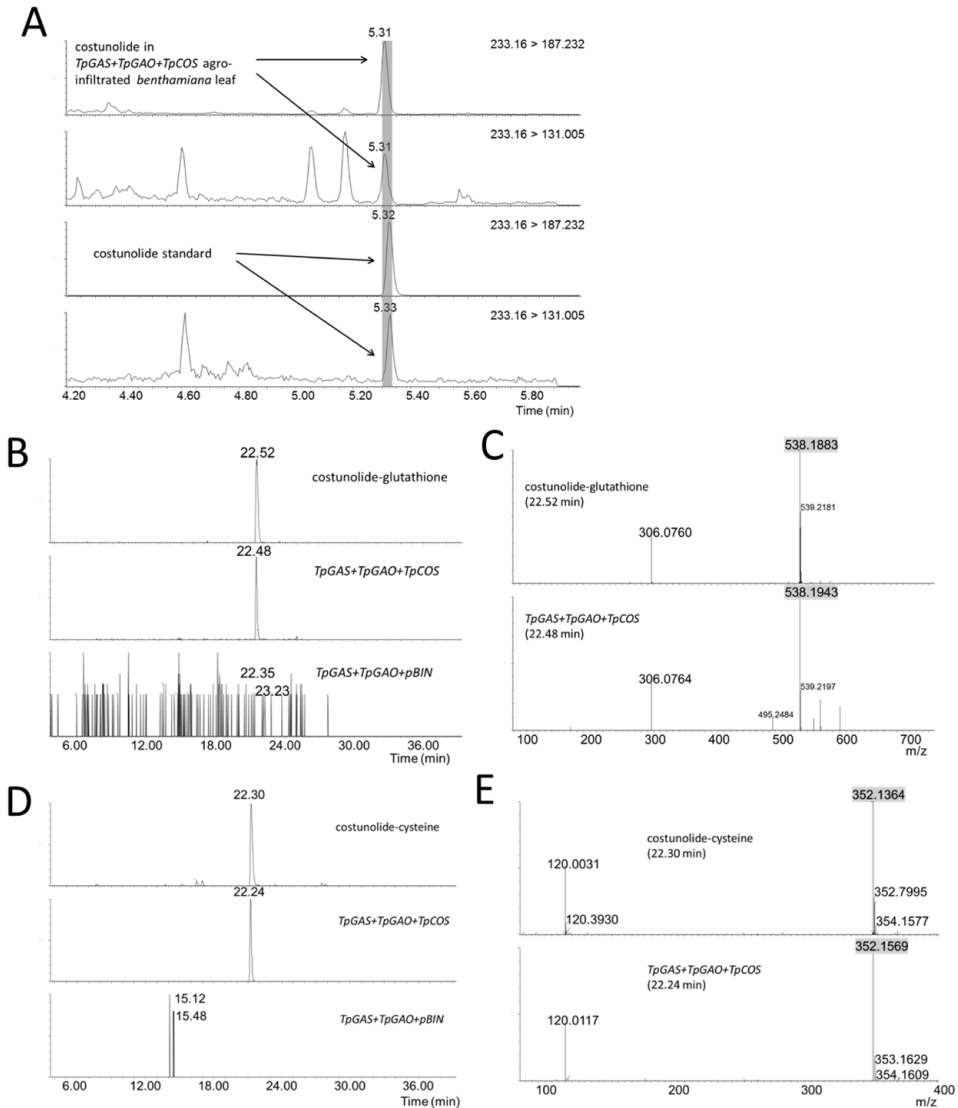
Supplementary Figure 2. Alignment of deduced amino acid sequence of *TpGAO* (germacrene A oxidase), *TpCOS* (costunolide synthase), and other GAOs and COSs from Asteraceae species. Amino acid sequences were obtained from cDNAs deposited at NCBI. germacrene A oxidase from *Tanacetum parthenium* (*TpGAO*, KC964544), from *Lactuca sativa* (*LsGAO*; GU198171), *Cichorium intybus* (*CiGAO*; GU256644), *Saussurea lappa* (*SiGAO*; GU256646), *Helianthus annuus* (*HaGAO*; GU256645), and *Barnadesia spinosa* (*BsGAO*; GU256647); costunolide synthase from *Tanacetum parthenium* (*TpCOS*, KC964544), from *Lactuca sativa* (*LsCOS*; AEI59780), and *Cichorium intybus* (*CiCOS*; AEG79727).



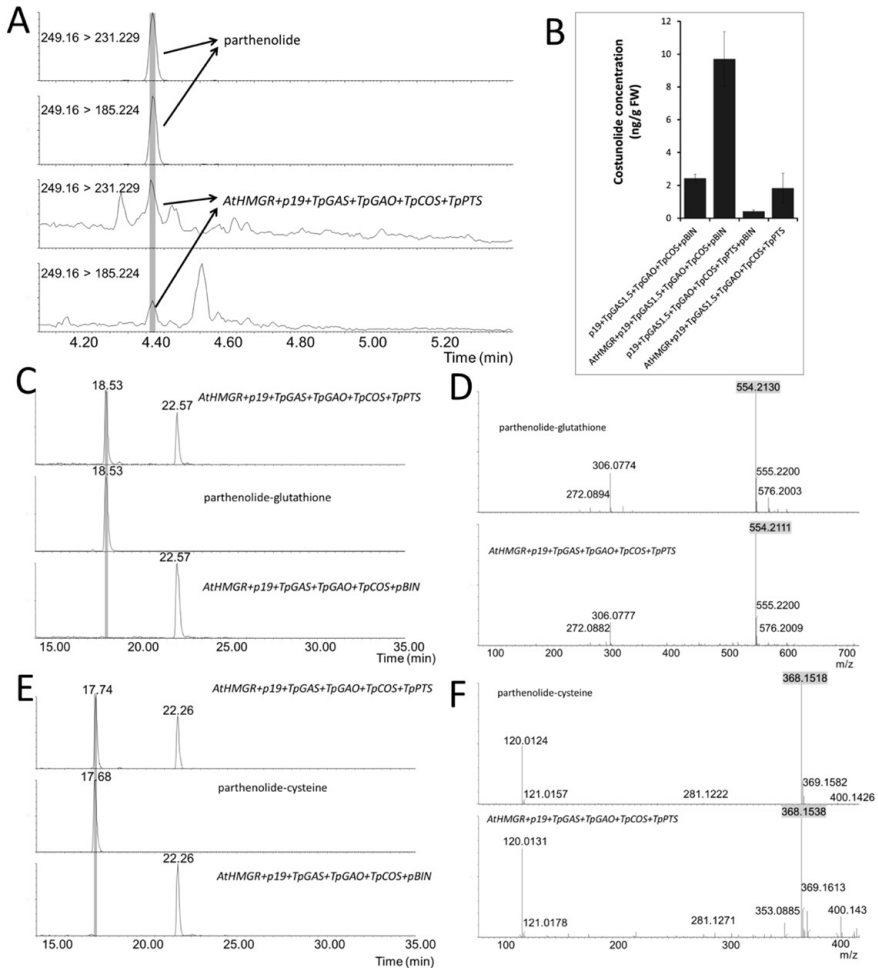
Supplementary Figure 3. Functional characterisation of *TpGAO* and *TpCOS* in yeast. (A) GC-MS chromatograms showing the metabolites produced by yeast transformed with the indicated genes. Line a, negative control; line b, the yeast transformed with *TpGAS+TpGAO*; line c, yeast transformed with *TpGAS+TpGAO+TpCOS*. 1 = germacra-1(10),4,11(13)-trien-12-oic acid; 2 = costunolide. (B) The mass spectra of compound 1 (a) and compound 2 (b) produced by yeast, and elematrien-12-oic acid (c) and costunolide standards (d). (C) Cope rearrangement of germacra-1(10),4,11(13)-trien-12-oic acid to elematrien-12-oic acid.



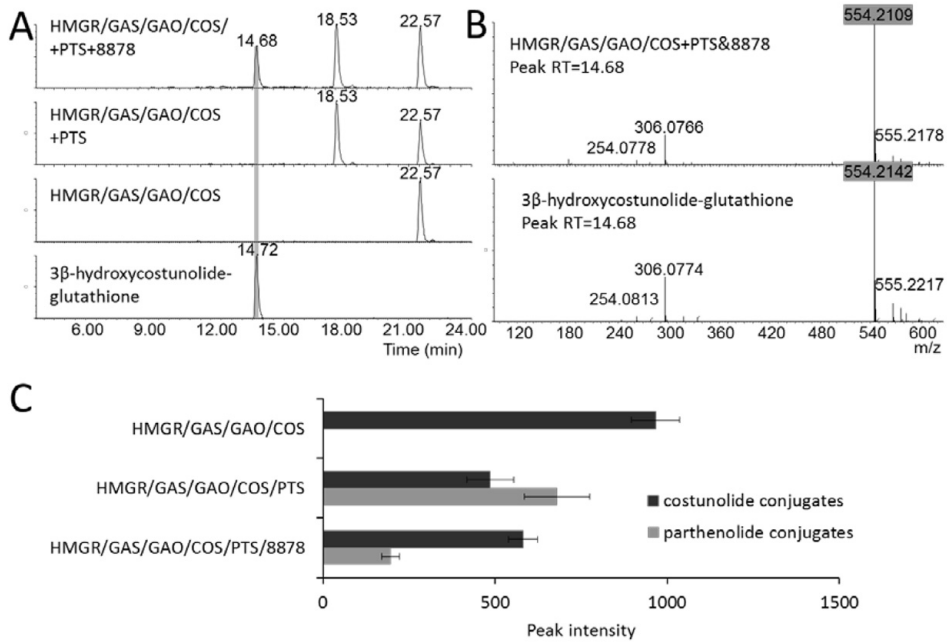
Supplementary Figure 4. Germacrene A production in *Nicotiana benthamiana* infiltrated by *pBIN* (empty vector), *TpGAS+pBIN*, and *TpGAS+TpGAO*. Volatiles emitted from *N. benthamiana* leaves infiltrated with the indicated genes were measured by GC-MS. *TpGAS*, *Tanacetum parthenium* germacrene A synthase; *TpGAO*, *Tanacetum parthenium* germacrene A oxidase.



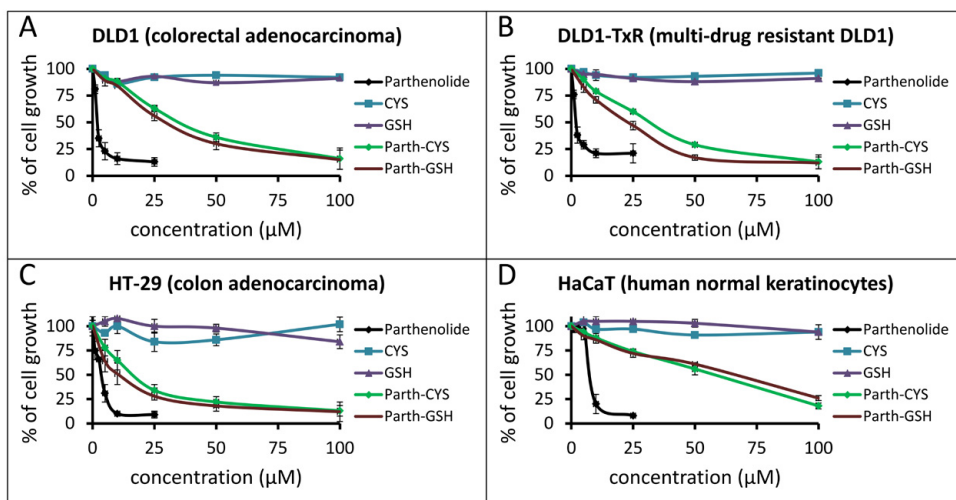
Supplementary Figure 5. Pathway reconstitution of costunolide biosynthesis in *N. benthamiana*. (A) UPLC-MRM-MS analysis of free costunolide (MRM transitions 233.16>187.232 and 233.16>131.005) in *N. benthamiana* leaves infiltrated with *TpGAS+TpGAO+TpCOS* and *TpGAS+TpGAO+pBIN*. (B) LC-QTOF-MS chromatograms (ion selection at m/z 306) of the costunolide-glutathione conjugate formed in an enzyme assay of costunolide and glutathione with glutathione-S transferase, and of extracts of *N. benthamiana* leaves agro-infiltrated with *TpGAS+TpGAO+TpCOS* and *TpGAS+TpGAO+pBIN* (control). (C) In source MS spectrum of peak 22.48 and costunolide-glutathione conjugate (RT=22.52). Grey boxes indicate the parent ion at $[M-H]^- = 538.20$. (D) LC-QTOF-MS chromatograms (ion selection at m/z 120) of the costunolide-cysteine conjugate formed in an enzyme assay of costunolide and cysteine with glutathione-S transferase, and of extracts of *N. benthamiana* leaves agro-infiltrated with *TpGAS+TpGAO+TpCOS* and *TpGAS+TpGAO+pBIN* (control). (E) In source MS spectrum of peak 22.24 and costunolide-cysteine conjugate (RT=22.30 min). Grey boxes indicate the parental ion at $[M-H]^- = 352.14$.



Supplementary Figure 6. Pathway reconstitution of parthenolide biosynthesis in *N. benthamiana*. (A) UPLC-MRM-MS analysis of parthenolide (MRM transitions 249.16>231.229 and 249.16>185.224) in *N. benthamiana* leaves infiltrated with AtHMGR+P19+TpGAS+TpGAO+TpCOS+TpPTS. (B) Costunolide concentration in *N. benthamiana* leaves infiltrated with P19+TpGAS+TpGAO+TpCOS, AtHMGR+P19+TpGAS+TpGAO+TpCOS, P19+TpGAS+TpGAO+TpCOS+TpPTS and AtHMGR+P19+TpGAS+TpGAO+TpCOS+TpPTS. (C) LC-QTOF-MS chromatograms (ion selection at m/z 306) of *N. benthamiana* leaves agro-infiltrated with AtHMGR+p19+TpGAS+CiGAO+CiCOS+TpPTS, the parthenolide-glutathione conjugate formed in an enzyme assay of parthenolide and glutathione with glutathione-S transferase, and of an extract of *N. benthamiana* leaves agro-infiltrated with AtHMGR+p19+TpGAS1.5+CiGAO+CiCOS+pBIN. (D) In source MS spectrum of peak 18.53 and the parthenolide-glutathione conjugate (RT=18.53 min). Grey boxes indicate the parent ion at $[M-H]^- = 554.20$. (E) LC-QTOF-MS chromatograms (ion selection at m/z 120) of *N. benthamiana* leaves agro-infiltrated with AtHMGR+p19+TpGAS+CiGAO+CiCOS+TpPTS, the parthenolide-cysteine conjugate formed in an enzyme assay of parthenolide and glutathione with glutathione-S transferase and of an extract of *N. benthamiana* leaves agro-infiltrated with AtHMGR+p19+TpGAS1.5+CiGAO+CiCOS+pBIN. (F) In source MS spectrum of peak 18.53 and parthenolide-cysteine conjugate (RT=18.53 min). Grey boxes indicate the parent ion at $[M-H]^- = 368.15$.



Supplementary Figure 7. Functional characterisation of *Tp8878* in *N. benthamiana*. (A) LC-QTOF-MS chromatograms (ion selection at m/z 306) of *N. benthamiana* leaves agro-infiltrated with *AtHMGR+p19+TpGAS+CiGAO+CiCOS+TpPTS+Tp8878*, the 3β -hydroxycostunolide-glutathione conjugate formed in an enzyme assay of 3β -hydroxycostunolide and glutathione with glutathione-S transferase, and of an extract of *N. benthamiana* leaves agro-infiltrated with *AtHMGR+p19+TpGAS1.5+CiGAO+CiCOS+TpPTS* or with *AtHMGR+p19+TpGAS1.5+CiGAO+CiCOS+pBIN* as controls. (B) In source MS spectrum of peak 14.68 and 3β -hydroxycostunolide-glutathione conjugate (RT=14.72 min). Grey boxes indicate the parent ion at $[M-H]^- = 554.20$. (C) Relative content of costunolide conjugates (glutathione and cysteine) in *N. benthamiana* agro-infiltrated with *AtHMGR+p19+TpGAS+CiGAO+CiCOS+TpPTS*, *AtHMGR+p19+TpGAS+CiGAO+CiCOS*, and *AtHMGR+p19+TpGAS+CiGAO+CiCOS+TpPTS+Tp8878* analysed by LC-QTOF-MS.



Supplementary Figure 8. Anti-cancer activity of parthenolide, parthenolide-cysteine and parthenolide-GSH. Displayed is the cell growth inhibition by parthenolide, cysteine (CYS), glutathione (GSH), parthenolide- CYS, and parthenolide-GSH in (A) DLD1 colorectal carcinoma cell line; (B) DLD1-TxR multi-drug resistant cancer cell line derived from DLD1; (C) HT-29 colon carcinoma cell line and (D) in HaCaT normal human keratinocytes. The data are averages of five independent experiments ($n=5$) \pm S.D.

References

- Fischedick JT, Standiford M, Johnson DA, De Vos RCH, Todorović S, Banjanac T, Verpoorte R, Johnson JA. 2012. Activation of antioxidant response element in mouse primary cortical cultures with sesquiterpene lactones isolated from *Tanacetum parthenium*. *Planta Medica*(EFirst).
- Liu Q, Majdi M, Cankar K, Goedbloed M, Charnikhova T, Verstappen FWA, de Vos RCH, Beekwilder J, van der Krol S, Bouwmeester HJ. 2011. Reconstitution of the costunolide biosynthetic pathway in yeast and *Nicotiana benthamiana*. *PLoS ONE* 6(8): e23255.
- Majdi M, Liu Q, Karimzadeh G, Malboobi MA, Beekwilder J, Cankar K, Vos Rd, Todorović S, Simonović A, Bouwmeester H. 2011. Biosynthesis and localization of parthenolide in glandular trichomes of feverfew (*Tanacetum parthenium* L. Schulz Bip.). *Phytochemistry* 72(14-15): 1739-1750.
- Outchkourov N, Peters J, De Jong J, Rademakers W, Jongasma M. 2003. The promoter-terminator of chrysanthemum *rbcS1* directs very high expression levels in plants. *Planta* 216(6): 1003-1012.
- Pompon D, Louerat B, Bronine A, Urban P. 1996. Yeast expression of animal and plant P450s in optimized redox environments. *Methods in Enzymology* 272: 51-64.
- Schmittgen TD, Livak KJ. 2008. Analyzing real-time PCR data by the comparative CT method. *Nature Protocols* 3(6): 1101-1108.
- Urban P, Mignotte C, Kazmaier M, Delorme F, Pompon D. 1997. Cloning, yeast expression, and characterization of the coupling of two distantly related *Arabidopsis thaliana* NADPH-Cytochrome P450 reductases with P450 CYP73A5. *Journal of Biological Chemistry* 272(31): 19176-19186.

Chapter 5

Kauniolide synthase, a cytochrome P450 terpenoid cyclase that catalyses the first step in guaianolide sesquiterpene lactone biosynthesis

Qing Liu, David Manzano Irimi Pateraki, Lea Ricard, Ric de Vos, Sander van de Krol, Harro Bouwmeester

In preparation for submission.

Abstract

Sesquiterpene lactones are terpenoids with a skeleton of 15 carbons, which are important for human as flavourings and fragrances and possess a wide range of pharmacological activities, including anticancer, anti-inflammatory, antifungal and anti-bacterial activities. The core skeletons of sesquiterpene lactones are classified as guaianolide, pseudoguaianolide, germacranolide, eudesmanolide or helenanolides. However, how these sesquiterpene lactone are made remains unknown. The putative first committed step in guaianolide biosynthesis has been hypothesised to be the epoxidation or hydroxylation of the branch point germacranolide sesquiterpene lactone, costunolide, followed by a cyclisation reaction. Here we used metabolic profiling, 454 sequencing of a glandular trichome cDNA library and expression profiling of P450 genes to identify the enzyme catalysing this reaction in feverfew, *Tanacetum parthenium*. The cytochrome P450, kauniolide synthase (TpKS), catalyses the formation of the guaianolide sesquiterpene lactone, kauniolide from costunolide, through the intermediate 3 β -hydroxycostunolide. We hypothesise that the enzyme catalyses the formation of kauniolide from costunolide via hydroxylation at C₃. Subsequent dehydration at C₃ induces double bond migration from C₄-C₅ to C₃-C₄. Attack of the resulting C₅ carbocation by the C₁-C₁₀ double bond subsequently results in cyclisation. The full biosynthetic pathway of kauniolide from the general sesquiterpene precursor FPP was reconstituted in *Nicotiana benthamiana* by transient co-expression of all the biosynthetic genes. In contrast to most P450s that only oxidise their substrates, TpKS oxidises its substrate and cyclises it, making it a special type of cytochrome P450.

Introduction

Sesquiterpene lactones (STLs) are a major class of plant secondary metabolites, characterized by their α -methylene γ -lactone moiety on the 15-carbon core backbone (Picman, 1986). Many of these colourless, bitter tasting, lipophilic molecules form the active constituents of extracts from a variety of medicinal plants used in traditional medicine (Rodriguez *et al.*, 1976; Zhang *et al.*, 2005). Bioactivity of STLs varies from anti-inflammatory (Lyss *et al.*, 1998) and anti-cancer (Koo *et al.*, 2001) to anti-malarial (Klayman, 1985), all of which are beneficial to human health. The majority of STLs have been reported in the Asteraceae, with over 4000 different STLs that have been identified (de Kraker *et al.*, 2002). Although all these STLs differ in the details of their structure, the backbone of all of them consists of a limited set of core skeletons that are classified as guaianolide, pseudoguaianolide, germacranolide, eudesmanolide or helenanolide (Picman, 1986; Fischer, 1990; Neerman, 2003) (Fig. 1a).

Guaianolides consist of a bicyclic 5,7-ring and have been reported in a variety of plants and other organisms, but mainly in the Asteraceae and Apiaceae (Simonsen *et al.*, 2013). Guaianolides represent a large number of naturally occurring STLs that have been used in traditional medicine throughout the history of mankind for treating various diseases (Schall & Reiser, 2008). The guaianolides exhibit anti-tumor, anti-schistosomal, anthelmintic, antimicrobial, contraceptive, root-growth stimulatory, anti-feedant, and germination inhibitory activities (Rodriguez *et al.*, 1976; Drew *et al.*, 2009; K & Merillon, 2013). Thapsigargin, for example, induces apoptosis in mammalian cells and eventually leads to the death of the cell (Søhoel *et al.*, 2006). A thapsigargin derived drug is currently undergoing clinical trials (phase II) for the treatment of breast, kidney and prostate cancer (Denmeade *et al.*, 2003; Janssen *et al.*, 2006). Another guaianolide, 11,13-dehydrocompressanolide from feverfew (*Tanacetum parthenium*), has been reported to have activity against leishmaniasis, which is one of the major infectious diseases affecting the poorest regions of the world (da Silva *et al.*, 2010). Several other bioactive guaianolides have also been reported from feverfew and chicory (*Cichorium intybus*), such as artecanin, tanaparthin- β -peroxide, leucodin and dehydrocostus lactone (de Kraker *et al.*, 2002; Fishedick *et al.*, 2012).

Despite the importance of guaianolides, their biosynthesis has not yet been elucidated. The biogenesis of guaianolides presumably proceeds through costunolide, as a guaianolide, leucodin, was found to be formed by the incubation of costunolide with chicory root enzyme extract (de Kraker *et al.*, 2002). The most basic guaianolide and putative precursor of leucodin, likely is kauniolide (Fig. 1b). However, it is not clear whether kauniolide is directly derived from costunolide or through parthenolide and two alternative kauniolide biosynthesis pathways have been suggested. One proceeds via parthenolide through an annular cyclization of the ring by a cyclase, followed by an elimination reaction by a guaianolide dehydroxylase (Qi *et al.*, 1995; Zhai *et al.*, 2012) (Figure 1b, presumed route 1). Alternatively, the pathway proceeds through direct enzymatic hydroxylation at C3 of costunolide, resulting in the intermediate 3 β -hydroxycostunolide, while the guaianolide skeleton is subsequently formed via C1,C5-cyclization by a germacrene cyclase (de Kraker *et al.*, 1998) (Figure 1b, presumed route

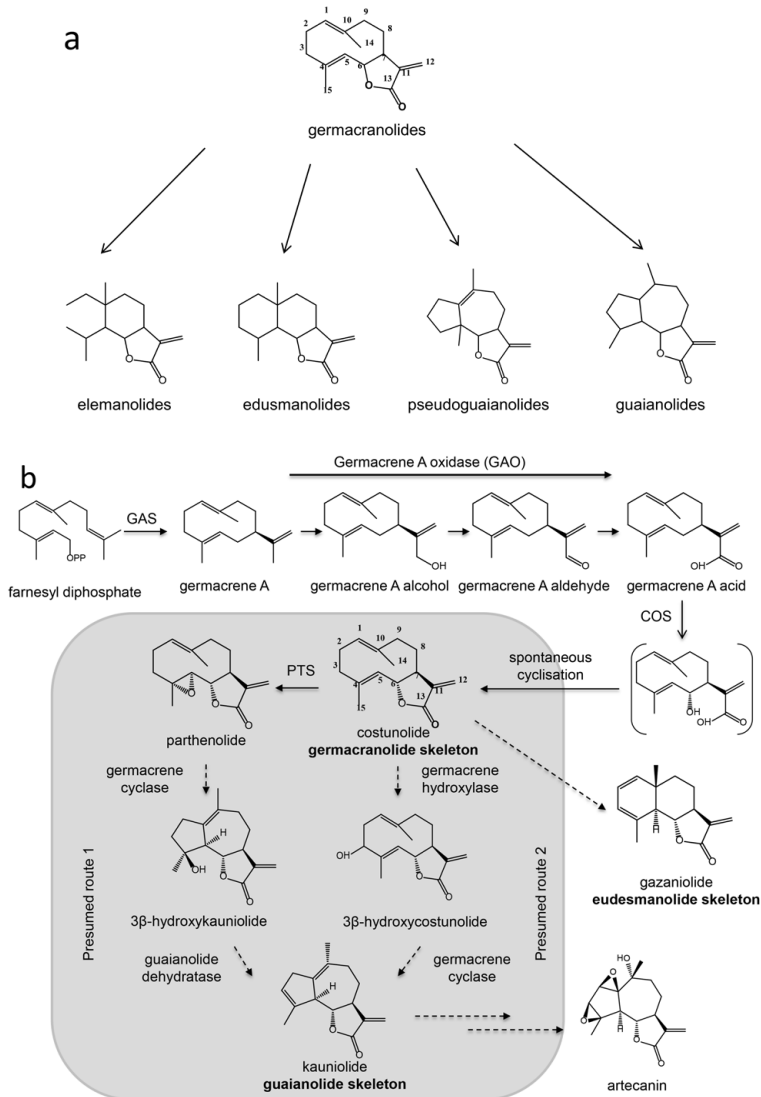


Figure 1. (a), Core skeleton of guaianolides, pseudoguaianolide, germacranolide, edusmanolide and helenanolide sesquiterpene lactones (STLs), and examples of some members of these STL classes. (b), Presumed biosynthetic pathway of guaianolide type sesquiterpene lactones in plants. GAS, germacrene A synthase; COS, costunolide synthase; PTS, parthenolide synthase. Costunolide is formed by conversion of farnesyl diphosphate (FDP) to germacrene A, catalysed by (+)-germacrene A synthase (GAS) (de Kraker *et al.*, 1998). Subsequently, germacrene A is converted to germacrene-1(10),4,11(13)-trien-12-oic acid by the cytochrome P450 enzyme, germacrene A oxidase (GAO) (de Kraker *et al.*, 2001). Genes encoding GAS and GAO have been isolated from several Asteraceae species (Bennett *et al.*, 2002; Bouwmeester *et al.*, 2002; Berteau *et al.*, 2006; Nguyen *et al.*, 2010; Cankar *et al.*, 2011; Liu *et al.*, 2011). Germacrene-1(10),4,11(13)-trien-12-oic acid is subsequently oxidised by costunolide synthase (COS) to 6 α -hydroxy-germacrene-1(10),4,11(13)-trien-12-oic acid, which undergoes spontaneous lactone ring formation to yield costunolide (Ikezawa *et al.*, 2011; Liu *et al.*, 2011). Costunolide is thought to be precursor for both guaianolide and eudesmanolide types of sesquiterpene lactones. Two alternative pathways have been suggested for the formation of the first basic guaianolide skeleton, kauniolide (Piet, 1996).

2). We have recently demonstrated that feverfew has a cytochrome P450 enzyme that can catalyse this C3-hydroxylation (Chapter 4).

Here we set out to determine whether kauniolide is derived from parthenolide or costunolide by identifying and isolating the gene(s) involved in biosynthesis of the guaianolide skeleton from feverfew (*Tanacetum parthenium*). We previously described the characterisation of the feverfew genes leading to the production of costunolide (Chapter 3) and parthenolide (Chapter 4), both of which are germacranolide STLs (de Kraker *et al.*, 2002). As several guaianolides have been reported in feverfew (Bork *et al.*, 1997; Pareek *et al.*, 2011; Fishedick *et al.*, 2012) we assumed that a guaianolide synthase should be present in feverfew. We assumed that this reaction should be catalysed by a cytochrome P450. To identify this P450, we determined the expression profile of a series of P450 gene candidates - that we retrieved from our feverfew trichome cDNA library - and compared their expression profile with the STL accumulation profile in developing ovaries. The enzyme encoded by one of these candidates, *Tp8879*, catalysed the conversion of costunolide, but not parthenolide, into the guaianolide kauniolide. This shows that the branch point in the biosynthesis of guaianolide and germacranolide type sesquiterpene lactones is the ubiquitous STL costunolide. The full kauniolide pathway encoded by farnesyl diphosphate synthase (FPS), germacrene A synthase (GAS), germacrene A oxidase (GAO), costunolide synthase (COS) and kauniolide synthase was successfully reconstituted by transient expression in *Nicotiana benthamiana*. As kauniolide forms the basic skeleton from which other guaianolides are likely derived, the identification of kauniolide synthase provides the basis for metabolic engineering approaches for the production of a range of different medicinal guaianolides.

Results

Identification and cloning of guaianolide skeleton biosynthesis candidate genes

Previously we have shown that the genes encoding the enzymes of the costunolide and parthenolide biosynthesis pathway, *TpGAS*, *TpGAO*, *TpCOS* and *TpPTS*, all have a similar expression pattern during ovary development, and that this expression pattern closely follows the accumulation of both costunolide and parthenolide in ovaries respectively (Figure 2a,b,c; Chapter 4). The genes involved in biosynthesis of germacrene A acid (Nguyen *et al.*, 2010), costunolide (Ikezawa *et al.*, 2011; Liu *et al.*, 2011) and parthenolide (Chapter 4) all encode P450 enzymes (*TpGAO*, *TpCOS* and *TpPTS*) of class CYP71 and share a relatively high amino acid sequence similarity in feverfew (Chapter 4). We assumed that the enzyme acting on either parthenolide or costunolide to form kauniolide would also be a P450 of class CYP71 and that the expression pattern of this gene may show similar profile as *TpGAO*, *TpCOS* and *TpPTS* (Figure 2a). From the 59 class CYP71 P450 sequences in the feverfew trichome cDNA sequence database (Majdi *et al.*, 2011) the expression profile over different ovary developmental stages was assessed (Chapter 4). The basic guaianolide kauniolide was not detected in the ovary extracts, presumably because it is rapidly converted to artemisinin, which is detected in feverfew ovaries (Figure 2c). The accumulation profile in developing ovaries of artemisinin

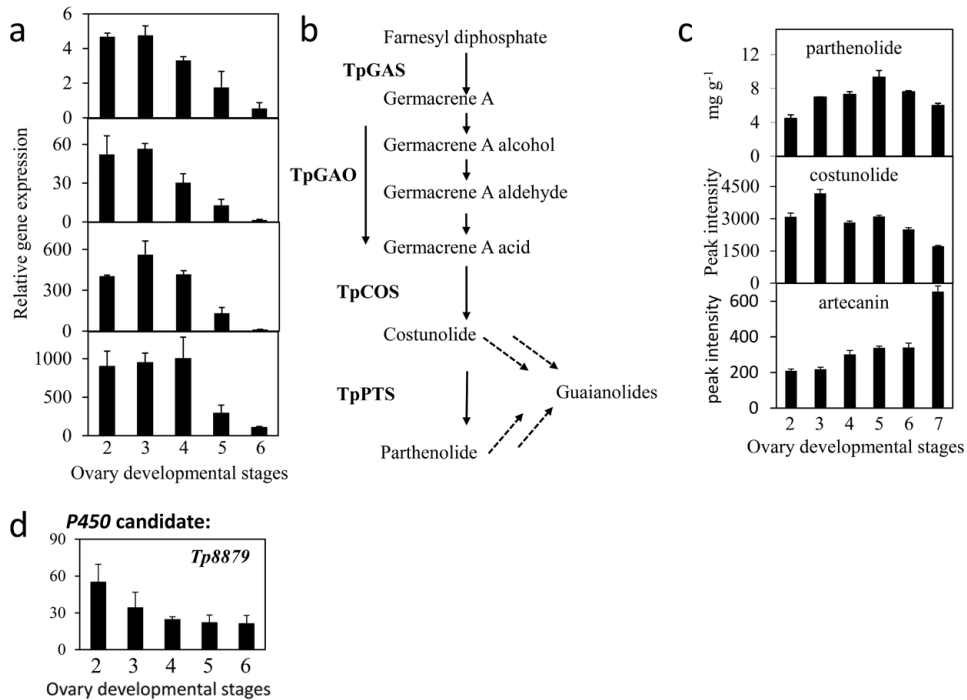


Figure 2. Parthenolide, costunolide and artemcanin content, and expression profile of parthenolide synthetic pathway genes as well as kaunioldie synthase candidate gene during ovary development. (a) Gene expression profile of feverfew *germacrene A synthase* (*TpGAS*), *germacrene A oxidase* (*TpGAO*), *costunolide synthase* (*TpCOS*), and *parthenolide synthase* (*TpPTS*) during ovary development. Bars represent means ($n = 3$) \pm S.E. (b) Simplified scheme for biosynthetic pathway of guaianolides. (c) Parthenolide, costunolide and artemcanin (a guaianolide) content in different developmental stages of feverfew ovaries. (d) Gene expression profile of kauniolide synthase candidate gene (*Tp8879*) during ovary development. Bars represent means ($n = 3$) \pm S.E.

differs from that of costunolide and parthenolide: both costunolide and parthenolide levels decline at later stages of ovule development, which may be a reflection of the reduced gene expression level at later stages of ovule development. In contrast, the artemcanin levels remain increasing throughout ovule development suggesting that expression of genes involved in the biosynthesis of guaianolide-like compounds persists throughout ovule development. Such expression profile was identified in candidate gene *Tp8879* (Figure 2d). The full sequence of this gene was retrieved and used to design primers to isolate the full length ORF for cloning into yeast expression vector pYED60 for enzymatic characterization.

Functional characterization of candidate *Tp8879* in yeast

To test the catalytic activity of candidate *Tp8879*, microsomes of yeast expressing the *Tp8879* ORF were isolated and incubated with costunolide or parthenolide. Analysis of the products formed from costunolide by LC-Orbitrap-FTMS showed a small new peak ($[M+H]^+ = 231.13780$) not present in control samples. The mass of this new compound is 2 D

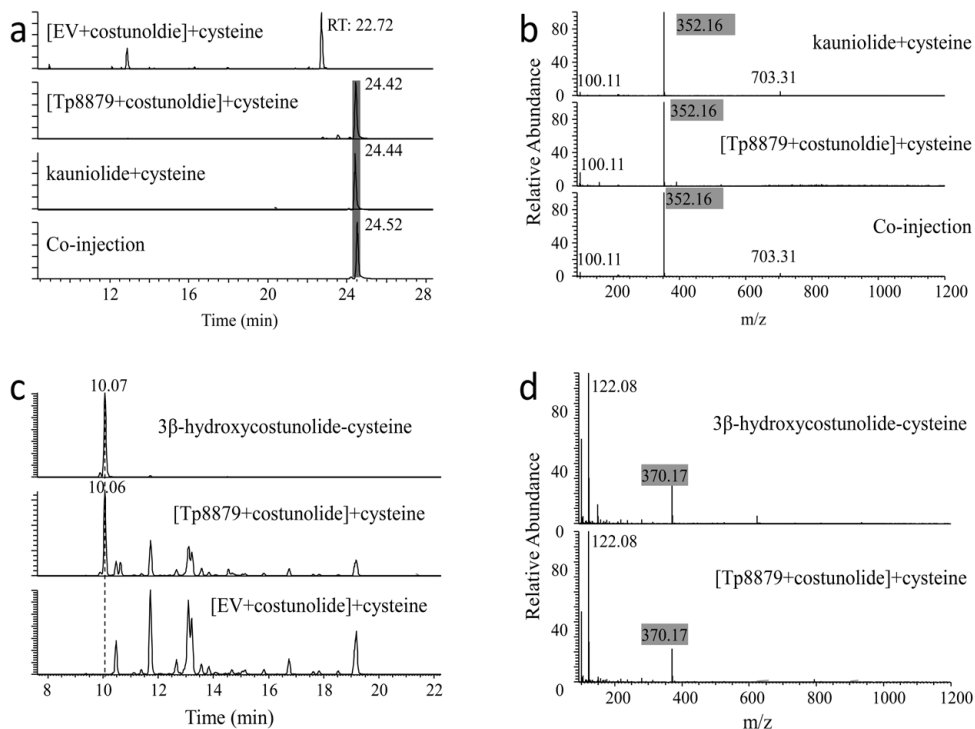


Figure 3. Identification of kauniolide in yeast microsomal assays. (a) LC-Orbitrap-FTMS chromatograms at $m/z=352.15771$ (10 ppm, positive ionization mode, mass for kauniolide-cysteine conjugate) of extracts of microsomes expressing empty vector fed with costunolide and incubated afterwards with cysteine (control) (top panel), extracts of microsomes expressing *Tp8879* fed with costunolide and incubated afterwards with cysteine (2nd panel), kauniolide-cysteine conjugate formed in an enzyme assay of kauniolide and cysteine with glutathione-S transferase (3rd panel), co-injection of the latter two (bottom panel). (b) MS spectrum of peak RT=24.45 min for kauniolide-cysteine conjugate (top panel), cysteine conjugated compounds in microsomes expressing *Tp8879* fed with costunolide (middle panel), and co-injection of the former two (bottom panel). Grey boxes indicate the parental ion at $[M+H]^+=352.16$. (c) LC-Orbitrap-FTMS chromatograms at $m/z=370.16827$ (10 ppm, positive ionization mode, mass for 3 β -hydroxycostunolide-cysteine conjugate) of 3 β -hydroxycostunolide-cysteine conjugate formed in an enzyme assay of 3 β -hydroxycostunolide and cysteine with glutathione-S transferase (top panel), cysteine conjugated products formed by microsomes expressing *Tp8879* fed with costunolide (2nd panel), and the co-injection of those two extracts (3rd panel). Microsomes expressing empty vector fed with costunolide and treated with cysteine was used as control. (d) MS spectrum of peak RT=10.07 min for 3 β -hydroxycostunolide-cysteine conjugate (top panel) and cysteine conjugated compounds in microsomes expressing *Tp8879* fed with costunolide (bottom panel). Grey boxes indicate the parental ion at $[M+H]^+=370.17$.

less than that of costunolide ($[M+H]^+=233.15244$), suggesting introduction of a double bond or ring closure in costunolide. From previous experience we know that some compounds may escape detection by LC-Orbitrap-FTMS, because of low ionisation. Ionisation may be improved by conjugation of the compound to be detected to cysteine ($[M]=121.01464$), which for many sesquiterpene lactones can be achieved non-enzymatically and irreversibly by add-

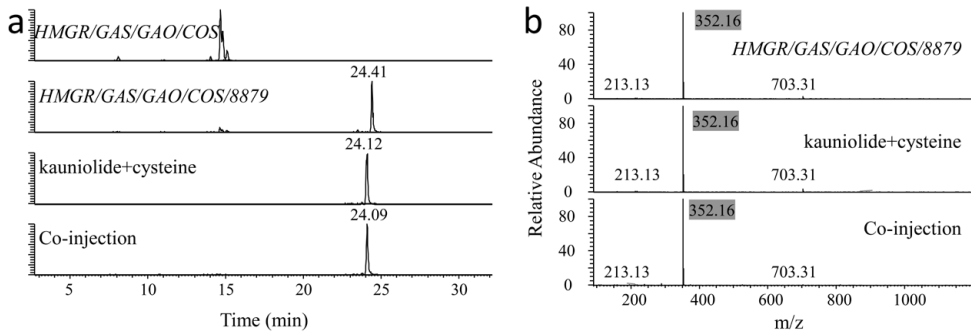


Figure 4. Characterisation of kauniolide biosynthesis in *N. benthamiana*. (a) LC-Orbitrap-FTMS chromatograms of $[M+H]^+=352.15771$ (kauniolide-cysteine conjugate). Top panel: Extract of *N. benthamiana* leaves agro-infiltrated with *AtHMGR+p19+TpGAS+CiGAO+CiCOS*. 2nd panel: Extracts of *N. benthamiana* leaves agro-infiltrated with *AtHMGR+p19+TpGAS+CiGAO+CiCOS+Tp8879*. 3rd panel: 3: kauniolide-cysteine conjugate formed in an enzyme assay of kauniolide and cysteine with glutathione-S transferase. Bottom panel: co-injection of (2) and (3). (b) MS spectrum of peak RT=24.41 min for *N. benthamiana* leaves agro-infiltrated with *AtHMGR+p19+TpGAS+CiGAO+CiCOS+Tp8879*, MS spectrum of peak RT=24.10 for kauniolide-cysteine conjugate and co-injection of the latter two. Grey boxes indicate the parental ion at $[M+H]^+=352.16$.

ing cysteine to the reaction mixture (Liu *et al.*, 2011). To test whether products are better detected after conjugation to cysteine, the Tp08879 assay product formed from costunolide was incubated for 1 hr with cysteine. Two compounds conjugated to cysteine were identified with mass $[M+H]^+=352.15771$ and $[M+H]^+=370.16827$. Using several sesquiterpene lactone standards conjugated to cysteine we could establish that the product from Tp8879 conjugated to cysteine with the mass $[M+H]^+=352.15771$ is kauniolide-cysteine: its mass and mass spectrum matched that of a kauniolide-cysteine standard and the peak co-eluted with a kauniolide-cysteine standard after co-injection (Figure 3a and b). The product with mass $[M+H]^+=370.16827$ is 3β -hydroxycostunolide-cysteine: its mass and mass spectrum matched that of a 3β -hydroxycostunolide-cysteine standard (Figure 3c and d). The peak intensity ratio of kauniolide-cysteine / 3β -hydroxycostunolide-cysteine was 6.7:1. No product peaks were detected in the microsomes fractions incubated with parthenolide, also not when the assay mix was incubated with cysteine to enhance detection of putative products (data not shown). The results of the incubation with costunolide suggest that Tp8879 is a kauniolide synthase which may produce 3β -hydroxycostunolide as intermediate. However, when microsomes of yeast cells expressing Tp8879 were provided directly with this putative intermediate 3β -hydroxycostunolide (or 3β -hydroxy parthenolide), no new peaks were detected, suggesting that the enzyme encoded by Tp8879 can not further convert this putative enzymatic intermediate.

Reconstitution of the kauniolide biosynthetic pathway in *Nicotiana benthamiana*

To verify the function of kauniolide synthase (TpKS) *in planta*, TpKS was cloned into a binary expression vector under control of the 35S-promoter and the full biosynthetic pathway of kauniolide was reconstituted in *N. benthamiana* by agro-infiltration. *A. tumefaciens* lines

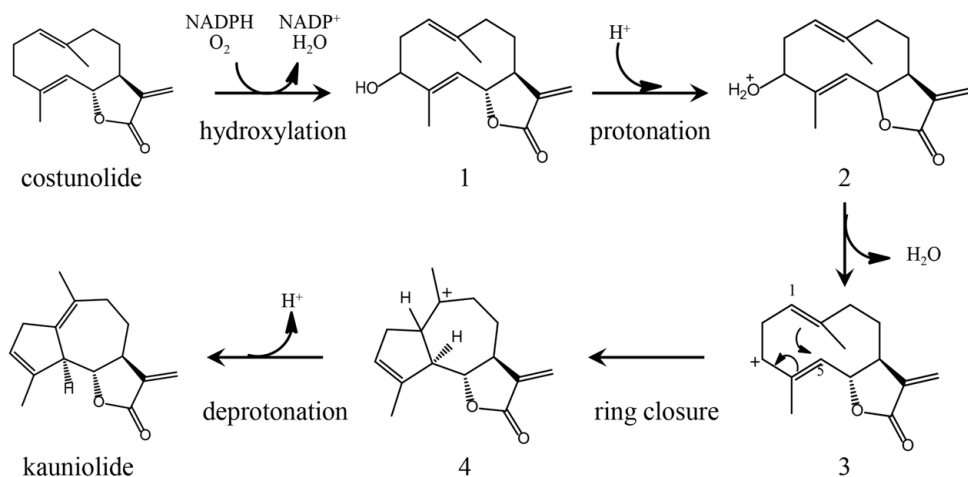


Figure 5. Proposed mechanism for the enzyme catalysed formation of kauniolide from costunolide. First, costunolide is hydroxylated at C₃ to form 3β-hydroxycostunolide (1), which is a NADPH/O₂ dependent step. Then the protonation of the 3β-hydroxycostunolide gives cation 3β-hydroxycostunolide (2). After losing one H₂O, 2 undergoes cation transition (3) and 1-5 cyclisation, which gives cation kauniolide (4). Finally, a selective deprotonation towards the bridgehead carbon atom of 4 gives kauniolide.

with the costunolide pathway constructs, *TpGAS*, *CiGAO* and *CiCOS*, as well as *AtHMGR* (to boost substrate availability) were co-infiltrated into *N. benthamiana* with and without the *A. tumefaciens* strain containing *Tp8879*. Leaves were harvested 4 days post-agroinfiltration and extracted with methanol for analysis by LC-Orbitrap-FTMS. Compared with the control (costunolide pathway without *Tp8879*) two new peaks were detected at RT=24.41 min and RT=24.66 min. The compound eluting at RT=24.41 min was identified as kauniolide-cysteine (Figure 4) and the peak at RT=24.66 min was identified as a kauniolide-glutathione conjugate (data not shown). No free kauniolide was detected.

Discussion

Here we show that cyclisation of the macrocyclic germacranolide to the bicyclic guaianolide sesquiterpene lactones is catalysed by a cytochrome P450 monooxygenase. This enzyme, kauniolide synthase, catalyses the formation of kauniolide from costunolide. The enzymatic reaction likely involves hydroxylation at C3 of costunolide to form 3β-hydroxycostunolide. Protonation followed by dehydration at C3 induces double bond migration from C₄-C₅ to C₃-C₄. Attack of the resulting C₅ carbocation by the C₁-C₁₀ double bond subsequently results in cyclisation. Kauniolide has the most basic guaianolide STL structure, and hence most likely serves as the universal precursor for all the different guaianolides found in nature of which many have medicinal properties. One example is the guaianolide artecanin (Figure 1). Artecanin is the only guaianolide STL detected in feverfew and hence likely derived from kauniolide, through further functionalization. To clone kauniolide synthase we compared metabolite profiles with gene expression profiles, to select a candidate kauniolide synthase from 59

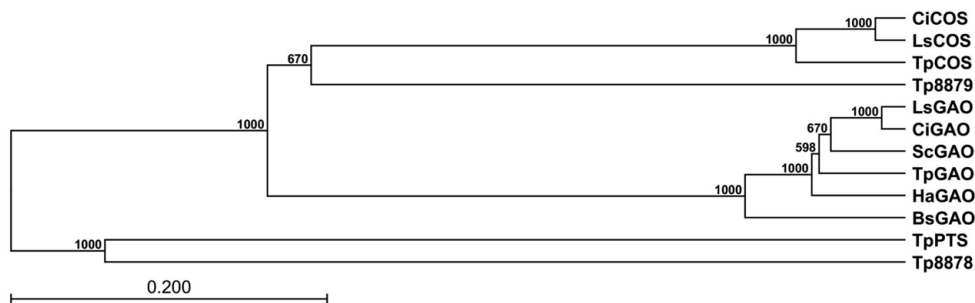


Figure 6. Phylogenetic tree of *TpKS* (*Tp8879*), *TpPTS*, costunolide/parthenolide 3 β -hydroxylase (*Tp8878*), and other GAOs and COSs in *Asteraceae* plants. Bootstrap values were shown in percentage value from 1,000 replicates.

P450 CYP71 sequences that were identified in a feverfew trichome cDNA library (Chapter 4). Accumulation levels of artemisinin increased throughout ovule development unlike those of costunolide and parthenolide (Figure 2). We therefore selected a candidate gene, *Tp8879*, that showed continued expression throughout ovule development for testing as kauniolide synthase. Subsequently, *Tp8879* was indeed shown to encode a kauniolide synthase (*TpKS*).

Enzyme assays showed that *TpKS* uses costunolide, the simplest germacranolide, as substrate and not parthenolide. This places costunolide at the branch point of the guaianolide and germacranolide STL biosynthesis pathways. A side product of the *TpKS* enzyme assay with costunolide as substrate was 3 β -hydroxycostunolide, although this product was not detected in the *in planta* pathway reconstitution. Although this may be an indication that kauniolide is formed from costunolide by *TpKS* through the intermediate 3 β -hydroxycostunolide, *TpKS* did not accept 3 β -hydroxycostunolide as substrate. The cyclisation of 3 β -hydroxycostunolide is not spontaneous, as another P450 (*Tp8878*) oxidises costunolide at the same carbon position (C₃) to form a stable 3 β -hydroxycostunolide product (Chapter 4). Results thus suggest that *TpKS* has additional catalytic capability compared with *Tp8878*, enabling an additional protonation reaction as indicated in Figure 5. Apparently this protonation reactions needs to follow the hydroxylation reaction while the substrate is still bound to the enzyme. Once intermediate 3 β -hydroxycostunolide is released it can not be used as substrate anymore as was evident from the lack of activity in enzyme assays with kauniolide synthase using 3 β -hydroxycostunolide as substrate. The proposed multiple step enzymatic mechanism of *TpKS* is not without precedent. Several plant P450s have been reported to catalyse multiple oxidations of their substrate. For example, amorphadiene synthase, CYP71AV1, from *Artemisia annua* converts amorphadiene to the corresponding alcohol, aldehyde and acid sequentially (Teoh *et al.*, 2006) and germacrene A oxidases from chicory, lettuce and feverfew have been reported to convert germacrene A to the corresponding alcohol, aldehyde and acid form (Nguyen *et al.*, 2010; Cankar *et al.*, 2011). However these P450s oxidise their substrate at the same carbon position. *TpKS* is able to oxidise its substrate followed by a protonation, double bond migration and carbocation-driven cyclization (Figure 5), which makes it a special type of P450.

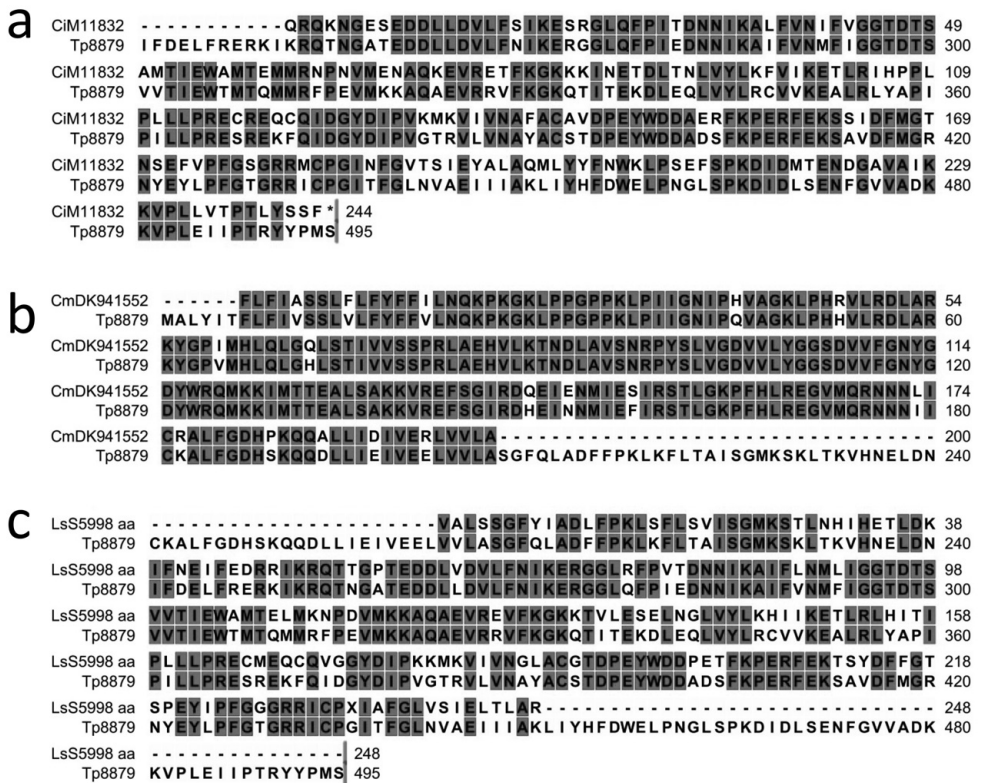


Figure 7. Alignment of feverfew kauniolide synthase (TpKS) with ESTs from Asteraceae. (a) CiM11832 from *Cichorium intybus* (NCBI accession no. EH687049.1); (b) CmDK94552 from *Chrysanthemum x morifolium* (NCBI accession no. DK94552); (c) LsS5998 from *Lactuca sativa* (NCBI accession no. DY983368).

Costunolide thus seems to form a central intermediate both for the different types of germacranolides and the different types of guaianolides in the majority of Asteraceae plants. Costunolide synthase has been hypothesized to have emerged relatively early in Asteraceae evolution (Ikezawa *et al.*, 2011) from germacrene A oxidase (GAO), and is present in several Asteraceae species, as shown in the phylogenetic tree in Figure 6. Several ESTs from Asteraceae in the NCBI database (ncbi.nlm.nih.gov) show high (over 80%) amino acid sequence identity to TpKS (Figure 7) and these genes may therefore be good candidates for kauniolide synthase in these plant species. Although TpGAO, TpCOS, TpPTS, Tp8878 and TpKS all belong to the same CYP71 family, TpKS is more similar to TpCOS (~48% amino acid sequence identity) than to TpPTS and Tp8878 (~32% and 37% amino sequence identity, respectively), suggesting that the evolution of *TpKS* is more constrained than that of TpPTS and Tp8878 (Figure 7).

As thousands of guaianolides have been reported in plants and other organisms (Simonsen

et al., 2013), the identification of TpKS, which catalyses the formation of the simplest guaianolide, kauniolide, makes the biosynthesis of guaianolides derived from it feasible. Indeed, co-expression of all kauniolide pathway genes in a heterologous host, *N. benthamiana*, resulted in the production of kauniolide, showing the potential of engineering of this pathway into alternative hosts. For the production of further functionalised guaianolide STLs additional enzymes will be required. The expression profile of TpKS differs from that of earlier enzymatic steps in the guaianolide biosynthesis pathway and may thus be used to select other P450 genes with similar expression pattern, for example the ones responsible for the formation of artecanin (Figure 1).

Materials and methods

Isolation and cloning of full length candidate genes from feverfew

A previously reported EST library constructed from mRNA isolated from feverfew (*Tanacetum parthenium*) trichomes was used for gene isolation (Chapter 2)(Majdi *et al.*, 2011). Fifty nine candidate cytochrome P450 contigs of the CYP71 group were identified by sequence homology to known sesquiterpene monooxygenases. One of them was selected for functional characterization based on its expression profile during ovary development. RACE PCR (Clontech) was used to obtain the 5'- and 3'-sequence of the candidate contigs. The full length cDNA of the candidate gene was amplified from feverfew cDNA with the addition of NotI/PacI restriction sites. The cDNA was subsequently cloned into the yeast expression vector pYEDP60 (Pompon *et al.*, 1996) and sequenced.

Gene expression analysis

Gene expression levels of candidates genes were measured by quantitative real time RT-PCR. Total RNA and cDNA were obtained from ovaries of feverfew flowers collected at developmental stages 2 to 6 as previously reported (Majdi *et al.*, 2011). Real time RT-PCR was performed using a LightCycler 480 (Roche Diagnostics). The LightCycler experimental run protocol used was: 95°C for 10 min, 95°C for 10 s, 60°C for 30 s for 40 cycles and finally a cooling step to 40°C. LightCycler Software 1.5.0 was used for data analysis. For efficiency determination, a standard curve of six serial dilution points (ranging from 200 to 6.25 ng) was made in triplicate. Primer pairs for *TpGAS* and *TpActin* were described previously (Majdi *et al.*, 2011). The following primer pairs were used for *TpGAO*, *TpCOS* and *TpPTS* amplification: forward *TpGAO* 5'-TGCAGCTCCCGCTTGCTAATATAC-3', reverse *TpGAO* 5'-AGTCTTTCTTTGAACCGTGGCTCC-3', forward *TpCOS* 5'-TAGCTTCATCCCGGAGCGATTTGA-3', reverse *TpCOS* 5'-AAATTCTTCGGCCCCGACCAAATG-3', forward *TpPTS* 5'-AGACATTACGTTTACACCCTCCCG-3', reverse *TpPTS* 5'-ATCACGACACAA-GTCCCAGGGAAA-3', forward *Tp8879* 5'-AGTTCCTTACGGCCATTTCTGGGA-3', reverse 5'-AGAAGATCGTCCTCAGTTGCTCCA-3'. Quantification of transcript levels was done in three independent biological replicates and for each biological replicate three technical replicates were used. Actin was used as a housekeeping gene. The Δ CT was calculated

as follows: $\Delta CT = CT (\text{Target}) - CT (\text{Actin})$. The fold change value was calculated using the expression $2^{-\Delta CT}$ (Schmittgen & Livak, 2008).

Plasmid construction for gene expression in yeast

Candidates *Tp8879* was cloned into pYED60 using NotI/PacI restriction sites. The obtained construct, named *Tp8879::pYED60*, was transformed into the WAT11 (Urban *et al.*, 1997) yeast strain. After transformation yeast clones were selected on SD minimal medium supplemented with amino acids, but omitting uracil and adenine sulphate for auxotrophic selection of transformants.

Yeast microsomes isolation and *in vitro* microsomes assay

Microsomes of yeast transformed with candidate *Tp8879* were isolated as described by Pompon *et al.* (1996) with modifications. Transformed yeast cell cultures were grown in 50 mL SGI medium for 36 hours at 30°C. By adding 250 mL YPL medium containing 2% galactose, the induction was performed for 24 hours at 30°C. Then cells were collected and chilled on ice for 20 min. After centrifugation at 4,900 x g for 10 min, pellets were re-suspended in 100 mL extraction buffer (50 mM Tris-HCl pH 7.5, 1 mM EDTA, 0.6 M sorbitol and 10 mM β -mercaptoethanol) and incubated for 10 min at room temperature. Following centrifugation at 4,900 x g for 10 min, the pellet was washed three times with extraction buffer (without resuspending the pellet). Cells were re-suspended in 3 mL extraction buffer (without β -mercaptoethanol) and transferred to a 50 mL Falcon tube. The centrifuge bottle was washed with another 2 mL of extraction buffer (without β -mercaptoethanol) and this was also transferred to the same 50 mL Falcon tube. About 25 mL of glass beads (450-500 μm) were used to lyse the cells by shaking for 10 min in a cold room. The lysed cells were transferred to a 25 mL centrifuge tube and centrifuged at 10,500 x g for 10 min. The supernatant was centrifuged at 195,000 x g for 2 h. The pelleted microsomal fraction was re-suspended in 4 mL chilled 50 mM Tris-HCl buffer pH 7.5 containing 1 mM EDTA and 20% (v/v) glycerol using a chilled glass Tenbroeck homogenizer. Yeast microsomes were then aliquoted in pre-cooled 1.5 mL eppendorf tubes and stored at -80 °C until use.

All enzyme assays were carried out using 40 mM potassium buffer pH 7.5. Reaction mixture that contains 14.4% (v/v) isolated microsomes, 0.2 mM substrate (10 mM stock in DMSO), 2mM NADPH (10 mM stock in 100 mM potassium buffer), 40mM potassium buffer (1 M, pH 7.5), and 45.2% (v/v) was incubated for 2.5 h at 25 °C with shaking (200 rpm). Then the mixture was centrifuged at 12000 rpm for 10 min. The supernatant was filtered through 0.22 μm filter before injection into LC-MS.

LC-Orbitrap-MS analysis of yeast microsomes assay mixture

To analyse microsomes assay mixtures, a LC-LTQ-Orbitrap FTMS system (Thermo Scientific) consisting of an Accela HPLC, an Accela photodiode array detector, connected to an LTQ/Orbitrap hybrid mass spectrometer equipped with an ESI source was used. Chromatographic separation took place on an analytical column (Luna 3 μ C18/2 100A; 2.0 \times 150 mm; Phenomenex, USA). Degassed eluent A [ultra-pure water: formic acid (1000:1, v/v)] and eluent

B [acetonitril:formic acid (1000:1, v/v)] were used at a flow rate of 0.19 mL min⁻¹. A linear gradient from 5 to 75% acetonitrile in 45 min was applied, which was followed by 15 min of washing and equilibration. FTMS full scans (m/z 100–1200) were recorded with a resolution of 60000, whereas for MSn scans a resolution of 15000 was used. The FTMS was externally calibrated in negative mode using sodium formate clusters in the range m/z 150–1200, and automatic tuning was performed on m/z 384.93. Injection volume was 5 μ l.

Plasmid construction for expression in *Nicotiana benthamiana*

For transient expression in *N. benthamiana*, *TpGAS*, *TpGAO*, *TpCOS*, *TpPTS* and *Tp8879* were cloned into ImpactVector1.1 (<http://www.impactvector.com/>) to express them under the control of the Rubisco (RBC) promoter (Outchkourov *et al.*, 2003). *TpGAS* was also cloned into ImpactVector1.5 to fuse it with the RBC promoter and the CoxIV mitochondrial targeting sequence as we have demonstrated before that mitochondrial targeting of sesquiterpene synthases results in improved sesquiterpene production (Liu *et al.*, 2011). An LR reaction (Gateway-LR Clonase TM II) was carried out to clone each gene into the pBinPlus binary vector (Vanengelen *et al.*, 1995) between the right and left borders of the T-DNA for plant transformation.

Transient expression in *Nicotiana benthamiana*

A. tumefaciens infiltration (agro-infiltration) for transient expression in *Nicotiana benthamiana* was performed as described by Liu *et al.* (2011). *A. tumefaciens* batches were grown at 28 °C at 220 rpm for 48 h in LB media with proper antibiotics. Cells were harvested by centrifugation at 4000xg for 20 min and then resuspended in MES buffer (10 mM MES, 10 mM MgCl₂ and 100 μ M acetosyringone to a final OD₆₀₀ of \sim 1, followed by incubation at room temperature under shaking at 50 rpm for 150 min. For co-expression, equal volumes of the *Agrobacterium* batches were mixed. Batch mixtures were infiltrated into leaves of three-week-old *N. benthamiana* plants by pressing a 1 mL syringe against the abaxial side of the leaf and slowly injecting into the leaf. After infiltration the plants were grown for another four and half days and then harvested for analysis.

LC-QTOF-MS analysis of leaf extracts

Extraction of agro-infiltrated leaves and LC-QTOF-MS (liquid chromatography, coupled to quadrupole time-of-flight mass spectrometry) analysis were performed as described by Liu *et al.* (2011). For extraction, 100 mg of fresh leaves were ground in liquid nitrogen and extracted with 300 μ l methanol:formic acid (1000:1, v/v). After brief vortexing and sonication for 15 min, the extracts were centrifuged at 13,000 rpm for 5 min and filtered through a 0.22 μ m inorganic membrane filter (RC4, Sartorius, Germany), and later injected into LC-QTOF-MS for analysis. A Waters Alliance 2795 HPLC connected to a Waters 2996 PDA detector and subsequently a QTOF Ultima V4.00.00 mass spectrometer (Waters, MS technologies, UK) operating in negative ionization mode was used. An analytical column (Luna 3 μ C18/2 100A; 2.0 \times 150 mm; Phenomenex, USA) attached to a C18 pre-column (2.0 \times 4 mm; Phenomenex, USA) was used. Degassed eluent A [ultra-pure water: formic acid (1000:1, v/v)] and eluent B

[acetonitril:formic acid (1000:1, v/v)] were used at a flow rate of 0.19 mL min⁻¹. Masses were recorded between *m/z* 80 and *m/z* 1500; leucine encephalin ([M-H]⁻=554.2620) was used as a lock mass for on-line accurate mass correction. The gradient of the HPLC started at 5% eluent B and increased linearly to 75% eluent B in 45 min, after which the column was washed and equilibrated for 15 min before the next injection. Injection volume was 5 µl.

Cysteine conjugation

Cysteine conjugation was performed as described by Liu *et al.* (2011). In brief, glutathione (GSH) (150 mM) or cysteine (150 mM) in 7 µl potassium buffer (100 mM; pH 6.5), and standards (30 mM) in 7 µl ethanol were added to 1000 µl potassium buffer (100 mM; pH 6.5). The reaction was initiated by adding 7 µl of GST (1g L⁻¹, in 100 mM potassium buffer; pH 6.5) into the mixture. Complete assay mixtures without GST enzyme or either of the substrates were used as controls. After incubation for 30 min at room temperature, samples were kept at -20 °C until analysis. Costunolide was purchased from TOCRIS Bioscience (United Kingdom). Parthenolide, 3β-hydroxycostunolide, and 3β-hydroxyparthenolide, isolated from dried aerial parts of feverfew plants, were provided by Dr. Justin T. Fishedick of PRISNA (Fishedick *et al.*, 2012). Kauniolide was provided by Prof. Yue Chen, Nankai University, China (Zhai *et al.*, 2012).

References

- Bennett MH, Mansfield JW, Lewis MJ, Beale MH. 2002. Cloning and expression of sesquiterpene synthase genes from lettuce (*Lactuca sativa* L.). *Phytochemistry* 60(3): 255-261.
- Berteau CM, Voster A, Verstappen FWA, Maffei M, Beekwilder J, Bouwmeester HJ. 2006. Isoprenoid biosynthesis in *Artemisia annua*: Cloning and heterologous expression of a germacrene A synthase from a glandular trichome cDNA library. *Archives of Biochemistry and Biophysics* 448(1-2): 3-12.
- Bork PM, Schmitz ML, Kuhnt M, Escher C, Heinrich M. 1997. Sesquiterpene lactone containing Mexican Indian medicinal plants and pure sesquiterpene lactones as potent inhibitors of transcription factor NF-kappa B. *FEBS Letters* 402(1): 85-90.
- Bouwmeester HJ, Kodde J, Verstappen FWA, Altug IG, de Kraker JW, Wallaart TE. 2002. Isolation and characterization of two germacrene A synthase cDNA clones from chicory. *Plant Physiology* 129(1): 134-144.
- Cankar K, Houwelingen Av, Bosch D, Sonke T, Bouwmeester H, Beekwilder J. 2011. A chicory cytochrome P450 mono-oxygenase CYP71AV8 for the oxidation of (+)-valencene. *FEBS Letters* 585(1): 178-182.
- da Silva BP, Cortez DA, Violin TY, Filho BPD, Nakamura CV, Ueda-Nakamura T, Ferreira ICP. 2010. Antileishmanial activity of a guaianolide from *Tanacetum parthenium* (L.) Schultz Bip. *Parasitology International* 59(4): 643-646.
- de Kraker JW, Franssen MCR, Dalm MCF, de Groot A, Bouwmeester HJ. 2001. Biosynthesis of germacrene A carboxylic acid in chicory roots. Demonstration of a cytochrome P450 (+)-germacrene A hydroxylase and NADP(+)-dependent sesquiterpenoid dehydrogenase(s) involved in sesquiterpene lactone biosynthesis. *Plant Physiology* 125(4): 1930-1940.
- de Kraker JW, Franssen MCR, de Groot A, Konig WA, Bouwmeester HJ. 1998. (+)-Germacrene A biosynthesis - The committed step in the biosynthesis of bitter sesquiterpene lactones in chicory. *Plant Physiology* 117(4): 1381-1392.
- de Kraker JW, Franssen MCR, Joerink M, de Groot A, Bouwmeester HJ. 2002. Biosynthesis of costunolide, dihydrocostunolide, and leucodin. Demonstration of cytochrome P450-catalyzed formation of the lactone ring present in sesquiterpene lactones of chicory. *Plant Physiology* 129(1): 257-268.
- Denmeade SR, Jakobsen CM, Janssen S, Khan SR, Garrett ES, Lilja H, Christensen SB, Isaacs JT. 2003. Prostate-specific antigen-activated thapsigargin prodrug as targeted therapy for prostate cancer. *Journal of the National Cancer Institute* 95(13): 990-1000.

- Drew D, Krichau N, Reichwald K, Simonsen H. 2009. Guaianolides in apiaceae: perspectives on pharmacology and biosynthesis. *Phytochemistry Reviews* 8(3): 581-599.
- Fischedick JT, Standiford M, Johnson DA, De Vos RCH, Todorović S, Banjanac T, Verpoorte R, Johnson JA. 2012. Activation of antioxidant response element in mouse primary cortical cultures with sesquiterpene lactones isolated from *Tanacetum parthenium*. *Planta Medica*(EFirst).
- Fischer NH. 1990. *Biochemistry of the mevalonic acid pathway to terpenoids*. New York: Plenum Press.
- Ikezawa N, Goepfert JC, Nguyen DT, Kim S-U, O'Maille PE, Spring O, Ro D-K. 2011. Lettuce costunolide synthase (CYP71BL2) and its homolog (CYP71BL1) from sunflower catalyze distinct regio- and stereo-selective hydroxylations in sesquiterpene lactone metabolism. *Journal of Biological Chemistry* 286(24): 21601-21611.
- Janssen S, Rosen DM, Ricklis RM, Dionne CA, Lilja H, Christensen SB, Isaacs JT, Denmeade SR. 2006. Pharmacokinetics, biodistribution, and antitumor efficacy of a human glandular kallikrein 2 (hK2)-activated thapsigargin prodrug. *The Prostate* 66(4): 358-368.
- K GR, Merillon JM. 2013. *Natural Products*. Berlin Heidelberg: Springer-Verlag.
- Klayman DL. 1985. Qinghaosu (Artemisinin) - an antimalarial drug from China. *Science* 228(4703): 1049-1055.
- Koo TH, Lee J-H, Park YJ, Hong Y-S, Kim HS, Kim K-W, Lee JJ. 2001. A sesquiterpene lactone, costunolide, from *Magnolia grandiflora* inhibits NF- κ B by targeting I κ B phosphorylation. *Planta Medica* 67(02): 103,107.
- Liu Q, Majdi M, Cankar K, Goedbloed M, Charnikhova T, Verstappen FWA, de Vos RCH, Beekwilder J, van der Krol S, Bouwmeester HJ. 2011. Reconstitution of the costunolide biosynthetic pathway in yeast and *Nicotiana benthamiana*. *PLoS ONE* 6(8): e23255.
- Lyss G, Knorre A, Schmidt TJ, Pahl HL, Merfort I. 1998. The anti-inflammatory sesquiterpene lactone Helenalin inhibits the transcription factor NF- κ B by directly targeting p65. *Journal of Biological Chemistry* 273(50): 33508-33516.
- Majdi M, Liu Q, Karimzadeh G, Malboobi MA, Beekwilder J, Cankar K, Vos Rd, Todorović S, Simonović A, Bouwmeester H. 2011. Biosynthesis and localization of parthenolide in glandular trichomes of feverfew (*Tanacetum parthenium* L. Schulz Bip.). *Phytochemistry* 72(14-15): 1739-1750.
- Neerman MF. 2003. Sesquiterpene lactones: a diverse class of compounds found in essential oils possessing antibacterial and antifungal properties. *International Journal of Aromatherapy* 13(2): 114-120.
- Nguyen DT, Gopfert JC, Ikezawa N, Macnevin G, Kathiresan M, Conrad J, Spring O, Ro DK. 2010. Biochemical conservation and evolution of germacrene A oxidase in asteraceae. *Journal of Biological Chemistry* 285(22): 16588-16598.
- Outchkourov NS, Peters J, de Jong J, Rademakers W, Jongsma MA. 2003. The promoter-terminator of chrysanthemum *rbcs1* directs very high expression levels in plants. *Planta* 216(6): 1003-1012.
- Pareek A, Suthar M, Rathore SG, Bansal V. 2011. Feverfew (*Tanacetum parthenium* L.): A systematic review. *Pharmacognosy Review* 5(9): 103-110.
- Picman AK. 1986. Biological activities of sesquiterpene lactones. *Biochemical Systematics and Ecology* 14(3): 255-281.
- Piet DP. 1996. *Transannular cyclisation reactions and the germacrene system mediated by enzymes from Cichorium intybus*. Proefschrift Wageningen thesis, Piet [S.I.].
- Pompon D, Louerat B, Bronine A, Urban P. 1996. Yeast expression of animal and plant P450s in optimized redox environments. *Methods in Enzymology* 272: 51-64.
- Qi S, Gomez-Barrios ML, Hopper EL, Hjortso MA, Fischer NH. 1995. Biosynthetic studies of lactucin derivatives in hairy root cultures of *Lactuca floridana*. *Phytochemistry* 40(6): 1659-1665.
- Rodriguez E, Towers GHN, Mitchell JC. 1976. Biological activities of sesquiterpene lactones. *Phytochemistry* 15(11): 1573-1580.
- Schall A, Reiser O. 2008. Synthesis of biologically active guaianolides with a trans-annulated lactone moiety. *European Journal of Organic Chemistry* 2008(14): 2353-2364.
- Schmittgen TD, Livak KJ. 2008. Analyzing real-time PCR data by the comparative CT method. *Nature Protocols* 3(6): 1101-1108.
- Simonsen HT, Weitzel C, Christensen SB. 2013. *Guaianolide sesquiterpenoids: Pharmacology and biosynthesis*. Berlin Heidelberg: Springer-Verlag.
- Søhoel H, Jensen A-ML, Møller JV, Nissen P, Denmeade SR, Isaacs JT, Olsen CE, Christensen SB. 2006. Natural products as starting materials for development of second-generation SERCA inhibitors targeted towards prostate cancer cells. *Bioorganic & Medicinal Chemistry* 14(8): 2810-2815.
- Teoh KH, Polichuk DR, Reed DW, Nowak G, Covello PS. 2006. *Artemisia annua* L.(Asteraceae) trichome-specific cDNAs reveal CYP71AV1, a cytochrome P450 with a key role in the biosynthesis of the antimalarial sesquiterpene lactone artemisinin. *FEBS Letters* 580(5): 1411-1416.
- Urban P, Mignotte C, Kazmaier M, Delorme F, Pompon D. 1997. Cloning, yeast expression, and characterization

of the coupling of two distantly related *Arabidopsis thaliana* NADPH-Cytochrome P450 reductases with P450 CYP73A5. *Journal of Biological Chemistry* 272(31): 19176-19186.

Vanengelen FA, Molthoff JW, Conner AJ, Nap JP, Pereira A, Stiekema WJ. 1995. Pbinplus - an improved plant transformation vector based on Pbin19. *Transgenic Research* 4(4): 288-290.

Zhai JD, Li D, Long J, Zhang HL, Lin JP, Qiu CJ, Zhang Q, Chen Y. 2012. Biomimetic semisynthesis of arglabin from parthenolide. *The Journal of Organic Chemistry* 77(16): 7103-7107.

Zhang S, Won YK, Ong CN, Shen HM. 2005. Anti-cancer potential of sesquiterpene lactones: bioactivity and molecular mechanisms. *Current Medicinal Chemistry - Anti-Cancer Agents* 5(3): 239-249.

Chapter 6

General discussion

Qing Liu

Plant secondary metabolites are an important source for the development of new drugs. For example, antimalarial drug artemisinin, was isolated from a herb *Artemisia annua* which has been used for many centuries in Chinese tradition medicine as a treatment for fever and malaria (Klayman, 1985). Another terpenoid paclitaxel (taxol), first isolated from the pacific yew tree (*Taxus brevifolia*), has been considered as the most successful anticancer drugs (Heinig *et al.*, 2013). Parthenolide, a sesquiterpene lactone present in feverfew, is a promising lead for the development of an anti-cancer drug and has attracted a lot of attention from medical institutes and companies. The elucidation of the biosynthetic pathway of parthenolide should improve the availability of parthenolide, and possibly parthenolide derivatives with improved chemical properties, and hence speed up the development of parthenolide-based anti-cancer drugs. The aim of the study presented in this thesis was to elucidate the biosynthetic pathway of parthenolide and related sesquiterpene lactones and to deliver the proof of concept for the heterologous production of these compounds in a heterologous host plant. With the cDNA library of feverfew trichomes at hand, the parthenolide biosynthetic pathway was elucidated by isolating all the structural genes (Figure 1). Moreover, the whole pathway was reconstituted in a heterologous plant species, *Nicotiana benthamiana*, through transient expression (agro-infiltration). Besides the genes involved in the parthenolide biosynthetic pathway, we also isolated P450s that catalyse branches of the main pathway (Figure 1): Tp8878, a 3 β -hydroxylase, which can hydroxylate both costunolide and parthenolide at C₃ and Tp8879, kauniolide synthase, which can cyclise costunolide to form kauniolide. Another P450, Tp8886, can oxidise kauniolide to an alcohol or epoxide, but the exact identity of the product has not been determined yet.

Strategies to enhance medicinal compound yield from medicinal plants

One of the drawbacks of using plants as a source for the production of drugs is that many plant species produce the bioactive terpenoids in only low quantities. Sometimes this is because the biosynthesis of those terpenoids is restricted to specialized cells (e.g. trichome, laticifer) which form only a small portion of the cells in a certain tissue, e.g. leaf, root, ovary. To increase the production of bioactive terpenoids in medicinal plants where these compounds naturally occur, the options are limited, as most medicinal plants are difficult to cultivate, to multiply or to transform.

However, there are exceptions to this rule. For the anti-malarial drug artemisinin, for example, transformation of the host plant *Artemisia annua* has been established (Weathers *et al.*, 1994; Vergauwe *et al.*, 1996; Han *et al.*, 2005). Overexpression of genes involved in the biosynthetic pathway or transport of artemisinin in *A. annua* increased the yield of artemisinin by more than two-fold (Jing *et al.*, 2008; Wang *et al.*, 2011; Zhang *et al.*, 2012). In addition to this transgenic approach, the yield of artemisinin in *A. annua* could also be promoted through cultivation, such as exposure to salinity stress (Qian *et al.*, 2010) or through abscisic acid treatment (Jing *et al.*, 2009). For feverfew, as transformation has not yet been established, the promotion of parthenolide yield is limited to agricultural practices, such as harvesting time

of specific cells that synthesize the product can greatly enhance the chances of identifying the relevant genes from sequencing of mRNA isolated from these specific cell types. For the identification of genes involved in parthenolide biosynthesis, the trichomes were isolated from ovaries and used for cDNA library construction and subsequent 454 sequencing. The isolation of specific metabolic pathway genes from mRNA isolated from glandular trichomes has been reported for several plant species, including mint (*Mentha piperita*) (Alonso *et al.*, 1992; Rajaonarivony *et al.*, 1992; Lange *et al.*, 2000), basil (*Ocimum basilicum*) (Gang *et al.*, 2002; Iijima *et al.*, 2004; Xie *et al.*, 2008), *A. annua* (Teoh *et al.*, 2006; Zhang *et al.*, 2008; Ting *et al.*, 2013), tomato (*Solanum lycopersicum*) (Fridman *et al.*, 2005; Besser *et al.*, 2009; Schillmiller *et al.*, 2009), and hop (*Humulus lupulus*) (Wang *et al.*, 2002; Nagel *et al.*, 2008; Xu *et al.*, 2013).

With the EST sequences in hand, the next challenge is to recognize the potential candidate genes, which usually starts by comparing the sequences to those available in public databases such as NIST. Vice versa, known terpene synthase gene sequences are used to blast against the specific sequence database to identify terpene synthases. Terpene synthases can be recognized as they share a common aspartate-rich DDxxD motif which is thought to be involved in the coordination of divalent metal ions for substrate binding (Lesburg *et al.*, 1997). Similar strategies may be used to identify cytochrome P450s which may be involved in the further modification of the terpenoid products. Especially for the P450 enzymes, this approach will render multiple candidate genes from which the right one still needs to be selected. For instance, in this thesis, fifty nine candidate P450s genes were identified for the parthenolide biosynthetic pathway in the feverfew trichome cDNA database. An efficient way to select the most likely candidate gene from such a large group of candidates is to use a combination of expression and metabolite profiling. Expression profiling does not require full length sequence information and when different tissues or developmental stages of a tissue are available that display a trend in metabolite accumulation, the metabolite profile can be compared to the expression profile of the candidate genes over the same tissue samples. In this way the list of 58 candidate P450 genes could be reduced to nine top candidates.

In this thesis, we noticed that all the P450s in the same biosynthetic pathway belonged to the same group, e.g. both GAO and COS belong to the CYP71 group, which helped us to identify P450s involved in the following steps, e.g. PTS (CYP71CA1, Chapter 4). Actually the identification of GAO was based on the discovery of amorphadiene oxidase (CYP71AV1), a gene that can oxidise amorphadiene to artemisinic acid (Teoh *et al.*, 2006). As the structure of germacrene A is close to that of amorphadiene, GAO was assumed to share high amino acid sequence similarity to that of CYP71AV1, leading to the finding of GAO (CYP71AV8) (Nguyen *et al.*, 2010; Cankar *et al.*, 2011). Later on, the identification of GAO (CYP71AV8) inspired the identification of COS from lettuce (CYP71BL2) (Ikezawa *et al.*, 2011), chicory (CYP71BL3, Chapter 3) (Liu, Q *et al.*, 2011) and feverfew (Chapter 4), as well as parthenolide synthase, kauniolide synthase and kauniolide oxidase from feverfew (Chapter 4 and 5).

Candidate gene characterisation

Once the candidate sequences have been identified, their full length sequences need to be ob-

tained by RACE-PCR after which the cDNA can be cloned into different expression vectors. Terpene synthase genes can be expressed in *E. coli* for functional characterisation while yeast should be used for expressing proteins that are targeted to microsomal membranes, such as P450s. Plants offer the advantage that they carry out more complex post-translational modifications than the other two expression hosts. In this thesis, the function of the terpene synthase gene, *TpGAS*, was identified by expression in *E. coli*, yeast and *N. benthamiana* (Chapter 2). The function of P450 candidates was identified by expression in yeast and *N. benthamiana* (Chapter 3, 4 and 5).

For candidate genes that operate downstream in the terpenoid biosynthetic pathway, the characterisation by expression in yeast is difficult when specific substrates are not readily available for feeding assays. This problem can be overcome by co-expression of the genes that encode enzymes making the putative substrate of the candidate enzyme to be tested. For the identification of *LsCOS*, for example, candidate genes were co-transformed in yeast with *GAS*+*GAO* that together makes the substrate for *LsCOS*, Germacra-1(10),4,11(13)-trien-12-oic acid (Ikezawa *et al.*, 2011). Another option would be to combine microsomes from multiple independent yeast cultures expressing single genes in one combined *in vitro* assay. In this thesis, we mixed the microsomes of yeast expressing *kauniolide synthase* (*TpKS*) and another P450 candidate, *Tp8886*, together. After feeding the mixture with the substrate of *KS*, costunolide, a new peak of oxidised kauniolide (based on molecular mass spectrum) was detected by LC-MS. The oxidised kauniolide is not from an epoxidation as the retention of this new peak is not the same as either of its kauniolide-epoxidized compounds (data not shown). We were unable to identify this new product yet, and it is also not present in feverfew! This demonstrates the power of combinatorial biochemistry where we combine enzymes into new pathways, producing compounds that may even be new to nature and could potentially have novel biological activity.

Agrobacterium-mediated transient gene expression is often used for identification of new viral suppressors of RNA silencing (Thomas *et al.*, 2003) and screening and functional analysis of unidentified genes (Hashimoto *et al.*, 2012; Kanagarajan *et al.*, 2012). The system has been further used to test whole groups of genes in pathway reconstitution experiments through agro-co-infiltration in plant, such as *N. benthamiana* (van Herpen *et al.*, 2010), lettuce (Joh *et al.*, 2005), and tobacco (Yang *et al.*, 2000). When expression constructs are available for all known steps of the pathway (starting with the specific TPS) and all candidate genes are cloned into individual expression vectors, such agro-infiltration assays may be used to test activity of the transiently expressed novel genes in *N. benthamiana*. By using this way, genes from the artemisinin biosynthesis pathway in *Artemisia annua* have been identified and characterized (Ting *et al.*, 2013), and so does the genes of the costunolide and parthenolide biosynthetic pathway of feverfew in this thesis (Chapter 4).

Product detection and identification

Targeted detection

Different techniques could be used for the detection of products. When the standard of a dedicated product is available, targeted analysis could be applied by GC-MS, LC-QTOF-MS, LC-Orbitrap-FTMS, and LC-MRM-MS/MS. In this thesis, the content of costunolide and parthenolide in transformed yeast extract or agro-infiltrated *N. benthamiana* leaves was qualified and quantified by standards (Chapter 3 and 4).

Chemical modification: Some compounds are difficult to detected either because they are not well extracted by the solvent used or they show poor ionisation during analysis by QTOF. Such compound may be easier to detect after a simple modification. In this thesis, the product of *TpKS* was hardly detectable when expressed in yeast. Cysteine was added to the reaction mixture as we have known from previous work that the product could be conjugated with cysteine through Michael-reaction. A new obvious peak was detected and later on identified as kauniolide-cysteine (Chapter 5).

Standards through bulk isolation: To identify the products of candidates, standards need to be available. But for the complicated sesquiterpene biosynthesis pathways most substrates and products are unknown and are not commercially available. One option to obtain specific standard compounds is through bulk isolation and purification from host plant tissue. For example, several sesquiterpene lactones have been isolated from bulk feverfew plant tissue material for which the structure of the purified compound was elucidated by NMR (Fischedick *et al.*, 2012). Those compounds were later crucial to identify two novel compounds produced by parthenolide candidates, 3 β -hydroxycostunolide and 3 β -hydroxyparthenolide (Chapter 4).

Standards through chemical synthesis: Another option to obtain standards would be chemical synthesis of the predicted compound. In this thesis, a unknown product of one of the candidate genes was identified as kauniolide based on references chemically synthesized (Zhai *et al.*, 2012) (Chapter 5). A third option would be using *in vitro* synthesized compounds as reference. In this thesis, two novel conjugates of costunolide were found in agro-infiltrated *N. benthamiana* leaves. Based on their molecular masses, they are assumed to be cysteine and glutathione conjugated of costunolide. Through *in vitro* enzyme assay, costunolide-glutathione and costunolide-cysteine were synthesized and used to identify those two novel compounds (Chapter 3). Similar strategy was used to identify parthenolide-glutathione and parthenolide-cysteine later (Chapter 4). We have to admit the limitation of this option, which is better used when other options are not available.

NMR elucidation: When no standards are available to identify the product, NMR may be applied to elucidate the structure, as NMR is in principle the most uniform detection technique and is essential for the unequivocal identification of unknown compounds. This strategy has been successfully applied to the structure of two novel compounds, artemisinic acid-12- β -diglucoside (van Herpen *et al.*, 2010) and geranoyl-6-O-malonyl- β -D-glucopyranoside (Yang *et al.*, 2011). However, structure elucidation by NMR can be very time and energy consuming, as the sensitivity of NMR is relatively low compared with MS.

Untargeted detection

When searching for unknown/novel compound is required, unbiased metabolomics detec-

tion is needed and could be applied by GC-MS, LC-QTOF-MS. For example, an un-target LC-MS profiling of extract from maize leaves overexpressing geraniol synthase was performed to find the major product of the overexpressed gene as geranic acid glycoside (Yang *et al.*, 2011). In this thesis, similar untargeted approach was applied and two novel conjugates costunolide-cysteine and costunolide-glutathione were identified in agro-infiltrated *N. benthamiana* leaves (Chapter 3).

Functional characterisation of candidate genes can be done by monitoring product accumulation, or substrate consumption when products of genes are not detectable. In this thesis, the identification of *TpGAO* was conducted by co-expressing it with *TpGAS* in *N. benthamiana*. Although no new product was detected, we noticed that the production of germacrene A (substrate) was decreased dramatically in *N. benthamiana* expressing *TpGAS/TpGAO* compared to the one expressing *TpGAS* only. By expressing *TpGAO* in yeast, we were able to detect its products, germacrene A alcohol, germacrene A aldehyde and germacrene A acid (Chapter 4).

Whole pathway reconstitution

Many plant-derived terpenoids have pharmaceutical and industrial applications, such as parthenolide, but their natural resources for extraction are often limited and, in many cases, their chemical synthetic routes are not commercially available. Metabolic engineering, either in the native producer or a heterologous host, is the only realistic alternative to improve yield and accessibility. The reconstruction of a biosynthesis pathway that involve multiple genes in stable transformed heterologous plants can be complicated as introduction of multiple genes under the same promoter may lead to silencing problems. Step wise introduction of pathways in stable transformed plants may also be hampered by accumulation of toxic intermediates which may cause selection of low expressing transformants. Transient gene expression system, mediated by *Agrobacterium*, in intact plant leaves is a rapid and useful method for metabolic engineering. By this method many different heterologous proteins can be produced without the need to generate transgenic plants, which is tedious, time consuming and sometimes difficult for many plant species (Fischer *et al.*, 1999; Fischer *et al.*, 2004).

Several platforms have been reported to be suitable for transient expression, e.g. *N. benthamiana* (Nafisi *et al.*, 2007; van Herpen *et al.*, 2010), *Nicotiana tabacum* (tobacco) (Yang *et al.*, 2000), and *Lactuca sativa* (lettuce) (Joh *et al.*, 2005). Transient gene expression has several advantages over stable expression. First, the transient gene expression technique is simple and easy to perform and the results can be assayed one week post-agroinfiltration (Kapila *et al.*, 1997), compared to months (to years) for stable transformation. Second, several genes can be introduced into plants at the same time through transient expression. (ref). In my thesis I introduced up to 15 genes have been successfully introduced into *N. benthamiana* plants through transient expressing and used that for the discovery of the P450 genes involved in STL biosynthesis in feverfew (Chapter 4 and 5). Finally, the relative expression level of the genes may also be manipulated by changing the relative amount of *Agrobacterium* carrying

each of the genes, which is difficult to achieve by stable transformation.

Using transient expression in *N. benthamiana*, only about 50% of costunolide was converted to parthenolide when *TpPTS* was added to the pathway (Chapter 4). This is likely caused by the co-infiltration of too many genes at the same time, such that not all cells are transformed with the whole pathway. The more multiple independent agrobacterium strains are co-infiltrated, the higher the chance that some cells are not being transfected with all the pathway genes. When *TpGAS* was transiently expressed in *N. benthamiana*, a huge peak of peak of germacrene A could be detected by GC-MS. When *TpGAO* was co-expressed with *TpGAS*, the peak area of germacrene A decreased by than more 90%. However, we were not able to detected any new peaks produced by *TpGAO*. Nevertheless when we co-expressed *TpCOS* or *CiCOS* with *TpGAS* and *TpGAO* or *CiGAO* we could detected costunolide and its conjugates, showing that Germacra-1(10),4,11(13)-trien-12-oic acid is produced upon expression of *GAS* and *GAO* (and is available to costunolide synthase when that is co-expressed), but is apparently conjugated to something that we cannot detect with our mass spectrometer.

Strategies for boosting flux through the pathway

To increase productivity during pathway reconstitution, it is important to boost the flux through the pathway or make use of pathway precursors more efficiently. Several strategies can be used to achieve that, including targeted expression, eliminating competing endogenous enzyme activity, Boosting precursor availability, and construction of an artificial metabolon.

Targeted expression

As the biosynthesis of different terpenoids is highly compartmentalized, enzymes need to be targeted to the appropriate location to achieve better production of terpenoids. For example, by expressing a limonene synthase gene from *Perilla frutescens*, with different targeting signal (plastid, cytosolic, endoplasmic reticulum), in tobacco (*Nicotiana tabacum*), Ohara *et al.* (2003) found that the specific activity of limonene synthase was generally higher in transgenics expressing the plastid localization construct compared to those containing the cytosolic enzyme. In this thesis, by targeting *TpGAS* to the mitochondria, the production of germacrene A in *N. benthamiana* was increased 15-fold compared with cytosolic localisation (Chapter 3).

Eliminating competing endogenous enzyme activity

When reconstituting biosynthetic pathways by transiently expressing multiple genes in a heterologous host plant, losses may occur if intermediate products are recognized by endogenous enzymes which divert carbon flux from the desired product route. For example, when *GAS+GAO+COS* were co-infiltrated in *N. benthamiana*, more than 90% of the costunolide produced was conjugated either to cysteine or to glutathione. When *PTS* was co-infiltrated with *GAS+GAO+COS*, the concentration of costunolide conjugate decreased by 50%, showing that the heterologous *PTS* competes with the endogenous glutathione S transferase conjugating costunolide. Elimination or restriction of endogenous competing reactions has been

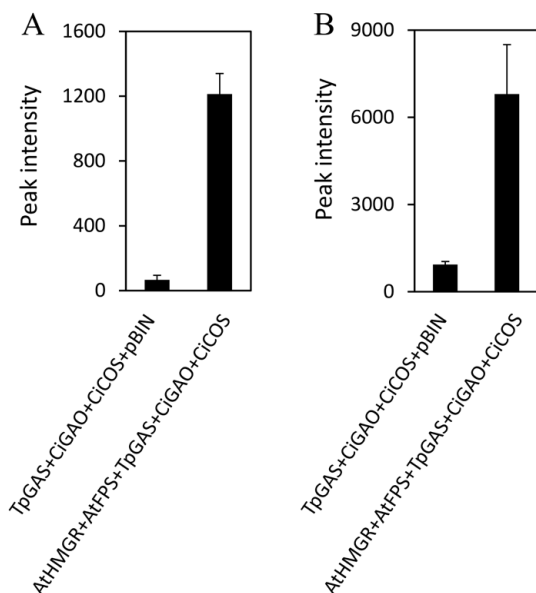


Figure 2. Boosting production of costunolide by co-expression of *AtHMGR* and *AtFPS* through agro-infiltration in *Nicotiana benthamiana* leaves. (A) Y-axis: the peak intensity of free costunolide measured by LC-triple quad-MS. X-axis: set of genes used for the agro-infiltration. (B) Y-axis: the peak intensity of costunolide conjugates measured by LC-QTOF-MS. X-axis: set of genes used for the agro-infiltration.

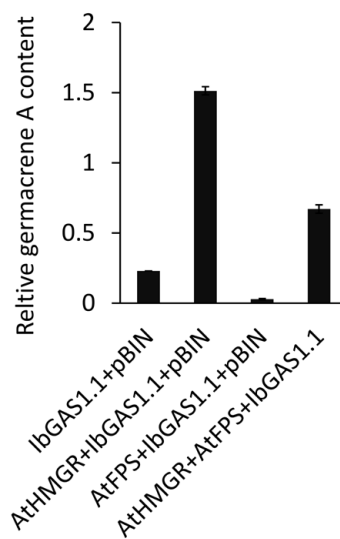


Figure 3. Contribution for the boosting of agro-infiltration production by *AtHMGR* and *AtFPS*. *AtHMGR* and/or *AtFPS* were used to co-infiltrate with *IbGAS* in *N. benthamiana*. The product, germacrene A, was collected and measured by GC-MS.

shown to increase production of target compounds in yeast (Ro *et al.*, 2006; Paddon *et al.*, 2013). The advantage of a transient expression/ production system would be that inhibition of competing reactions in mature leaves would be of little consequence during the 4-5 days of transient parthenolide production, while permanent elimination of such competing reactions in stable transformants could potentially lead to reduced plant fitness. On the other hand, storage of target metabolites as conjugates may have the advantage that the storage capacity of the vacuole is used and that high concentrations can be reached without phytotoxic effects (1995).

Boosting precursor availability: The overexpression of genes encoding enzymes such as 3-hydroxy-3-methylglutaryl-CoA reductase (HMGR), deoxyxylulose 5-phosphate synthase (DXS) and prenyltransferases, has been used to elevate terpenoid levels in plants (Degenhardt *et al.*, 2003; Wu *et al.*, 2006). Overexpression of *HMGR* and *farnesyl diphosphate synthase* (*FPS*; farnesyl diphosphate is the immediate C15 precursor for sesquiterpene biosynthesis) together with *amorphaadiene synthase* resulted in an 80-fold increase in the production of the artemisinin precursor, amorphaadiene (van Herpen *et al.*, 2010). In my thesis work, I used the same *AtHMGR* together with *AtFPS* to boost the production of costunolide 7-fold (free form) and 20-fold (conjugated form) (Figure 2). Later we found that the boosting activity was due

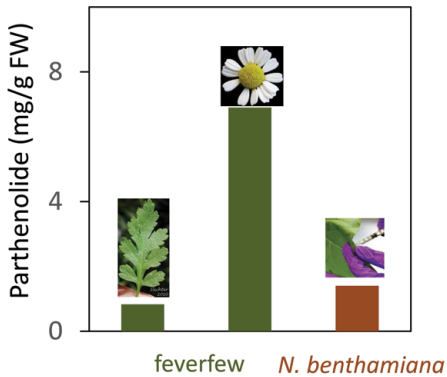


Figure 4. Total parthenolide (free plus conjugated) content in *N. benthamiana* leaves infiltrated with the whole parthenolide biosynthetic pathway and feverfew leaves and flowers. In agro-infiltrated leaves, both free and conjugated parthenolide are present, in feverfew leaves and flowers only free parthenolide.

undesired crosstalk between different metabolic pathways (Møller, 2010). As the expression of parthenolide biosynthetic pathway genes in feverfew is highly coordinated and there is competition between heterologous genes and endogenous *N. benthamiana* genes, construction of an artificial metabolon using a common scaffold protein could coordinate the flux of heterologous enzyme products/substrates and prevent the competition for heterologous metabolites by endogenous enzymes.

Comparing feverfew and *N. benthamiana* yields of parthenolide

When the whole biosynthetic pathway of parthenolide was reconstituted in *N. benthamiana* in combination with boosting by co-expression of *AtHMGR*, the production of free and conjugated parthenolide in the leaves of *N. benthamiana* was 1.4 mg/g FW (Chapter 4). This is higher than the (free) parthenolide content in feverfew leaves, but lower than the content in feverfew flowers (Figure 4). Nevertheless, there are several advantages of producing parthenolide through agro-infiltration in *N. benthamiana* over production with feverfew. First, it takes 4 weeks for *N. benthamiana* plants to be ready for agro-infiltration, and leaves could be harvested 4-5 days later, compared to 3 months for feverfew plants to be ready for harvest. Second, the industrial culturing of *N. benthamiana* – including large-scale agro-infiltration – is available, which can ensure a stable plant supply, thus stable supply of parthenolide.

At present the parthenolide amount produced in agro-infiltrated *N. benthamiana* leaves is probably not yet high enough for industrial-scale production when compared with feverfew. However, in the evaluation of production capacity of feverfew plants and an industrial scale agroinfiltration of pre-grown tobacco plants the time aspects should also be taken into account. The yield from *N. benthamiana* is obtained 4-5 days after agro-infiltration, while that

to *AtHMGR*, while *AtFPS* did not contribute (Figure 3). A possible explanation for that could be that the product of *AtFPS* is not available to the downstream *GAS*. In subsequent experiments (Chapter 4 and 5), only *AtHMGR* was therefore used to boost production in agro-infiltration.

Construction of an artificial metabolon: Metabolons are multienzyme complexes which allow the direct passage of product from one enzymatic reaction to a consecutive enzyme in a metabolic pathway (Møller, 2010). The advantage of a metabolon is that it can limit the diffusion of intermediates into the surrounding medium, facilitates fast turnover of labile or toxic intermediates, and may prevent

from feverfew requires at least 10 weeks of growth followed by a second harvest from the same plants after an additional 27 weeks (<http://www2.ca.uky.edu/ktrdc/Bulletin%20KTRDC-IB-3.pdf>). In 2009, feverfew seed was sold for \$424/kg and the buyer price for dried feverfew was about \$3.20/kg. Premiums paid for organically produced product in Canada have fluctuated from year to year and are buyer dependent. Yields of feverfew in Saskatchewan can vary from 2,000 kg/ha to 5,000 kg/ha dry herb (about 20,000-50,000 kg FW/ha). (<http://www.agriculture.gov.sk.ca/Default.aspx?DN=5a05a8da-ff3e-490b-b280-5f7b22b803b>). Assuming that the yield from feverfew is per year and mainly consists of leaf material (with similar content per gr/FW as agroinfiltrated *N. benthamiana* plants), one would need to infiltrate 200,000-500,000 *N. benthamiana* plants (at about 100 gr FW/plant) per year to reach similar yields as with a hectare of feverfew. This mounts to about 4000 plant infiltrations per week.

Options for host plant engineering

Instead of using a heterologous plant host, there are also advantages to engineering the homologous host, if that host can be transformed. Several strategies for metabolic engineering of medicinal plants have been used to boost the production of terpenoids, such as overexpressing enzymes and boosting transcriptional regulation.

Engineering enzymes

The production of terpenoids can be boosted through overexpression of biosynthetic genes. The artemisinin content in *A. annua* was enhanced 2.4-fold through over-expression of two of its biosynthetic genes, *CYP71AV1* and *cytochrome P450 reductase (CPR)*, in the host plant (Jing *et al.*, 2008). When FPS was co-overexpressed with these two biosynthetic genes, artemisinin production was enhanced 3.6-fold (Chen *et al.*, 2012). A similar strategy could be applied to feverfew when its transformation is established.

Boosting transcriptional regulation

The use of transcription factors to up-regulate an entire terpenoid pathway (or large parts of it) has so far not been reported (Lange & Ahkami, 2012). However, there are transcription factors, such as ERF/AP2 type (van der Fits & Memelink, 2000; Yu *et al.*, 2012), WRKY (Xu *et al.*, 2004) and MYC (Hong *et al.*, 2012), that have been reported to be involved in transcriptional regulation of terpenoid biosynthesis in several different plant species. The understanding of transcriptional regulation of terpenoid biosynthesis may enable us to manipulate the biosynthesis pathway of terpenoids in cell or tissue cultures of medicinal plants. In *Catharanthus roseus*, overexpression of AP2/ERF transcription factor *ORCA3* resulted in enhanced expression of several terpene indole-alkaloid biosynthetic genes and, consequently, in increased accumulation of the terpenoid indole alkaloid products (van der Fits & Memelink, 2000). Overexpression of *ORCA2* lead to enhanced accumulation of catharanthine and vindoline in hairy roots (Liu, D-H *et al.*, 2011). In *Artemisia annua*, overexpression of AP2/ERF transcription factors *AaERF1* and *AaERF2* resulted in elevated transcript levels of both *ADS* and *CYP71AV1* and consequently in increased accumulation of artemisinin and artemisinic acid (Yu *et al.*, 2012). Overexpression of *AaORA* - the expression of which could directly be

linked to expression of *ADS*, *CYP71AV1* and *DBR2* that encode enzymes of the artemisinin pathway - in transgenic *A. annua* resulted in an about 50% increase in artemisinin and 35% in DHAA content (Lu *et al.*, 2013). In my thesis I show that the expression of the genes involved in the biosynthetic of parthenolide all show similar profiles, suggesting that these genes are under the regulation of a single transcription factor. Selection of transcription factors that show similar expression profiles as the pathway genes can help us to narrow down the number of candidates. If this transcription factor can be identified, overexpression in feverfew could probably increase the production of parthenolide.

Increasing the polarity of terpenoids

Water solubility is a crucial part of the terpenoid biological activity as poor solubility will make pharmacological use of the compound difficult. This poor water solubility is for example a limitation for the use of parthenolide as a drug. Solubility of a compound may be improved by, among others, amino acid conjugation, hydroxylation and glycosylation. Parthenolide amino analogs could be converted into water-soluble organic acid salts through Michael addition reactions, and this increased their water solubility and bioavailability (Guzman *et al.*, 2007; Neelakantan *et al.*, 2009). In my thesis, cysteine and glutathione conjugates of parthenolide were produced upon pathway reconstitution in *N. benthamiana*. These conjugates are more water-soluble than parthenolide and showed high activity against colon cancer cells, with only slightly lower activity than parthenolide (Chapter 4). Glycosylation has been reported to often change the biological activity of terpenoids as well as improve their pharmacokinetic parameters (Rivas *et al.*, 2013). Hydroxylation, many of which are performed by P450 oxidases, may cause new bioactivity to the compounds as well as improve their water solubility (McGarvey & Croteau, 1995). In this thesis, through the hydroxylation at C3 position of costunolide and parthenolide, their water-solubility was increased while their bioactivity was not affected (Chapter 4).

Future challenges

In my thesis work I have elucidated the entire biosynthetic pathway of parthenolide and have reconstituted this pathway *in planta*. The future challenge lies in how to bring the production of parthenolide to a level high enough for industrial production. Solutions for that challenge include optimization of the enzymatic activity of the pathway genes, boosting of precursor availability, and restriction of competing pathways, like what has been done for the production of artemisinin precursors in yeast (Paddon *et al.*, 2013). Besides those, solutions may also include targeting the expression of the pathway to other sub-cellular compartments, coordination of each gene's expression level and/or artificial metabolon formation, to reach an optimum flux through the pathway. Finally, as only a few P450 candidates out of the 59 within the CYP71 group have been identified in this thesis, some of the remaining P450s may be able to convert parthenolide to more water-soluble derivatives while keeping its activity. This would possibly make parthenolide interesting enough to warrant large-scale efforts to use

the knowledge generated in my thesis for the large-scale biotechnological production of this natural compound.

References:

- Alonso WR, Rajaonarivony JI, Gershenzon J, Croteau R. 1992. Purification of 4S-limonene synthase, a monoterpenic cyclase from the glandular trichomes of peppermint (*Mentha x piperita*) and spearmint (*Mentha spicata*). *Journal of Biological Chemistry* 267(11): 7582-7587.
- Besser K, Harper A, Welsby N, Schauvinhold I, Slocombe S, Li Y, Dixon RA, Broun P. 2009. Divergent regulation of terpenoid metabolism in the trichomes of wild and cultivated tomato species. *Plant Physiology* 149(1): 499-514.
- Cankar K, Houwelingen Av, Bosch D, Sonke T, Bouwmeester H, Beekwilder J. 2011. A chicory cytochrome P450 mono-oxygenase CYP71AV8 for the oxidation of (+)-valencene. *FEBS Letters* 585(1): 178-182.
- Chen Y, Shen Q, Wang Y, Wang T, Wu S, Zhang L, Lu X, Zhang F, Jiang W, Qiu B. 2012. The stacked over-expression of FPS, CYP71AV1 and CPR genes leads to the increase of artemisinin level in *Artemisia annua* L. *Plant Biotechnology Reports*: 1-9.
- Degenhardt J, Gershenzon J, Baldwin IT, Kessler A. 2003. Attracting friends to feast on foes: engineering terpene emission to make crop plants more attractive to herbivore enemies. *Current Opinion in Biotechnology* 14(2): 169-176.
- Fischedick JT, Standiford M, Johnson DA, De Vos RCH, Todorović S, Banjanac T, Verpoorte R, Johnson JA. 2012. Activation of antioxidant response element in mouse primary cortical cultures with sesquiterpene lactones isolated from *Tanacetum parthenium*. *Planta Medica* 78(18): 1725-1730.
- Fischer R, Stoger E, Schillberg S, Christou P, Twyman RM. 2004. Plant-based production of biopharmaceuticals. *Current Opinion in Plant Biology* 7(2): 152-158.
- Fischer R, Vaquero-Martin C, Sack M, Drossard J, Emans N, Commandeur U. 1999. Towards molecular farming in the future: transient protein expression in plants. *Biotechnology and Applied Biochemistry* 30(2): 113-116.
- Fonseca JM, Rushing JW, Rajapakse NC, Thomas RL, Riley MB. 2005. Parthenolide and abscisic acid synthesis in feverfew are associated but environmental factors affect them dissimilarly. *Journal of Plant Physiology* 162(5): 485-494.
- Fridman E, Wang J, Iijima Y, Froehlich JE, Gang DR, Ohlrogge J, Pichersky E. 2005. Metabolic, genomic, and biochemical analyses of glandular trichomes from the wild tomato species *Lycopersicon hirsutum* identify a key enzyme in the biosynthesis of methylketones. *The Plant Cell* 17(4): 1252-1267.
- Gang DR, Lavid N, Zubieta C, Chen F, Beuerle T, Lewinsohn E, Noel JP, Pichersky E. 2002. Characterization of phenylpropene O-methyltransferases from sweet basil facile change of substrate specificity and Convergent evolution within a plant o-methyltransferase family. *The Plant Cell* 14(2): 505-519.
- Guzman ML, Rossi RM, Neelakantan S, Li XJ, Corbett CA, Hassane DC, Becker MW, Bennett JM, Sullivan E, Lachowicz JL, Vaughan A, Sweeney CJ, Matthews W, Carroll M, Liesveld JL, Crooks PA, Jordan CT. 2007. An orally bioavailable parthenolide analog selectively eradicates acute myelogenous leukemia stem and progenitor cells. *Blood* 110(13): 4427-4435.
- Han J-l, Wang H, Ye H-c, Liu Y, Li Z-q, Zhang Y, Zhang Y-s, Yan F, Li G-f. 2005. High efficiency of genetic transformation and regeneration of *Artemisia annua* L. via *Agrobacterium tumefaciens*-mediated procedure. *Plant Science* 168(1): 73-80.
- Hashimoto M, Komatsu K, Maejima K, Okano Y, Shiraishi T, Ishikawa K, Takinami Y, Yamaji Y, Namba S. 2012. Identification of three MAPKKKs forming a linear signaling pathway leading to programmed cell death in *Nicotiana benthamiana*. *BMC Plant Biology* 12(1): 103.
- Heinig U, Scholz S, Jennewein S. 2013. Getting to the bottom of taxol biosynthesis by fungi. *Fungal Diversity*: 1-10.
- Hong G-J, Xue X-Y, Mao Y-B, Wang L-J, Chen X-Y. 2012. *Arabidopsis* MYC2 interacts with DELLA proteins in regulating sesquiterpene synthase gene expression. *The Plant Cell* 24(6): 2635-2648.
- Iijima Y, Gang DR, Fridman E, Lewinsohn E, Pichersky E. 2004. Characterization of geraniol synthase from the peltate glands of sweet basil. *Plant Physiology* 134(1): 370-379.
- Ikezawa N, Goepfert JC, Nguyen DT, Kim S-U, O'Maille PE, Spring O, Ro D-K. 2011. Lettuce costunolide synthase (CYP71BL2) and its homolog (CYP71BL1) from sunflower catalyze distinct regio- and stereo-selective hydroxylations in sesquiterpene lactone metabolism. *Journal of Biological Chemistry* 286(24): 21601-21611.
- Jing F-y, Zhang L, Li M-y, Tang K-x. 2008. Over-expressing CYP71AV1 and CPR genes enhances artemisinin content in *Artemisia annua* L. *Journal of Agricultural Science and Technology* 10: 64-70.
- Jing F, Zhang L, Li M, Tang Y, Wang Y, Wang Y, Wang Q, Pan Q, Wang G, Tang K. 2009. Abscisic acid (ABA) treatment increases artemisinin content in *Artemisia annua* by enhancing the expression of genes in artemisinin

- biosynthetic pathway. *Biologia* **64**(2): 319-323.
- Joh LD, Wroblewski T, Ewing NN, VanderGheynst JS. 2005.** High-level transient expression of recombinant protein in lettuce. *Biotechnology and Bioengineering* **91**(7): 861-871.
- Kanagarajan S, Muthusamy S, Gliszczynska A, Lundgren A, Brodelius PE. 2012.** Functional expression and characterization of sesquiterpene synthases from *Artemisia annua* L. using transient expression system in *Nicotiana benthamiana*. *Plant Cell Reports* **31**(7): 1309-1319.
- Kapila J, De Rycke R, Van Montagu M, Angenon G. 1997.** An *Agrobacterium*-mediated transient gene expression system for intact leaves. *Plant Science* **122**(1): 101-108.
- Klayman DL. 1985.** Qinghaosu (artemisinin): an antimalarial drug from China. *Science* **228**(4703): 1049-1055.
- Lange BM, Ahkami A. 2012.** Metabolic engineering of plant monoterpenes, sesquiterpenes and diterpenes - current status and future opportunities. *Plant Biotechnology Journal* **11**(2): 169-196.
- Lange BM, Wildung MR, Stauber EJ, Sanchez C, Pouchnik D, Croteau R. 2000.** Probing essential oil biosynthesis and secretion by functional evaluation of expressed sequence tags from mint glandular trichomes. *Proceedings of the National Academy of Sciences* **97**(6): 2934-2939.
- Lesburg CA, Zhai G, Cane DE, Christianson DW. 1997.** Crystal structure of pentalenene synthase: mechanistic insights on terpenoid cyclization reactions in biology. *Science* **277**(5333): 1820-1824.
- Liu D-H, Ren W-W, Cui L-J, Zhang L-D, Sun X-F, Tang K-X. 2011.** Enhanced accumulation of catharanthine and vindoline in *Catharanthus roseus* hairy roots by overexpression of transcriptional factor ORCA2. *African Journal of Biotechnology* **10**: 3260-3268.
- Liu Q, Majdi M, Cankar K, Goedbloed M, Charnikhova T, Verstappen FWA, de Vos RCH, Beekwilder J, van der Krol S, Bouwmeester HJ. 2011.** Reconstitution of the costunolide biosynthetic pathway in yeast and *Nicotiana benthamiana*. *PLoS ONE* **6**(8): e23255.
- Lu X, Zhang L, Zhang F, Jiang W, Shen Q, Zhang L, Lv Z, Wang G, Tang K. 2013.** AaORA, a trichome specific AP2/ERF transcription factor of *Artemisia annua*, is a positive regulator in the artemisinin biosynthetic pathway and in disease resistance to *Botrytis cinerea*. *New Phytologist* **198**(4): 1191-1202.
- Marrs KA, Alfenito MR, Lloyd AM, Walbot V. 1995.** A glutathione-s-transferase involved in vacuolar transfer encoded by the maize gene *Bronze-2*. *Nature* **375**(6530): 397-400.
- McGarvey DJ, Croteau R. 1995.** Terpenoid metabolism. *The Plant Cell* **7**(7): 1015.
- Moller BL. 2010.** Dynamic metabolons. *Science* **330**(6009): 1328-1329.
- Nafisi M, Goregaoker S, Botanga CJ, Glawischnig E, Olsen CE, Halkier BA, Glazebrook J. 2007.** Arabidopsis cytochrome P450 monooxygenase 71A13 catalyzes the conversion of indole-3-acetaldoxime in camalexin synthesis. *The Plant Cell* **19**(6): 2039-2052.
- Nagel J, Culley LK, Lu Y, Liu E, Matthews PD, Stevens JF, Page JE. 2008.** EST analysis of hop glandular trichomes identifies an O-methyltransferase that catalyzes the biosynthesis of xanthohumol. *The Plant Cell* **20**(1): 186-200.
- Neelakantan S, Nasim S, Guzman ML, Jordan CT, Crooks PA. 2009.** Aminoparthenolides as novel anti-leukemic agents: Discovery of the NF- κ B inhibitor, DMAPT (LC-1). *Bioorganic & Medicinal Chemistry Letters* **19**(15): 4346-4349.
- Nguyen DT, Gopfert JC, Ikezawa N, Macnevin G, Kathiresan M, Conrad J, Spring O, Ro DK. 2010.** Biochemical conservation and evolution of germacrene A oxidase in asteraceae. *Journal of Biological Chemistry* **285**(22): 16588-16598.
- Ohara K, Ujihara T, Endo T, Sato F, Yazaki K. 2003.** Limonene production in tobacco with *Perilla* limonene synthase cDNA. *Journal of Experimental Botany* **54**(393): 2635-2642.
- Paddon C, Westfall P, Pitera D, Benjamin K, Fisher K, McPhee D, Leavell M, Tai A, Main A, Eng D. 2013.** High-level semi-synthetic production of the potent antimalarial artemisinin. *Nature* doi:10.1038/nature12051.
- Qian Z, Gong K, Zhang L, Lv J, Jing F, Wang Y, Guan S, Wang G, Tang K. 2010.** A simple and efficient procedure to enhance artemisinin content in *Artemisia annua* L. by seeding to salinity stress. *African Journal of Biotechnology* **6**(12).
- Rajaonarivony JI, Gershenzon J, Miyazaki J, Croteau R. 1992.** Evidence for an essential histidine residue in 4S-limonene synthase and other terpene cyclases. *Archives of biochemistry and biophysics* **299**(1): 77-82.
- Rivas F, Parra A, Martinez A, Garcia-Granados A. 2013.** Enzymatic glycosylation of terpenoids. *Phytochemistry Reviews*: 1-13.
- Ro DK, Paradise EM, Ouellet M, Fisher KJ, Newman KL, Ndungu JM, Ho KA, Eachus RA, Ham TS, Kirby J, Chang MCY, Withers ST, Shiba Y, Sarpong R, Keasling JD. 2006.** Production of the antimalarial drug precursor artemisinic acid in engineered yeast. *Nature* **440**(7086): 940-943.
- Schilmiller AL, Chauvinhold I, Larson M, Xu R, Charbonneau AL, Schmidt A, Wilkerson C, Last RL, Pichersky E. 2009.** Monoterpenes in the glandular trichomes of tomato are synthesized from a neryl diphosphate precursor rather than geranyl diphosphate. *Proceedings of the National Academy of Sciences* **106**(26): 10865-10870.

- Toeh KH, Polichuk DR, Reed DW, Nowak G, Covello PS. 2006.** *Artemisia annua* L. (Asteraceae) trichome-specific cDNAs reveal CYP71AV1, a cytochrome P450 with a key role in the biosynthesis of the antimalarial sesquiterpene lactone artemisinin. *FEBS Letters* **580**(5): 1411-1416.
- Thomas CL, Leh V, Lederer C, Maule AJ. 2003.** Turnip crinkle virus coat protein mediates suppression of RNA silencing in *Nicotiana benthamiana*. *Virology* **306**(1): 33-41.
- Ting HM, Wang B, Rydén AM, Woittiez L, Herpen T, Verstappen FW, Ruyter-Spira C, Beekwilder J, Bouwmeester HJ, Krol A. 2013.** The metabolite chemotype of *Nicotiana benthamiana* transiently expressing artemisinin biosynthetic pathway genes is a function of CYP71AV1 type and relative gene dosage. *New Phytologist* **199**(2): 352-366.
- van der Fits L, Memelink J. 2000.** ORCA3, a jasmonate-responsive transcriptional regulator of plant primary and secondary metabolism. *Science Signaling* **289**(5477): 295.
- van Herpen TWJM, Cankar K, Nogueira M, Bosch D, Bouwmeester HJ, Beekwilder J. 2010.** *Nicotiana benthamiana* as a production platform for Artemisinin precursors. *PLoS ONE* **5**(12): e14222.
- Vergauwe A, Cammaert R, Vandenberghe D, Genetello C, Inze D, Van Montagu M, Van den Eeckhout E. 1996.** *Agrobacterium tumefaciens*-mediated transformation of *Artemisia annua* L. and regeneration of transgenic plants. *Plant Cell Reports* **15**(12): 929-933.
- Wang E, Gan S, Wagner GJ. 2002.** Isolation and characterization of the CYP71D16 trichome specific promoter from *Nicotiana tabacum* L. *Journal of Experimental Botany* **53**(376): 1891-1897.
- Wang Y, Jing F, Yu S, Chen Y, Wang T, Liu P, Wang G, Sun X, Tang K. 2011.** Co-overexpression of the *HMGR* and *FPS* genes enhances artemisinin content in *Artemisia annua* L. *Journal of Medicinal Plants Research* **5**(15): 3396-3403.
- Weathers PJ, Cheetham RD, Follansbee E, Toeh K. 1994.** Artemisinin production by transformed roots of *Artemisia annua*. *Biotechnology Letters* **16**(12): 1281-1286.
- Wu S, Schalk M, Clark A, Miles RB, Coates R, Chappell J. 2006.** Redirection of cytosolic or plastidic isoprenoid precursors elevates terpene production in plants. *Nature Biotechnology* **24**(11): 1441-1447.
- Xie Z, Kapteyn J, Gang DR. 2008.** A systems biology investigation of the MEP/terpenoid and shikimate/phenylpropanoid pathways points to multiple levels of metabolic control in sweet basil glandular trichomes. *The Plant Journal* **54**(3): 349-361.
- Xu H, Zhang F, Liu B, Huhman DV, Sumner LW, Dixon RA, Wang G. 2013.** Characterization of the formation of branched short-chain fatty acid:CoAs for bitter acid biosynthesis in Hop glandular trichomes. *Molecular Plant* doi: 10.1093/mp/sst004.
- Xu Y-H, Wang J-W, Wang S, Wang J-Y, Chen X-Y. 2004.** Characterization of *GaWRKY1*, a cotton transcription factor that regulates the sesquiterpene synthase gene (+)- δ -cadinene synthase-A. *Plant Physiology* **135**(1): 507-515.
- Yang T, Stoopen G, Yalpani N, Vervoort J, de Vos R, Voster A, Verstappen FWA, Bouwmeester HJ, Jongsma MA. 2011.** Metabolic engineering of geranic acid in maize to achieve fungal resistance is compromised by novel glycosylation patterns. *Metabolic Engineering* **13**(4): 414-425.
- Yang Y, Li R, Qi M. 2000.** *In vivo* analysis of plant promoters and transcription factors by agroinfiltration of tobacco leaves. *The Plant Journal* **22**(6): 543-551.
- Yu Z-X, Li J-X, Yang C-Q, Hu W-L, Wang L-J, Chen X-Y. 2012.** The jasmonate-responsive AP2/ERF transcription factors *AaERF1* and *AaERF2* positively regulate artemisinin biosynthesis in *Artemisia annua* L. *Molecular Plant* **5**(2): 353-365.
- Zhai JD, Li D, Long J, Zhang HL, Lin JP, Qiu CJ, Zhang Q, Chen Y. 2012.** Biomimetic semisynthesis of arglabin from parthenolide. *Journal of Organic Chemistry* **77**(16): 7103-7107.
- Zhang L, Lu X, Shen Q, Chen Y, Wang T, Zhang F, Wu S, Jiang W, Liu P, Zhang L, Wang Y, Tang K. 2012.** Identification of putative ABCG transporter unigenes related to artemisinin yield following expression analysis in different plant tissues and in response to methyl jasmonate and abscisic acid treatments. *Plant Molecular Biology Reporter* **30**(4): 838-847.
- Zhang Y, Toeh KH, Reed DW, Maes L, Goossens A, Olson DJH, Ross ARS, Covello PS. 2008.** The molecular cloning of artemisinic aldehyde Δ 11(13) reductase and its role in glandular trichome-dependent biosynthesis of artemisinin in *Artemisia annua*. *Journal of Biological Chemistry* **283**(31): 21501-21508.

Summary

Parthenolide is the major bioactive compound of feverfew and has anti-inflammatory and anti-cancer activity. **Chapter 1** gives an overview of the history and current status of research on parthenolide in feverfew. As a promising anti-cancer drug, parthenolide has attracted a lot of attention from medical institutes and companies. A search with 'parthenolide' in Google patents yields more than 2000 hits on extraction of parthenolide or its use in treating cancer or other diseases. However, information on the parthenolide biosynthetic pathway is scarce. Elucidation of the full pathway to parthenolide would open up new opportunities for production of this compound in heterologous, more efficient production platforms.

To elucidate the biosynthetic pathway of parthenolide, knowledge on the tissue(s) in which parthenolide is produced and stored is important. In **Chapter 2**, parthenolide was found to highly accumulate particularly in floral trichomes, suggesting that this is also the preferred site of biosynthesis. These floral trichomes were subsequently used to isolate germacrene A synthase (*TpGAS*), the gene encoding the first dedicated step in parthenolide biosynthesis, using a degenerate primer PCR approach. The transcript level of *TpGAS* was indeed highest in glandular trichomes. The high expression of *TpGAS* in glandular trichomes which also contain the highest concentration of parthenolide, supports the assumption that glandular trichomes are the organ where parthenolide biosynthesis and accumulation occur.

During my work on **Chapter 2**, a Canadian group reported a germacrene A oxidase (GAO) from lettuce. As the 454 cDNA library of feverfew trichomes was not available yet, we decided to use a 454 cDNA library of chicory (which also produces costunolide) to continue screening candidate genes involved in the next step of the parthenolide biosynthetic pathway, costunolide synthase (COS). In **Chapter 3**, four P450s (belonging to the CYP71 group) were selected from the chicory cDNA library for functional characterisation in yeast. One of them, named CYP71BL3, was found to be costunolide synthase, and can catalyse the oxidation of germacra-1(10),4,11(13)-trien-12-oic acid to yield costunolide. The biosynthetic pathway of costunolide was reconstituted in *Nicotiana benthamiana* by transient expression (agro-infiltration) of *TpGAS*, *CiGAO* (which we also identified in the chicory library) and *CiCOS*, which resulted in costunolide production of up to 60 ng.g⁻¹ FW. In addition, two new compounds were formed that were identified as costunolide-glutathione and costunolide-cysteine conjugates.

When the 454 sequences of the feverfew trichome library became available, we continued to identify additional genes involved in the biosynthetic pathway of parthenolide. In **Chapter 4**, the parthenolide biosynthetic pathway was elucidated by isolating all the structural genes from feverfew, *TpGAS*, *TpGAO*, *TpCOS* and *TpPTS*. Moreover, the whole pathway was reconstituted in *N. benthamiana*, through transient expression. In the agro-infiltrated plants, parthenolide as well as a number of conjugates (with cysteine and glutathione) were produced. In an anti-cancer bioassay, these relatively polar conjugates were highly active against colon cancer cells, with only slightly lower activity than free parthenolide. Finally, also a gene encoding

a costunolide and parthenolide 3 β -hydroxylase was identified, which could potentially be used in biotechnological applications to produce hydroxylated parthenolide. The conjugation and hydroxylation of parthenolide open up new options to improve the water solubility of parthenolide and therefore its potential as a drug.

Besides genes involved in the biosynthetic pathway of parthenolide, we also identified two other P450 genes that can utilize costunolide as substrate. In **Chapter 5**, Tp8879 is identified. Tp8879 can cyclise the monocyclic germacranolide sesquiterpene lactone costunolide to form the bicyclic guaianolide sesquiterpene lactone kauniolide, and is hence called kauniolide synthase. The biosynthetic pathway of kauniolide was reconstituted in *N. benthamiana*, through transient expression.

This thesis combines a series of existing and new technologies for gene discovery – transcriptomics and metabolomics - as well as optimisation of plant metabolic engineering – using transient expression in *N. benthamiana* - and reports on novel combinatorial biochemistry occurring in metabolic engineering of heterologous plant hosts, resulting in novel sesquiterpene lactone derivatives with the potential to be new drug leads. The use of transient expression and metabolomics for unexpected product identification are technologies that will be of great value to others working in the field of metabolic engineering. The strategies for identification and characterization of candidate genes, the strategies and tools for metabolic engineering and the possibilities to further improve pathway metabolic engineering are discussed in **Chapter 6**.

Samenvatting

Parthenolide is de belangrijkste biologisch actieve stof in moederkruid (*Tanacetum parthenium*) en heeft zowel anti-ontstekings als anti-kanker activiteit. In **hoofdstuk 1** wordt een historisch overzicht gegeven van het onderzoek aan parthenolide in moederkruid. Als anti-kanker medicijn heeft parthenolide de belangstelling van medische instituten en de farmaceutische industrie. Een zoekopdracht in GOOGLE patenten geeft meer dan 2000 hits die variëren van extractie protocollen voor parthenolide tot het gebruik van parthenolide als medicijn tegen kanker. Echter, informatie over de biosynthese van parthenolide is in deze database niet te vinden. De opheldering van de parthenolide biosynthese route zou nieuwe mogelijkheden kunnen geven voor de productie van deze stof in efficiëntere productie systemen. Om de biosynthese route van parthenolide te ontrafelen, is kennis van de weefsels waar parthenolide wordt gemaakt en opgeslagen in de plant van belang. In **hoofdstuk 2** is vastgesteld dat parthenolide vooral ophoopt in de zogenaamde trichomen, die zich met name bevinden op de bloemen. Dit duidt er op dat de biosynthese ook voornamelijk in deze cellen actief is. Deze trichomen zijn vervolgens gebruikt om met behulp van gedegenereerde primers en PCR het germacreen A synthase gen (*TpGAS*) te isoleren dat codeert voor het eerste enzym in de parthenolide biosynthese route. De transcriptie van *TpGAS* was inderdaad het hoogst in de trichomen, waar ook de hoogste concentratie parthenolide wordt gevonden. Dit bevestigt dat de trichomen op de bloemen de weefsels zijn waar de parthenolide biosynthese plaatsvindt.

Tijdens mijn werk aan hoofdstuk 2 publiceerde een Canadese groep over een germacreen A oxidase (*GAO*) uit sla. Omdat in die tijd de sequentie informatie over de genen die in de moederkruid trichomen tot expressie komen nog niet bekend was hebben we besloten om gebruik te maken van een sequentie database van witlof (witlof maakt net als moederkruid ook costunolide, de waarschijnlijke precursor is van parthenolide). In **hoofdstuk 3** zijn vier cytochroom P450s (van de CYP71 klasse) geselecteerd uit de witlof sequentie database voor functionele karakterisering in gist. Eén van deze cDNAs (*CYP71BL3*) bleek inderdaad te coderen voor het costunolide synthase enzym (*COS*) dat de oxidatie van germacra-1(10),4,11(13)-trien-12-oic zuur naar costunolide katalyseert. De biosynthese route tot aan costunolide kon transient tot expressie gebracht worden in *Nicotiana benthamiana* middels agroinfiltratie van *TpGAS*, *CiGAO* en *CiCOS*, wat resulteerde in een costunolide productie van 60 ng.g⁻¹ FW. Bovendien werden twee nieuwe componenten gevormd, die werden geïdentificeerd als costunolide-glutathion en costunolide-cysteine conjugaten.

Toen de 454 sequenties van de moederkruid trichoom cDNA bank beschikbaar kwamen zijn we doorgegaan met de identificatie van additionele genen van de biosynthese route van parthenolide. In **hoofdstuk 4** is de hele parthenolide biosynthese route opgehelderd door isolatie en karakterisering van de moederkruid *TpGAS*, *TpGAO*, *TpCOS* en het parthenolide synthase, *TpPTS*. Ook werd nog een enzym geïdentificeerd dat parthenolide kan hydroxyleeren. De parthenolide biosynthese route werd in zijn geheel tot expressie gebracht in *N. benthamiana*. In de agro-geïnfiltreerde planten werden parthenolide en een aantal conjugaten

daarvan (met cysteine of glutathion) geproduceerd. In een anti-kanker assay bleek dat deze relatief polaire conjugaten zeer actief waren tegen darmkanker cellen, met maar iets minder activiteit dan vrij parthenolide. Omdat de conjugatie en hydroxylatie van parthenolide de wateroplosbaarheid verbeteren, opent dit nieuwe mogelijkheden voor de toepassing van parthenolide als medicijn. Naast genen van de biosyntheseroute van parthenolide hebben we ook twee andere P450 genen geïdentificeerd die coderen voor enzymen die costunolide als substraat gebruiken. In **hoofdstuk 5** is Tp8879 geïdentificeerd als een enzym dat het monocyclische germacranolide sesquiterpeen lacton costunolide om kan zetten in het bicyclische guaianolide sesquiterpeen lacton, kauniolide, en dit enzym is daarom kauniolide synthase genoemd. De biosynthese route van kauniolide werd gereconstitueerd in *N. benthamiana* door middel van transiente expressie. In mijn proefschrift heb ik een aantal bestaande en nieuwe technieken gecombineerd voor 'gene-discovery', te weten transcriptomics en metabolomics, en heb ik gewerkt aan de optimalisatie van de metabole engineering van planten, gebruikmakend van transiente expressie in *N. benthamiana*. Bovendien heb ik nieuwe 'combinatorial biochemistry' aangetoond, die optreedt tijdens de metabole engineering die ik heb uitgevoerd in de heterologe gastplant, *N. benthamiana*, wat resulteerde in nieuwe sesquiterpeen lacton derivaten met potentieel voor de ontwikkeling van nieuwe medicijnen. Het gebruik van transiente expressie en metabolomics voor de identificatie van onverwachte nieuwe producten zijn technologieën die van grote waarde zijn voor anderen die werken in het veld van de metabole engineering. De strategie voor het identificeren en karakteriseren van kandidaat genen en de strategie en mogelijkheden van metabole engineering om biosynthese en productie van belangrijke metabolieten verder te verbeteren worden bediscussieerd in **hoofdstuk 6**.

Acknowledgements

I'm feeling excited to finish my PhD, although it's my second PhD degree. During the past 4 years, I became a confident and independent researcher through the PhD training in Wageningen University. This could not have been achieved without the help from my promoters, supervisors, colleagues, co-operates, friends, and families. Here I would like to take this opportunity to express my thanks and appreciations to all of them.

First of all, I would like to thank my promoter Prof. dr. Harro Bouwmeester for giving me the opportunity to join his research group. Harro, I still remember the time when we first met. You went to China for a meeting, and I picked you up from the airport. During the way from the airport to your hotel, we discussed a lot of scientific issues. I was impressed by your contagious scientific curiosity and your quick response. After I started working in your group, I didn't do a very good job at the very beginning. I am grateful for your support. It is your continuous support that encouraged me to propose new ideas and new solution to overcome every difficulty. Your research vision and scientific thinking enlightened me to think and act like a scientist. Thanks a lot for your effort and help through every step of my PhD.

Special thanks go to my supervisor, Sander van de Krol. It is from you that I see one can enjoy playing with scientific research so well. Because of that, I begin to enjoy doing my research during the second half of my PhD study. One activity I would like to mention specially is the writing week (hard part) combined with boat trip (relaxed part) afterwards. It forced and helped us at the same time to start writing about whatever results we've got at that moment, which is really really helpful for me. Thank you for your elaborated instructions on my papers, PPT slides and this thesis, which helped me to improve my writing and presenting skills a lot.

My sincere thanks go to Carolien Ruyter-Spira. Thank you for your guidance during the first 8 months of my research in Plant Physiology. Your kindness and patience helped me to adjust to the new environment. I really appreciate that. By the way, it is with your help that I get used to planning my experiment for the coming month. Thank you for being supportive all the time.

I would like to thank the technician of my PhD project, Miriam Goedbloed. Thank you for your help with the cloning of most of the candidate genes in

this thesis.

I would like to thank the people in the TERPMED project, which my PhD project is a part of. Ric de Vos, thank you for being always available to answer my questions and help me out with experimental difficulties, especially LC-MS data analysis. Angelos K. Kanellis, thank you for your trust and inviting me to present my work in the TERPNET 2013 conference as an invited speaker. People from PRISNA, Justin Fishedick, Karel Lund, Annelies Schulte, thank you for all the standards you sent me. Albert Ferrer, David Manzano, Irene Pateraki, thank you for the nice cooperation. Alain Tissier, Kathleen Brückner, Ana Simonovic, Slađana Todorović, Dragana Bozic and Aalt-Jan van Dijk, thank you for all the discussions and suggestions during the TERPMED project meetings.

I would like to express my appreciation to my colleagues and friends in the Terpene lab 1.056. Francel, Bert and Jos, thank you for your help with LC-MS, GC-MS and qPCR analysis. I've learned a lot about how to operate those machines and analyse the data. Katja, thanks a lot for your help in and outside the lab. Rina, thanks for the help with all the administrative things. And all my PhD fellows in the lab, Neli, Aldana, Jimmy, Benyamin, Thierry, Lemeng, Jun, Bo, Yuanyuan, Mohammad, thanks you for creating such a pleasant working atmosphere. My friend Danijela, thank you for your help with the Inula work. I miss our discussions during the coffee break in the afternoon. My students Namraj, Rashmi, and Lea, thank you for your valued contribution to my PhD work.

To my friends in Wageningen, Ningwen Zhang and Ke Lin, Wei Song, Xi Cheng, Chunxu Song and Wei Qin, Yanfen Lin and Hieng Ming (Jimmy) Ting, Yanru Song and Xu Cheng, Na Li and Wei Liu, Hanzi He, Hui Li, Yanxia Zhang, Tingting Xiao, Lisha Zhang and Chenlei Hua, Xi Chen and Weicong Qi, Ying Li, Songlin Xie, Wei Gao, Suxian Zhu, Feng Zhu, Liping Gao, Jifeng Tang and Jinbo Wan, Xi Wan, Ke Peng, Xianwen Ji, Huchen Li, Bing Bai, Chunting Lang, Yan Wang, Margriet Roelse and Martijn Luking, Benyamin, Houshyani Hassanzadeh, I would like to thank you for your great company and support. With all of you, Ting and I had a very good time in the Netherlands.

I am very grateful to my promoter during my first PhD study in Huazhong Agricultural University in China, Prof. Xiuxin Deng. You opened the door of

scientific research to me and showed me how to become a qualified researcher.

I thank my loving parents Xianqi Wang and Xinzhen Liu. Thank you for being supportive all the time and giving me the opportunity to make my own decisions and follow my own path. Special thanks for my brother Xiaowei Wang. You have no idea how much I admired you when we were growing up. To my parents-in-laws, thank you for raising such an amazing daughter.

My daughter, Yiyi. Thank you for bringing so much happiness and joyfulness to the family. You are my angel. For sure, I will love you forever!

Finally, my wife and soul mate, Ting. I feel like the luckiest guy in the world to have spent the past 11 years and going to spend the rest of my life with you!

Curriculum Vitae

Qing Liu was born on 21 January 1982 in Songzi City, Hubei province, China. Qing performed his bachelor study between 1999 and 2003 with a major in Horticulture in Huazhong Agricultural University and with an additional major in English in Huazhong University of Science and Technology. From Sep-



tember 2003 to October 2008, he performed his first PhD study under the supervision of Professor Xiuxin Deng in Huazhong Agricultural University, focusing on 'Revealing the molecular mechanism of a red-flesh citrus mutant'. After that, he came to the Netherlands and temporarily worked as a research assistant in the group of Harro Bouwmeester at Wageningen UR. Started from August 2009, he became a PhD student in the same group under the supervision of Harro Bouwmeester and Sander van de Krol. This thesis summarizes the research of his study in elucidation of the sesquiterpene lactone biosynthetic pathway in feverfew, a medicinal plant.

Publication list

Publications related to this thesis:

- Liu, Q.**, Manzano, D., Tanić, D., Ricard, L., Ferrer, A., de vos, R., Krol, S.V.D., and Bouwmeester, H.J. (2013). Branching of guaianolide and germacrenolide type sesquiterpene lactone biosynthesis occurs at the common precursor costunolide. (In preparation for submission)
- Liu, Q.**, Manzano, D., Tanić, D., Ricard, L., Ferrer, A., de vos, R., Krol, S.V.D., and Bouwmeester, H.J. (2013). *In planta* reconstitution of the biosynthesis pathway of an anti-cancer drug. (In submission)
- Liu, Q.***, Majdi*, M., Cankar, K., Goedbloed, M., Charnikhova, T., Verstappen, F.W.A., de Vos, R.C.H., Beekwilder, J., van der Krol, S., and Bouwmeester, H.J. (2011). Reconstitution of the costunolide biosynthetic pathway in yeast and *Nicotiana benthamiana*. PLoS ONE 6, e23255.
- Majdi, M.*, **Liu, Q.***, Karimzadeh, G., Malboobi, M.A., Beekwilder, J., Cankar, K., Vos, R.d., Todorović, S., Simonović, A., and Bouwmeester, H. (2011). Biosynthesis and localization of parthenolide in glandular trichomes of feverfew (*Tanacetum parthenium* L. Schulz Bip.). Phytochemistry 72, 1739-1750.

Other publications:

- Liu, Q.**, Zhang, Y., Matusova, R., Charnikhova, T., Amini, M., Jamil, M., Huang, K., Timko, M., Fernandez-Aparicio, M., Westwood, J., Ruyter-Spira, C., Krol, S.V.D., and Bouwmeester, H.J. (2013). *ShMAX2* restores branching but not the Very Low Fluence Response in the *Arabidopsis thaliana max2* mutant. (In submission)
- Liu, Q.**, Zhu, A., Chai, L.J., Zhou, W.J., Yu, K.Q., Ding, J., Xu, J., and Deng, X.X. (2009). Transcriptome analysis of a spontaneous mutant in sweet orange (*Citrus sinensis* L. Osbeck) during fruit development. Journal of Experimental Botany 60, 801-813.
- Liu, Q.**, Xu, J., Liu, Y.Z., Zhao, X.L., Deng, X.X., Guo, L.L., and Gu, J.Q. (2007). A novel bud mutation that confers abnormal patterns of lycopene accumulation in sweet orange fruit (*Citrus sinensis* L. Osbeck). Journal of Experimental Botany 58, 4161-4171.
- Kohlen W*, Charnikhova T*, **Liu Q**, Bours R, Domagalska MA, Beguerie S, Verstappen F, Leyser O, Bouwmeester HJ, Ruyter-Spira C. (2011). Strigolactones are transported through the xylem and play a key role in shoot architectural response to phosphate deficiency in non-AM host *Arabidopsis thaliana*. Plant Physiology(155): 974-987.
- Xu J, Tao N, Cao H, **Liu Q**, Deng X. (2011). PRESENCE OF TWO VARIANTS OF LYCOPENE β -CYCLASE GENE IN GENOMES OF CITRUS AND ITS RELATIVES. BIOTECHNOLOGY & BIOTECHNOLOGICAL EQUIPMENT 25(3): 2452-2457.
- Pan Z, **Liu Q**, Yun Z, Guan R, Zeng W, Xu Q, Deng X. (2009). Comparative proteomics of a lycopene-accumulating mutant reveals the important role of oxidative stress on carotenogenesis in sweet orange (*Citrus sinensis* [L.] osbeck). Proteomics 9(24): 5455-5470.
- Xu Q, Yu K, Zhu A, Ye J, **Liu Q**, Zhang J, Deng X. (2009). Comparative transcripts profiling reveals new insight into molecular processes regulating lycopene accumulation in a sweet orange (*Citrus sinensis*) red-flesh mutant. BMC genomics 10(1): 540.
- Liu Y, **Liu Q**, Xiong J, Deng X. (2007). Difference of a citrus late-ripening mutant (*Citrus sinensis*) from its parental line in sugar and acid metabolism at the fruit ripening stage.

Science in China Series C: Life Sciences 50(4): 511-517.

Xu J, Tao N, **Liu Q**, Deng X. (2006). Presence of diverse ratios of lycopene/ β -carotene in five pink or red-fleshed citrus cultivars. *Scientia horticulturae* 108(2): 181-184.

Liu Y, **Liu Q**, Tao N. (2006). Efficient isolation of RNA from fruit peel and pulp of ripening navel orange (*Citrus sinensis* Osbeck). *Journal of Huazhong Agricultural University* 25.

* authors contributed equally to this publication.

**Education Statement of the Graduate School
Experimental Plant Sciences**

Issued to: Qing Liu
Date: 2 December 2013
Group: Plant Physiology, Wageningen University & Research Centre

1) Start-up phase	<i>date</i>
▶ First presentation of your project Gene discovery and metabolic engineering of pharmaceutically active sesquiterpene lactones	Feb 08, 2010
▶ Writing or rewriting a project proposal Gene discovery and metabolic engineering of pharmaceutically active sesquiterpene lactones	2009
▶ Writing a review or book chapter	
▶ MSc courses	
▶ Laboratory use of isotopes	
<i>Subtotal Start-up Phase</i>	<i>7.5 credits*</i>

2) Scientific Exposure	<i>date</i>
▶ EPS PhD student days Second European Retreat of Phd Students in Plant Sciences, Cologne, Germany EPS PhD student day, Wageningen University EPS ExPectationS Day (EPS Career Day), Wageningen University	Apr 15-17, 2010 May 20, 2011 Feb 01, 2013
▶ EPS theme symposia EPS Theme 3 Symposium 'Metabolism and Adaptation', Leiden University EPS Theme 3 Symposium 'Metabolism and Adaptation', Wageningen University	Feb 19, 2010 Feb 10, 2011
▶ NWO Lunteren days and other National Platforms ALW meeting 'Experimental Plant Sciences', Lunteren ALW meeting 'Experimental Plant Sciences', Lunteren ALW meeting 'Experimental Plant Sciences', Lunteren ALW meeting 'Experimental Plant Sciences', Lunteren	Apr 06-07, 2009 Apr 19-20, 2010 Apr 04-05, 2011 Apr 02-03, 2012
▶ Seminars (series), workshops and symposia Mini symposium: How to write a world-class paper? Seminar: 'Plant drug smugglers' about transport of secondary metabolites in plants' by Prof. Marc Boutry Seminar: 'Metabolomics-based functional genomics - from Arabidopsis to crops and medicinal plants' by Professor Kazuki Saito Seminar: 'Glandular trichomes of tomato: from terpene biosynthesis to trichome differentiation' by prof. Alain Seminar: Using the Nicotiana-TMV system to study resistance gene evolution and plant genome stability by Professor Hanhui Kuang Seminar series: Plant Physiology-Genetics, Wageningen University	Oct 26, 2010 Mar 13, 2013 Apr 08, 2013 May 03, 2013 Sep 11, 2013 2009-2013
▶ Seminar plus	
▶ International symposia and congresses EU meeting TERPMED project (Baecelona, Spain) EU meeting TERPMED project (Chania, Greece) EU meeting TERPMED project (Wageningen, The Netherlands) EU meeting TERPMED project (Kalmar, Sweden) TERPNET 2011 (Kalmar, Sweden) EU meeting TERPMED project (Halle, Germany) EU meeting TERPMED project (Leiden, The Netherlands) EU meeting TERPMED project (Baecelona, Spain) EU meeting TERPMED project (Chania, Greece) TERPNET 2013 (Chania, Greece) International Scientific Workshop on Plant Secondary Metabolism (Wuhan, China)	Jul 03, 2009 May 14, 2010 Oct 28, 2010 May 22, 2011 May 23-26, 2011 Nov 03-04, 2011 Apr 23-24, 2012 Oct 25-26, 2012 May 30-31, 2013 Jun 01-06, 2013 Jul 05-07, 2013
▶ Presentations Second Joint Retreat of Phd Students in Plant Sciences, Cologn, Germany (poster) Summer school 'Rhizosphere Signaling' Wageningen (oral) EU meeting TERPMED project Chania, Greece (oral) EU meeting TERPMED project Wageningen (oral) EPS Theme 3 Symposium Wageningen (oral) TERPNET 2011 Kalmar, Swden (poster) EU meeting TERPMED project Kalmar, Sweden (oral) EU meeting TERPMED project Halle, Germany (oral) EU meeting TERPMED project Leiden (oral) EU meeting TERPMED project Barcelona, Spain (oral) EU meeting TERPMED project Chania, Greece (oral) TERPNET 2013 Chania, Greece (oral) International Scientific Workshop on Plant Secondary Metabolism Wuhan, China (oral)	Apr 15-17, 2010 Aug 25, 2010 May 14, 2010 Oct 28, 2010 Feb 10, 2011 May 23-26, 2011 May 22, 2011 Nov 03-04, 2011 Apr 23-24, 2012 Oct 25-26, 2012 May 30, 2013 Jun 02, 2013 Jul 05-07, 2013
▶ IAB interview	Nov 05, 2012
▶ Excursions	
<i>Subtotal Scientific Exposure</i>	<i>27.6 credits*</i>

3) In-Depth Studies	<u>date</u>
▶ EPS courses or other PhD courses	
Summer school 'Rhizosphere Signaling'	Aug 23-25, 2010
Bioinformatics- A user's Approach	Aug 30-Sep 03, 2010
Plant Metabolomics	Apr 26-28, 2011
▶ Journal club	
Plant Research International, Bouwmeester & Jongsma associate group	2009-2012
Literature discussion: Plant physiology group, Wageningen University	2009-2013
▶ Individual research training	

Subtotal In-Depth Studies 6.3 credits*

4) Personal development	<u>date</u>
▶ Skill training courses	
PhD Competence Assessment, Wageningen University	Mar 16, 2010
Techniques for writing and presenting a scientific paper	Feb 14-17, 2012
Advanced Course Guide to Scientific Artwork	May 06-07, 2013
Adobe InDesign	May 08, 2013
How to write a convincing Research Proposal	May 27, 2013
▶ Organisation of PhD students day, course or conference	
Summer school 'Rhizosphere Signaling' session organiser	Aug 25, 2010
▶ Membership of Board, Committee or PhD council	

Subtotal Personal Development 4.2 credits*

TOTAL NUMBER OF CREDIT POINTS*	45.6
---------------------------------------	-------------

Herewith the Graduate School declares that the PhD candidate has complied with the educational requirements set by the Educational Committee of EPS which comprises of a minimum total of 30 ECTS credits

* A credit represents a normative study load of 28 hours of study.

Funding

The research of this thesis was funded by by the European Commission (EU-project TerpMed, Plant Terpenoids for Human Health: a chemical and genomic approach to identify and produce bioactive compounds, Grant agreement no.: 227448).



Financial support from Wageningen University and Research centre for printing this thesis is gratefully acknowledged.



A lot of science is detective work: observing, collecting evidence, finding clues, reconstructing events, establishing theories and drawing conclusions. Detective work with techniques straight out of Crime Scene Investigation (CSI) makes science almost romantic.

Adapted from Roelof Kleis & Bob Ramaker in RESOURCE magazine 2013.

Thesis layout: Qing Liu
Cover design: Ting Yang & Qing Liu